Effects of Initial Fire Attack Suppression Tactics on the Firefighter and Compartment Environment

by

Matthew R. Obach

A thesis
presented to the University of Waterloo
in fulfillment of the
thesis requirement for the degree of
Master of Applied Science
in
Mechanical Engineering

Waterloo, Ontario, Canada, 2011

I hereby declare that I am the sole author of this thesis. This is a true copy of the thesis, including any required final revisions, as accepted by my examiners.

I understand that my thesis may be made electronically available to the public.

Abstract

Full-scale experiments are conducted to study the effects of different water-based indirect and combination initial attack methods on the compartment environment and firefighter during compartment fire suppression, with an aim toward improving manual fire suppression effectiveness and firefighter safety. Hot layer temperatures typical of room fire conditions are developed in the test compartment using wood cribs. Five suppression methods including straight stream, penciling, continuous wide and narrow fog, and a wide angle burst method are examined for two different spray angles and nozzle pressures. Temperatures, heat flux, gas velocity, and gas concentrations are monitored for the duration of each experiment in the fire compartment, along with temperatures and gas concentrations in the area of the firefighter, just outside the compartment.

Realistic fire conditions are repeatedly established in the test compartment, with each fuel load allowing up to nine suppression applications per fire. The repeatability of the compartment temperatures are demonstrated by the consistent hot layer temperature stratification in the room, along with the uniformity of the hot layer throughout a test, and the consistency of the temperature from test to test. The repeatability of each suppression method is also demonstrated by comparing results of compartment cooling achieved in repeat tests.

Differences in average compartment temperature before and during suppression indicate that penciling tactics provide little cooling of the compartment. In narrow fog attacks, the hot layer is pushed toward the floor, resulting in increased temperatures in the lower layer, generally an undesired result. Wide angle fog methods may have greater impact on compartment temperature as compared to straight stream or narrow fog methods, however, they also result in large increases in temperature at the firefighter. Wide angle burst tactics less effectively cool the compartment gases than continuous methods, but also lead to less impact on the firefighter. Greater numbers of bursts increase cooling of the compartment, but at the expense of increased impact on the firefighter.

Including impact on the firefighter, continuous straight stream methods, at a nozzle discharge pressure of 700 kPa and aimed to the top of the rear compartment wall, appear the best choice for initial attack on the fire developed in these experiments. Due to variability between real fire scenarios and experiments such as these, significantly more study of the various suppression tactics is required before the most effective methods of suppression can be determined for a given set of fire scenarios.

Acknowledgements

I would like to thank my supervisor, Dr. Elizabeth Weckman, for her constant advice and support throughout the entire project. I would also like to thank Gord Hitchman for the countless hours in technical advising and manual labor he committed to the experimental set-up and testing.

I would like to thank Dr. Al Strong for imparting some of his wisdom in terms of fire and suppression behaviour and practices, as well as for always being prepared as my backup during testing. Rick Hummel, manager at the Waterloo Regional Emergency Services Training and Research Center, Capt. Steve MacInnis, Training Director, Kitchener Fire Department, and Capt. Blake Moogy, Training Officer, Kitchener Fire Department helped to educate and train me in firefighting practices and on the pumper truck, which was greatly appreciated. Rick also helped with scheduling and monitoring of the large-scale fire tests to ensure no problems were encountered in areas external to the test area. The work accomplished by Charles Lin in his two months at the lab was also greatly appreciated, as his efforts greatly facilitated the data reduction and analysis process. Help was also received from Andy Barber, Matt DiDomizio, and Andrew House from the University of Waterloo, Timo Tikka, from Lakehead University, Stephen Paskaluk from the University of Alberta, and Luke Robson from the University of Saskatchewan, in the set-up and operation of the large fire tests.

In addition, I would like to acknowledge financial contributions from the Natural Sciences and Engineering Research Council of Canada (NSERC), the Ontario Government Scholarship Program (OGSST), the Department of National Defense, and the University of Waterloo Live Fire Research Facility (UWLFRF).

Lastly, I would like to thank my wife, Lana, and the rest of my family for encouraging me to pursue this endeavor, and for all their support.

CONTENTS

LIST OF FIGURES ..... **XI**

LIST OF TABLES ..... **XV**

CHAPTER 1 ..... **1**

INTRODUCTION

CHAPTER 2 ..... **3**

LITERATURE REVIEW

2.1 COMPARTMENT FIRE DEVELOPMENT 3

2.1.1 Measurement Techniques in Compartment Fires *4*

2.2 COMPARTMENT FIRE SUPPRESSION 4

2.2.1 Manual Fire Suppression *5*

2.3 OBJECTIVES 11

CHAPTER 3 ..... **13**

EXPERIMENTAL APPARATUS AND TECHNIQUE

3.1 COMPARTMENT 13

3.2 INSTRUMENTATION 16

3.3 FUEL LOAD 28

3.3.1 Free Burn Characteristics of the Wood Cribs *28*

3.3.2 Compartment Loading *31*

3.4 SUPPRESSION 35

3.4.1 Equipment and Set-Up *35*

3.4.2 Energy Balance *37*

3.4.3 Flow Properties *38*

3.5 TEST PROCEDURE 40

3.5.1 Pre-Test Conditions *40*

3.5.2 Test Procedure *41*

3.6 MEASUREMENT UNCERTAINTY AND SOURCES OF ERROR 41

3.6.1 Temperature Measurement *42*

3.6.2 Heat Flux Measurement *43*

3.6.3 Velocity Measurement *44*

3.6.4 Gas Concentration Measurement *44*

3.7 SUMMARY 45

CHAPTER 4 ..... **47**

CHARACTERIZATION OF THE COMPARTMENT FIRE ENVIRONMENT

4.1 INTERFACE HEIGHT 48
4.2 UPPER LAYER AVERAGE TEMPERATURE 50
4.3 LATERAL AND AXIAL UNIFORMITY 51
4.4 UPPER LAYER TEMPERATURE REPEATABILITY 54
4.5 COMPARTMENT ENVIRONMENT PRIOR TO SUPPRESSION 55
4.5.1 Upper Layer Average Temperature *55*
4.5.2 Heat Flux out of the Compartment *56*
4.6 SUMMARY 57

CHAPTER 5 ..... **59**

RESULTS

5.1 REPEATABILITY 59
5.1.1 Characteristics of Suppression *59*
5.2 SUPPRESSION IMPACT ON THE COMPARTMENT AND FIREFIGHTER ENVIRONMENTS 63
5.2.1 Initial Impact of the Suppression Methods *65*
5.2.2 Impact Varying the Burst Method *68*
5.2.3 Impact from Increased Discharge Pressure *71*
5.2.4 Impact from Increased Discharge Angle *74*
5.3 PROTECTED VS. AMBIENT ENVIRONMENT AT THE FIREFIGHTER 77
5.3.1 Temperature *77*
5.3.2 Heat Flux *81*
5.4 GAS CONCENTRATION 83
5.5 OVERALL SUPPRESSION EFFECTIVENESS 86
5.6 SUMMARY 90

CHAPTER 6 ..... **91**

CLOSURE

6.1 CONCLUSIONS 91
6.1.1 Compartment Environment and Repeatability *91*
6.1.2 Methods of Suppression *92*
6.2 RECOMMENDATIONS FOR FUTURE WORK 93

REFERENCES **95**

LIST OF FIGURES

Figure 3.1. Fire compartment. 14
Figure 3.2. Picture showing the inside of the doors in the test compartment. 15
Figure 3.3. Compartment schematic with the thermocouple rakes included. 17
Figure 3.4. Picture showing the thermocouples mounted in the rakes and to the wall. 18
Figure 3.5. Uncovered floor mount heat flux gauge. 19
Figure 3.6. Covered floor mount heat flux gauge. 20
Figure 3.7. Bi-directional probe: (a) with attached thermocouple; (b) rake at the opening. 22
Figure 3.8. Thermocouples on the exterior wall of the compartment. 23
Figure 3.9. Bulkhead thermocouples on the backside of the compartment. 24
Figure 3.10. Firefighter sensors exposed to ambient. 27
Figure 3.11. Protected firefighter sensors: (a) covering removed; (b) covering in place. 27
Figure 3.12. Two wood cribs placed side by side. 28
Figure 3.13. Heat release rate curves for the three crib configurations tested. 30
Figure 3.14. Double the heat release rate for one module compared to two modules side by side 31
Figure 3.15. Compartment schematic with fuel load included. 32
Figure 3.16. Heat release rate curves for the six crib configuration. 34
Figure 3.17. Heat flux measured for different crib configurations in the compartment and calorimeter during the initial burning phase. 35
Figure 3.18. Suppression stand used in the experiments: (a) before instrumentation; (b) at the door. 36
Figure 3.19. Nozzle flow patterns. L-R: straight stream, narrow fog, wide fog. 40
Figure 4.1. Frame from the compartment video just prior to suppression. 48
Figure 4.2. Temperature and interface height before suppression. 49
Figure 4.3. Average upper layer temperature during a fire growth phase. 50

Figure 4.4. Instantaneous temperature measured by each upper layer thermocouple on the six vertical rakes at 200 seconds after ignition. 52

Figure 4.5. Temperature measured by the thermocouples on the centerline axis of the compartment at 200 seconds after ignition. 53

Figure 4.6. Average upper layer temperature during the fire growth phase for all crib burns..... 54

Figure 4.7. Heat flux measured just outside the compartment in ambient conditions for five tests. 56

Figure 5.1. Average compartment temperature difference for three penciling tests. 60

Figure 5.2. Upper bulkhead wall temperature for the three penciling tests. 61

Figure 5.3. Average compartment temperature difference for two narrow fog applications. 62

Figure 5.4. Average compartment temperature difference for two wide angle fog applications. 63

Figure 5.5. Average compartment temperature difference for each suppression method. 65

Figure 5.6. Typical temperature increase at the firefighter measured using five different suppression methods. 67

Figure 5.7. Average compartment temperature difference for different numbers of bursts. 69

Figure 5.8. Temperature increase at the firefighter observed from suppression using different number of bursts. 69

Figure 5.9. Temperature reduction in the compartment observed for the five suppression methods at two different discharge pressures, 410 and 700 kPa..... 72

Figure 5.10. Temperature increase at the firefighter for the narrow fog suppression method at two pressures. 74

Figure 5.11. Average compartment temperature difference for the five suppression methods at two different application angles, 20 and 30° above horizontal. 75

Figure 5.12. Temperature increase at the firefighter using two narrow fog tests, one at each angle. 76

Figure 5.13. Typical temperature profile of the thermocouples under the firefighter gear for one suppression test. 78

Figure 5.14. Typical ambient temperatures measured just outside the compartment using straight stream suppression. 79

Figure 5.15. Typical ambient temperatures measured just outside the compartment using burst suppression. 79

Figure 5.16. Typical heat flux measured by the skin simulant sensors for one suppression test. 81

Figure 5.17. Carbon monoxide levels measured near the firefighter for the suppression tests conducted during one compartment burn. 84

Figure 5.18. Peak carbon monoxide levels measured during each suppression method..... 85

Figure 5.19. Average compartment temperature difference caused by the four most effective suppression methods. 86

Figure 5.20. Temperature increase of the ambient air measured just outside the door for each of the four methods that provided the greatest amount of compartment cooling..... 88

Figure 5.21. Temperature increase measured under the firefighter suit for each of the four methods that produced the greatest amount of compartment cooling. 88

Figure 5.22. Peak carbon monoxide levels measured at the firefighter..... 89

LIST OF TABLES

Table 3.1. Heat flux gauge calibration data. 19

Table 3.2. Calibration equations for the eight pressure transducers. 21

Table 3.3. Thermal properties of the Dermis and Colorceran. 25

Table 3.4. Calibration 'slope' for each skin simulant sensor. 26

Table 3.5. Ventilation openings used for oxygen consumption calorimetry analysis in the compartment. 33

Table 3.6. Nozzle calibration test data. 39

Table 3.7. Flow rate determined for each flow pattern and flow tactic. 40

Table 5.1. Typical peak temperature rise under the firefighter gear for each suppression method. 78

Table 5.2. Typical peak temperature rise of the ambient gases just outside the door for each suppression method. 80

Table 5.3. Typical peak heat flux rise measured by the sensors exposed to ambient for each suppression method. 82

Table 5.4. Typical peak heat flux rise under the firefighter gear for each suppression method. 82

Table 5.5. Integrated compartment cooling by the four methods. 87

Chapter 1

INTRODUCTION

In the United States alone, close to 600 000 structure fires are fought annually [1], while over 10 000 are responded to annually in Ontario [2]. The National Fire Protection Association recommends that fire departments should be able to respond to a residential fire no later than 9 minutes after the fire is reported [3], which is similar to the 11 minute average response time of the fire departments in Ontario [4]. In a study by the U.S. Department of Homeland Security, it was found that fire departments in the United States had begun to address the fire 11 minutes after notification 90% of the time [5]. Depending on the method of ignition of the fire, fuel, and ventilation in the room, an 11-minute fire growth time can produce a range of different fires, from virtually non-existent or smoldering combustion, to very large, fully developed post flashover compartment fires [6].

The situation facing the fire department when they arrive on scene, therefore, can be very different even for similar response times. Depending on the conditions, the firefighters need to be ready to employ a number of different tactics to combat and suppress the fire. Along with knowing which tactic to use, firefighting personnel need equipment that can deliver a number of different tactics easily and efficiently, and need to understand the best method of deployment for each tactic in order to suppress the fire as quickly as possible, while keeping themselves and other occupants as safe as possible during the initial stage of fighting the fire.

In the following chapter, general literature on compartment fire development is first reviewed along with experimentally determined times required for a fire to grow to fully developed conditions. Typical test methods and equipment used in room fire experiments are also outlined. Following that, the literature on fire suppression is discussed with particular emphasis on manual suppression of compartment fires as well as initial attack methods used in manual fire suppression for municipal firefighting operations. The final section of the chapter discusses the research objective, improving manual fire suppression effectiveness and firefighter safety, and the methods by which the objective was satisfied.

Chapter 2

LITERATURE REVIEW

2.1 Compartment Fire Development

A fire starts when the proper mixture of air, fuel, and an ignition source of sufficient energy come into contact. After ignition, the fire will grow as it consumes more fuel in the compartment. In this initial stage, the fire is fuel controlled, and will grow unhampered as long as there is available fuel [7, 8]. If at any time there is not enough fuel to sustain combustion, the fire may die out at this stage [6]. It may also be possible for the fire to die out or continue to burn at a very slow rate if there is insufficient oxygen (air) supplied into the room at this time [6].

On the other hand, the fire will continue to grow in the compartment as long as there is sufficient fuel to feed the fire and adequate ventilation into the compartment that sufficient oxygen is being entrained into the fire to sustain the combustion [6]. As the fire grows, it will generate a hot layer in the compartment because the heated air and products of combustion rise towards the ceiling due to buoyancy [7]. Therefore, as a fire burns in a room, it entrains cool air into the base of the fire, and transports heated air and products of combustion into the upper part of the room [7]. In situations where there is little mixing between the two layers (no forced convection into or out of the room), a discernable boundary will be created between the upper (hot), and lower (cool) layers. This boundary is known as the layer interface [7], and may be measured in terms of its height above the floor, or interface height. Subsequent to the formation of an interface, that interface will remain intact as long as there is sufficient fuel and oxygen to keep the fire burning, and the ventilation is such that the hot layer is not escaping the room faster (or slower) than hot gases are being fed to it from the fire plume.

The heated gases in the upper layer increase the amount of heat transferred to the unburnt fuel in the compartment, increasing the rate of combustion [9]. As the depth and temperature build, the radiant heat from the upper layer can ignite all of the available fuel in the room, creating a fully developed fire [6]. In large fully developed fires, average upper layer temperatures are typically 500 to 600°C, with peaks up to 800°C [10–13].

A study conducted by Babrauskas, et. al. combined data from a number of tests on the time to flashover, or to when fully developed conditions would exist in a room fire. The time to flashover was determined for rooms containing materials ranging from polystyrene and polyurethane foams, to plywood and other wall lining materials, to fully furnished and lined rooms [14]. In all of the tests, 33 in total, the same room size, 2.4 m by 3.6 m by 2.4 m high, was used. In the 33 tests collated, the average time to flashover was 3.5 minutes, with a 3.5 minute standard deviation, with flashover occurring more than 11 minutes after the fire started in only one of the tests. The results of these tests confirm that, even if the fire department responds to a fire in less than the recommended time, fully developed fire conditions may very well exist in a room before they arrive.

2.1.1 Measurement Techniques in Compartment Fires

As mentioned, all of the compartment fire tests used in the determination of flashover times were conducted in a 2.4 m by 3.6 m by 2.4 m room [14], which is the same size as the room used for the ISO 9705 room fire tests [15]. The ISO 9705 test room has also been used in tests not specifically looking at flashover or wall lining materials [16]. In these tests, temperatures in the compartment are determined using Type-K thermocouples, which have properties well suited for temperature measurements in fire compartments [13, 16, 17]. For ease of implementation, rakes have been used containing a number of thermocouples wired to a chain or other member, which can be installed in the compartment so the temperature can be measured at multiple points along a vertical line [16].

Along with temperature, heat flux has also been measured to investigate properties of fires in compartments using Schmidt-Boelter or similar types of heat flux gauges [16, 17]. Gas species and concentration data has been collected in upper layers of compartment fires using copper tube probes [13]. The concentrations of the gases, usually oxygen, carbon dioxide, and carbon monoxide, are determined using paramagnetic and infrared gas sensors once the moisture and particulates are removed from the gas stream [13, 16]. The measured gas concentrations can be used to determine the heat release rate of the fire using the methods of oxygen consumption calorimetry [16–19].

2.2 Compartment Fire Suppression

Effective compartment fire suppression involves applying the correct amount of water to the proper location in a compartment in an attempt to control or extinguish a fire [20]. There are two broad categories of fire suppression distinguished by their mode of operation: automatic fire suppression and manual fire suppression. While many methods of automatic fire suppression are available, those that use water as a suppression agent most often employ sprinklers as the water distribution system. In an automatic fire suppression system, a sprinkler is pre-installed and plumbed into the building, and serves to both detect the fire and suppress it by spraying water into the area in reach of the sprinkler [21].

Research in the area of sprinkler suppression has considered suppression of both liquid and solid fuel fires in open areas and enclosures [22–25]. In the majority of automatic suppression research, water is used as the suppression agent because it is both readily available and easy to work with and apply [22]. In these experiments, it was determined that the direction of spray and sprinkler orientation, as well as the size of the suppression drops, are the important factors impacting the effectiveness of the sprinklers.

A number of studies have looked at the size of drops released, and the effect the droplet size has on sprinkler suppression effectiveness [26–29]. Research has suggested that the larger drops, on the order of 5 mm, are more effective at penetrating the fire plume, while smaller drops, on the order of 0.5 mm, cool the compartment environment more effectively [28]. This suggests a dual mode sprinkler that can produce both large and small drops may be effective at both cooling the compartment and suppressing the fire [28].

The effectiveness of automatic sprinklers that deploy water as a mist have also been studied. Full-scale tests of water mist suppression systems suggest that for small spaces, water mist may be more effective, as the mist is more apt to vapourize quickly and displace oxygen from the room aiding in suppression of the fire [30]. In all of the automatic suppression research, whether it be water mist or otherwise, researchers agree that minimizing the amount of water used while still achieving an acceptable level of suppression is the best way to keep damage to a minimum [28, 31].

For many years, researchers have been developing methods to determine the smallest amount of water required to suppress a compartment fire. One of the first methods was based on calculating the quantity of water needed to absorb all of the heat produced by the fire, and to displace the oxygen in the compartment(s) [32]. Other empirical and theoretical based methods, as well as computer simulations, have subsequently been developed [33–37]. These newer models consider a number of factors not included in the original model, such as building construction and occupancy, and the approach of the firefighters [34, 35]. Other models have also been proposed which approach the issue from a more theoretical standpoint, or use computer simulations to develop equations for the required amount of water [33, 37]. One consistency in all of this research is that total fire extinguishment is always considered.

2.2.1 Manual Fire Suppression

Unlike automatic suppression, manual fire suppression (or firefighting) relies on a human operator to deliver the suppression agent (water) via a hoseline and nozzle apparatus. A distinct advantage of manual suppression is the ability of the firefighter to choose from a number of different attack methods, depending on the situation. The equipment available for firefighting today supports a number of different choices of attack method.

Currently, the most commonly used handheld nozzle in the fire service to combat single compartment fires is a 38 mm (1 ½ inch) combination nozzle [38]. Typically, these hand held nozzles can deliver water at multiple flow volumes and spray settings simply by adjusting the nozzle [39], making them very practical for switching between different attack methods. When possible, the nozzle is attached via a 38 mm (1 ½ inch) hoseline to a pumper truck where the pump discharge pressure can be controlled, however, other water sources may also be used.

With the use of combination firefighting nozzles, different fire suppression tactics and spray patterns can be employed by a single firefighter. The three most common tactics or 'methods of attack' are the direct attack method, the indirect attack method, and the combination attack method. During a working fire, the attack method is chosen by a firefighter based on field factors such as visibility in the fire compartment, anticipated stage of fire development, and standard operating protocols of a given fire department. However, due to non-uniformity of fuel loads, compartment geometry in real fires, and the complex nature of fire itself, effective manual fire suppression can be more difficult than anticipated.

2.2.1.1 Methods of Attack

The direct attack method involves applying water directly towards the materials that are on fire in the compartment [32]. This method is usually employed when the compartment fire is still in its early stages of growth [32]. In this early stage, the average temperature of the gases (air and products of combustion) in the compartment is quite low, and the fire is still burning in the area of its origin [6]. With a limited amount of hot gas build-up in the compartment, visibility is good, and the burning fuel can be located and hit with a water stream to directly extinguish the fire.

The advantage of the direct attack method is that water is being put on the fire and fuel sources as soon as the attack begins. When the fire is in the initial stages and combustion is only controlled by the availability of the fuel, the direct attack method is a logical one to use. Applying water directly to the fuel not only suppresses the fire directly, but also cools the environment and hampers fire growth, as unburnt fuel will not ignite as easily once doused with water. If the fire is in a more advanced stage and fire growth is not necessarily controlled by the fuel of the source fire alone, then the direct attack may not be the best method, as it essentially ignores the hot layer that may be building, which can also contribute to fire spread [9].

When the fire is past the initial stages and it is the desire of the firefighters to attack and cool the built-up hot layer, then the indirect method of attack may be used. The indirect method of attack involves applying water to the heated atmosphere, but striking as little of the fuel or heated compartment walls as possible [32]. The purpose of the indirect method is to quickly cool the heated gases in the compartment [32]. Once the gases are cooled, the heated walls and ceiling will radiate heat to the cool gases and water in the upper layer, creating steam [32]. The purpose of the steam is to smother the fire by displacing oxygen in areas where a direct attack approach may not

be possible. Not directly cooling the heated compartment walls or ceiling sustains the production of steam for a longer time, making it easier to smother the fire. As the steam is produced only in the upper layer and not on the walls, it is also easier to direct the steam movement using the water spray, keeping it away from the firefighter. The downside of the indirect attack method is that water does not reach the fire and compartment walls, so only the smothering effect acts to extinguish the fire. If the steam is not able to complete this action, then a more direct approach may be necessary.

If a fire in a compartment is past the initial stages of growth, and it is decided that both the direct and indirect methods of attack may not be appropriate methods of suppression, then the combination method may be employed. The combination method involves applying water into the heated atmosphere, taking care to strike the heated compartment walls with the suppression water spray [32]. The purpose of this method is to both cool the upper layer of the compartment by spraying water into the area, and also to cool the surfaces in the fire, the available fuel, and to put water on the fire itself. If the combination method can be employed successfully, then both the upper layer gases and the burning fuel will be affected at the same time. It may not be possible to employ the combination method in a compartment, however, if the fire cannot be attacked via deflection of the nozzle spray off the upper layer surfaces. If this is the case, the smothering action of the indirect method may be more suited for fire suppression. Care must also be taken when using the combination method to ensure firefighter safety, as spraying all the heated surfaces in the compartment may create an abundance of steam that cannot be as easily controlled as with the indirect method, potentially leading to steam being directed back at the firefighter.

2.2.1.2 Nozzle Settings and Pressure

As well as the fundamental choice of direct, indirect, or combination methods of fire attack, there are many possible variations of each, depending on the nozzle settings used to deliver the water into the compartment. Basic nozzle parameters that can be set when using the current style of combination nozzle are the flow rate through the nozzle and the spray distribution. The flow rate through the nozzle is dependent on the nozzle flow rate selected (dial on the nozzle itself), as well as the pressure delivered to the nozzle. As mentioned above, water is typically delivered to the nozzle via a hoseline connected to a pumper truck.

The pressure of the water exiting the pumper truck is measured and displayed in the truck, but due to losses in the hoseline and other appliances (connectors), as well as elevation changes between the pump and nozzle discharge locations, the pressure of the water exiting the nozzle will be reduced. The pressure loss due to a change in elevation is easily calculated by adjusting the pump discharge pressure by ±10 kPa for each meter of elevation change [40]. The value of 10 is used because water exerts a pressure of approximately 10 kPa per meter of elevation [40]. If the nozzle is positioned at an elevation below the pump discharge, then the elevation pressure

calculated is added to the pump discharge pressure to obtain the nozzle pressure, and the calculated pressure is subtracted if the nozzle discharge is above the pump discharge (more pump pressure is needed to increase the elevation of the water).

The pressure loss due to friction in the hoseline is determined using the following equation [40]:

$$F_L = CQ^2L \tag{2.1}$$

where F_L is the pressure loss due to friction [kPa],
C is a hose loss coefficient,
Q is the flow rate in hundreds of liters through the hose (flow/100) [ℓ], and
L is the hose length in hundreds of meters (length/100) [m].

For new 38 mm diameter hoses, a value of 38 can be used for the loss coefficient (C) [40]. The pressure determined from the above formula for the frictional losses is always subtracted from pump discharge pressure to get the nozzle discharge pressure.

Any other appliances that are in line with the pump and nozzle may also create a pressure loss if the flow through the appliance is large enough. As a rule for fireline appliances, if the flow is less than 1400 ℓ/min, the appliances will not have a marked effect on the nozzle discharge pressure. All of the above calculations for pressure loss are carried out on scene in order to set the desired nozzle discharge pressure and water flow rate through the nozzle.

The nozzle spray distribution is adjusted at the nozzle. Spray patterns range from a straight stream of water, which has a negligible expansion of the spray, to a wide angle fog pattern, which can have an expansion angle upwards of 120°, with any available angle in-between. The advantage of the straight stream or smaller expansion angles is that the water spray will carry further, which can be useful for direct or combination attack methods. The water spray from the larger expansion angles does not carry as far, but smaller drops are created similar to a mist, which may be more appropriate for an indirect method of attack.

2.2.1.3 Initial Attack Methods

In practice, during any compartment fire where hot gases are accumulating, multiple methods of attack may be employed with the nozzle adjusted to deliver one or more water spray distributions. The indirect and combination methods are used in an attempt to control the fire environment, with the intent to make it easier for the firefighter to find the seat of the fire and use a direct attack method. As such, the indirect and combination method are often used as initial attack methods in a compartment where an appreciable hot upper layer has developed. There is debate, however, as to which initial attack method is the most appropriate when attacking particular types of compartment fires. Often, the method selected is not necessarily the best for

the given fire scenario, but rather the one used successfully by that fire department in the past [38]. As total fire extinguishment is studied in all of the research on automatic suppression, the effectiveness of the suppression as an initial attack method at controlling the fire and tenability of the compartment environment is not examined. To address all of these concerns, more scientific studies are needed into the physical interactions of the suppression water spray, compartment environment, firefighter, and firefighting operations during the initial attack of compartment fires.

During fire fighting operations, a wide range of initial attack methods can be deployed, depending on the compartment conditions and fire department practices. Initial fire attack can be accomplished using straight stream, narrow fog, or wide angle fog settings. During these applications, water can be applied continuously for the duration of the initial attack. Penciling tactics and a range of different burst methods such as those discussed by Grimwood can also be used as initial fire attack methods [38, 41].

The burst initial attack method discussed by Grimwood is an indirect method that involves applying short water burst into the upper layer of a fire compartment [41]. In this method, several short bursts of water, each around 0.5 seconds in duration, are applied into the heated upper layer of a compartment fire using a firefighting nozzle set to the wide angle fog position. The purpose of the bursts of fog is to introduce a small quantity of small water droplets (as small as the nozzle is capable of) as a spray into the heated upper layer. This fine spray should evaporate quickly and effectively cool the upper layer while producing as little steam as possible, since only small quantities of water are deployed during each burst.

The penciling initial attack method is a combination method that delivers water into the compartment using the straight stream nozzle setting [38]. For this method, water is applied in medium length bursts into the compartment. The burst duration is longer than that for the short burst method, usually around 2 seconds, with a 2 second break in between [38].

Some research has been conducted on the impact of different initial suppression attack methods on the compartment environment. In studies conducted at Lund University in Sweden, fires established in two different steel compartments were manually suppressed by firefighters using hoselines and nozzles fed at two different water supply pressures [42]. Suppression was continued until the fire was completely extinguished, with the nozzle position being advanced during some of the tests [43]. Results indicated that nozzle sprays fed at higher water pressures reduced the compartment temperature more quickly than lower pressure sprays, but that the overall compartment temperature did not always decrease to a lower value when higher pressure water sprays were used [43]. Similar high and low pressure tests were also conducted in a larger room, again with total fire extinguishment used as the end of test criteria [44]. The second set of experiments were aimed more at the impact of the suppression work on the firefighter in terms of body and skin temp, heart rate, etc., and did not focus on the compartment temperature. One important outcome of these experiments for the present research was that it was difficult for the

researchers to draw conclusions about the different suppression methods because of the number of variables involved, including different spray patterns, variability in firefighter movement and methods, and pressure variations between tests [43].

Experiments which focused on extinguishing wood crib fires using manual suppression techniques while varying the nozzle pressure were also conducted by Scheffey and Williams [45]. These experiments involved manual suppression of wood crib fires in an open environment (no enclosure) using an operator who was allowed to move freely around the crib to suppress the fire as they saw fit. From these experiments, it was determined that the nozzle discharge pressure did not greatly affect the time it took to suppress the fire. However, this set of experiments was conducted on fires in an open area and considered only total extinguishment of the burning fuel. A follow-up study was conducted where the same wood cribs were tested in a multi-level shipboard compartment using two different methods of attack, one direct - water applied directly at the fire, and one indirect - water aimed in the upper layer in order to produce steam and smother the fire [46]. The main focus of these experiments was to study the response time of the firefighting personnel, the benefit to those personnel of wearing personal protective gear, and the amount of water required to suppress internal fires as compared to that used in the open crib fire tests. It was noted that the short water burst tactic, where a short fog suppression burst was applied, the firefighter stayed low and advanced on the fire, and another burst was applied, was a worthwhile tactic when the fire was large. This suggests that as an initial attack method, short bursts of water into the fire compartment may be an appropriate tactic.

Grimwood also looked at the effectiveness of the burst method as applied in the upper layer in a compartment fire. Through experiment, it was found that the burst method produced less steam than comparable suppression activities conducted using a continuous wide angle fog approach. In the experiment, however, no temperatures were measured in the compartment, so the effective cooling of the upper layer of the compartment could not be scientifically analyzed [47].

Based on the above literature review, research in the area of fire suppression is not in its infancy, as studies on water requirements for suppression date back to the late '50s [32], and even before. In order to consider different scenarios, a number of updated empirical and computer models for fire suppression have been created. All of the research on both automatic and manual fire suppression by water, however, as well as the research on water requirements for firefighting, look at total extinguishment of the fire, using one or all methods of attack (as applicable). Further, this research does not consider the impacts that suppression activities have on the firefighter who deploys the different methods of initial fire attack. As such, there is a paucity of scientific research conducted on the impact of the different initial attack methods, whether an indirect or combination method, on the firefighter, or on controlling the fire environment. This is the area in which the present research will make one of its main contributions.

2.3 Objectives

The objective of this research project is to examine different manual suppression initial attack techniques in order to begin scientific assessment of, and drive appropriate improvements of firefighting tactics and firefighter safety. This objective will be completed by:

- Setting up and instrumenting an appropriate single fire compartment experiment with a fuel loading and ventilation parameters that produce a consistent and repeatable fire which maintains upper layer conditions similar to those observed in fully developed fires.
    - Average upper layer temperatures of 900 K desired for this research.
- Developing a method and apparatus that will allow different hoseline and nozzle based manual suppression methods to be delivered in a repeatable manner into the compartment fire.
- Characterizing different initial attack methods to determine:
    - How different methods cool the environment in the compartment during the developed conditions.
    - The effect of each method on the firefighter or occupants in the vicinity of the firefighter as each is applied to the fire compartment.

In the remaining chapters of this thesis, the experimental set-up, measurement techniques, and experimental procedure used are first described, followed by results from preliminary experiments that were used to determine fuel load and fire properties, and to characterize the suppression equipment. Temperature, heat flux, and carbon dioxide concentration data collected in the fire compartment and at locations around the simulated firefighter before and after suppression is presented in order to compare the different suppression methods. From all of the results, indications of appropriate initial attack suppression methods that could be deployed in this compartment fire are outlined. Conclusions are then drawn about both the experiment and suppression attack methods, and recommendations for continuing research are presented.

Chapter 3

EXPERIMENTAL APPARATUS AND TECHNIQUE

In order to examine the effects of the different initial attack suppression methods in a fully-developed compartment fire situation, hot layer temperatures similar to those that would occur in room fires (approximately 900 K) are created in the compartment using wood cribs as fuel. Five different suppression methods commonly used by the fire service as initial attack approaches are studied. Suppression water application times are held to a maximum of 5 seconds. Suppression methods include straight stream for 5 seconds, penciling (two applications each lasting 2 seconds with a 2 second break in between), narrow fog for 5 seconds, wide angle fog for 5 seconds, and a wide angle burst method (two bursts lasting around 1 second with a 2 second break in between). In all cases, suppression water is delivered via a standard hoseline and nozzle combination typical of those used by municipal fire departments in Canada. Along with changing the suppression tactic, the spray angle and nozzle pressure are varied to more fully understand interactions between the various suppression methods, the firefighter, and the compartment environment. Details of the experimental configuration and methods are discussed below.

3.1 Compartment

The fire compartment used in the suppression tests measures 2.4 m wide x 3.5 m long x 2.4 m tall, with one door opening (0.91 m wide x 1.75 m high) in the center of one narrow end wall. The bottom of the opening is located 0.05 m above the compartment floor, while the wall above the opening is 0.6 m high. The layout of the fire compartment used is shown schematically in Figure 3.1.

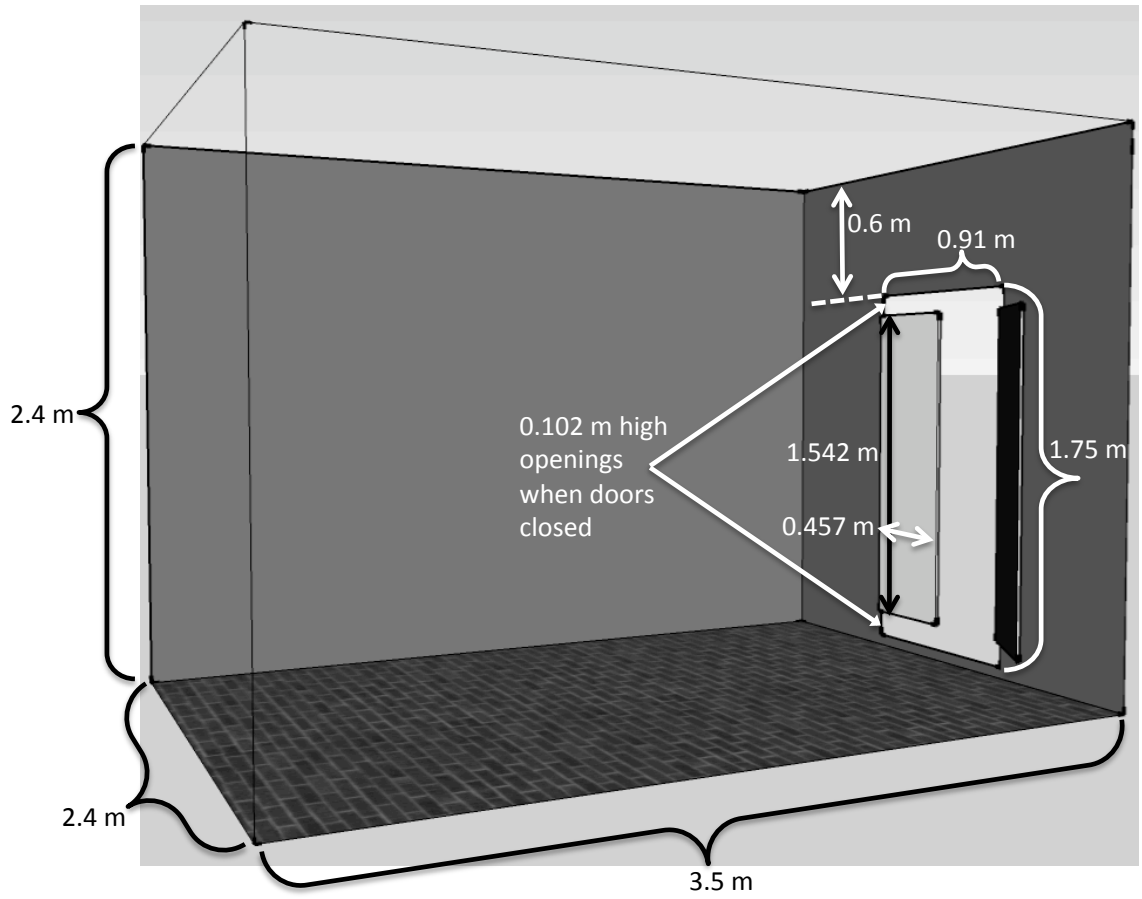

Figure 3.1. Fire compartment.

The interior compartment walls are 2 mm thick Corten steel, except for the bulkhead wall (end wall opposite the door) and a ceiling extension over the fire, which are 9.5 mm thick steel plate. The thicker steel plate has been added to the compartment to increase the wall stiffness in those areas that may experience direct flame impingement. On the outside of the compartment, the walls are insulated with a 25.4 mm thick layer of Fiberfrax Durablanket S high temperature insulation, then a 25.4 mm air gap, and covered with 18-gauge aluminum sheet. The roof is insulated with 50.8 mm of Fiberfrax Durablanket S insulation again covered with sheet aluminum. This results in an approximate thermal conductivity of 0.041 W/mK for the walls and 0.062 W/mK for the roof. In terms of both size and thermal properties, the compartment behaves similarly to an ISO 9705 test room [15].

The floor of the compartment is lined with 57.15 mm thick fireclay brick (152.4 mm x 76.2 mm) over a layer of 25.4 mm thick, 0.61 m square concrete block, resting on a corrugated steel grate. The layers of brick and concrete ensure a negligible amount of heat transfer through the floor, while still allowing any standing water to flow through the floor and out of the compartment.

The compartment door consists of two pieces of 3.175 mm thick steel, each measuring 1.524 m high x 0.457 m wide, hinged to the door frames to meet in the middle, and hung to leave a 0.102 m gap across the top and bottom when the doors are closed. A 12.7 mm thick sheet of Fiberfrax Duraboard LD insulation is affixed to the interior of each door to shield the steel from radiation. A hook is bolted to the outside of each door to facilitate movement of the doors during a fire test. The two doors were shown in the fire compartment schematic in Figure 3.1, and a picture of the actual doors can be seen in Figure 3.2.

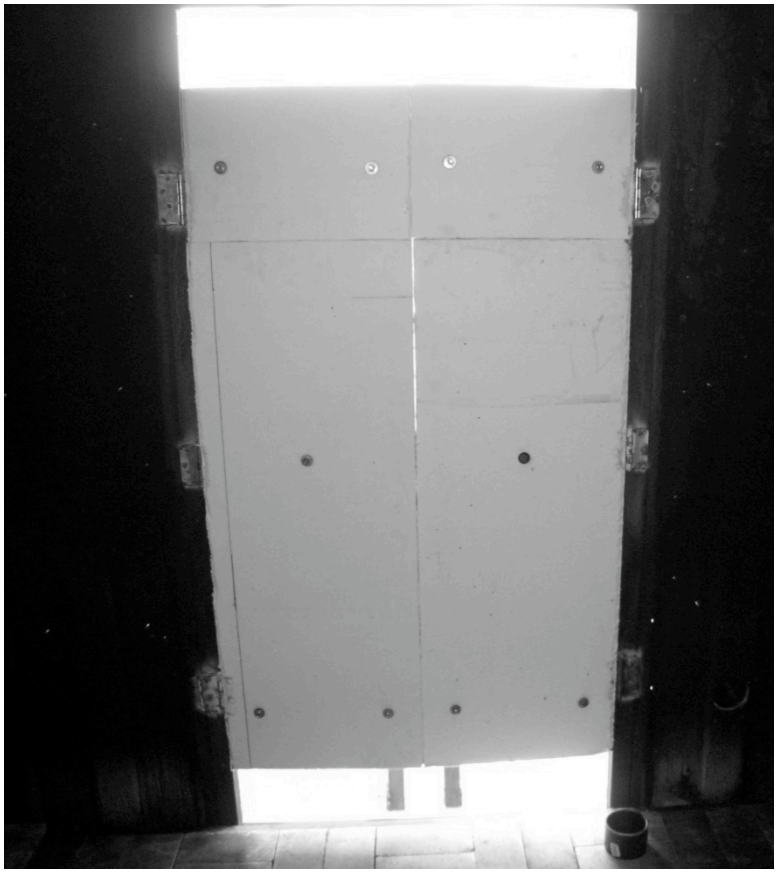

Figure 3.2. Picture showing the inside of the doors in the test compartment.

Double 1.524 m tall doors opening in the middle of the compartment were chosen over a more conventional door for reasons of safety, geometrical symmetry, and ease of use. When the doors are fully closed during a test, hot gases are able to exit the compartment through the upper gap, and cool air can enter under the doors. This ensures the fire will not choke completely, or worse, create the possibility of a dangerous backdraft situation [6]. The central door opening also increases the symmetry of airflow in the compartment in contrast to a conventional door that opens asymmetrically to one side. Any asymmetry in the airflow would cause the temperatures on

each side of the compartment to vary, making data analysis more complex. Lastly, the two doors are easier to open during each test because they do not swing as far into the compartment as a single door. Not only does this makes each door lighter, but it also makes it possible to locate instrumentation closer to the door opening, at half the distance than would otherwise be possible.

3.2 Instrumentation

Compartment and external air temperatures are measured using inconel-sheathed, ceramic wrapped Type-K (chromel-alumel) thermocouples. A thermocouple consists of two dissimilar metals that are joined together in a bead, located at the measurement point. When heated, a voltage is produced at the point of interest, and measured by the data acquisition system. Knowing the two metals that are used in the thermocouple, chromel and alumel in the case of Type-K thermocouples, makes it possible to correlate the voltage measured with the temperature increase [48]. The beads for all of the Type-K thermocouples used in this experiment for gas temperature measurement are approximately 1 mm in diameter.

Ten thermocouple rakes, each containing eight thermocouples, measure hot gas temperatures inside the compartment. Six vertical rakes are located 0.30 m from the side walls, with three rakes on each side of the compartment, positioned in planes 0.55, 1.70, and 3.10 m from the opening. The eight thermocouples on each rake are located at heights of 0.00, 0.50, 0.80, 1.10, 1.40, 1.70, 2.00, and 2.30 m off the floor. This arrangement leaves a 1.8 m wide unobstructed region to facilitate free gas and water movement through the center of the compartment.

Three horizontal rakes are positioned 2.15 m above the floor, in the same planes as the vertical rakes, i.e. at 0.55, 1.70, and 3.10 m from the opening. Thermocouples are located laterally at 0.15, 0.45, 0.75, and 1.05 m from the centerline in both directions. A final horizontal rake runs the length of the centerline of the compartment, 2.05 m off the floor, from the bulkhead to the door. Thermocouples on this rake are located at distances of 0.30, 0.95, 1.30, 2.00, 2.30, 2.60, 2.90, 3.30 m from the opening. The compartment schematic with the six vertical rakes and four horizontal rakes can be seen in Figure 3.3, along with a picture showing the mounting of the thermocouples in Figure 3.4.

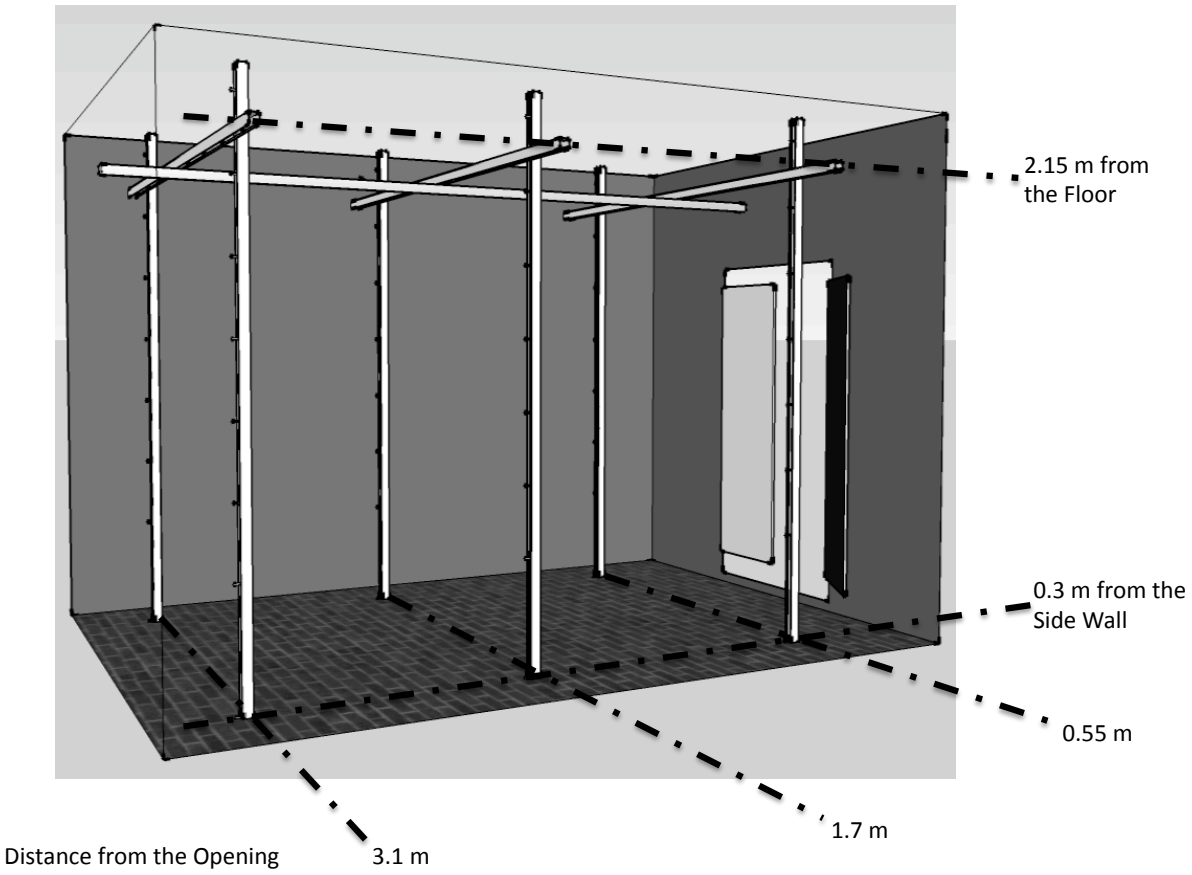

Figure 3.3. Compartment schematic with the thermocouple rakes included.

Surface temperatures are measured on the bulkhead, side walls, and ceiling of the compartment. Steel surface temperatures are obtained by welding the two individual Type-K thermocouple wires directly to the steel, spaced roughly 2 mm apart [49]. For aluminum surface temperature measurements, the Type-K thermocouple beads are taped directly to the aluminum sheet using high temperature aluminum tape. Bulkhead temperatures are measured at locations 0.10 m from the centerline and heights of 0.80, 1.40, 1.80, 2.00, and 2.20 m above the floor. Side wall temperatures are measured at positions 0.50, 1.10, 1.70, and 2.30 m above the floor at a distance of 1.70 m from the opening. Ceiling surface temperatures are measured on the centerline at distances of 2.90 and 3.30 m from the bulkhead.

The data from all thermocouple sensors (gas and surface) is acquired and stored using custom Labview programs via National Instruments cFP-2000 data loggers. In the experiment, 142 instruments were connected to the data loggers, with data recorded every 1.125 s (0.8 Hz).

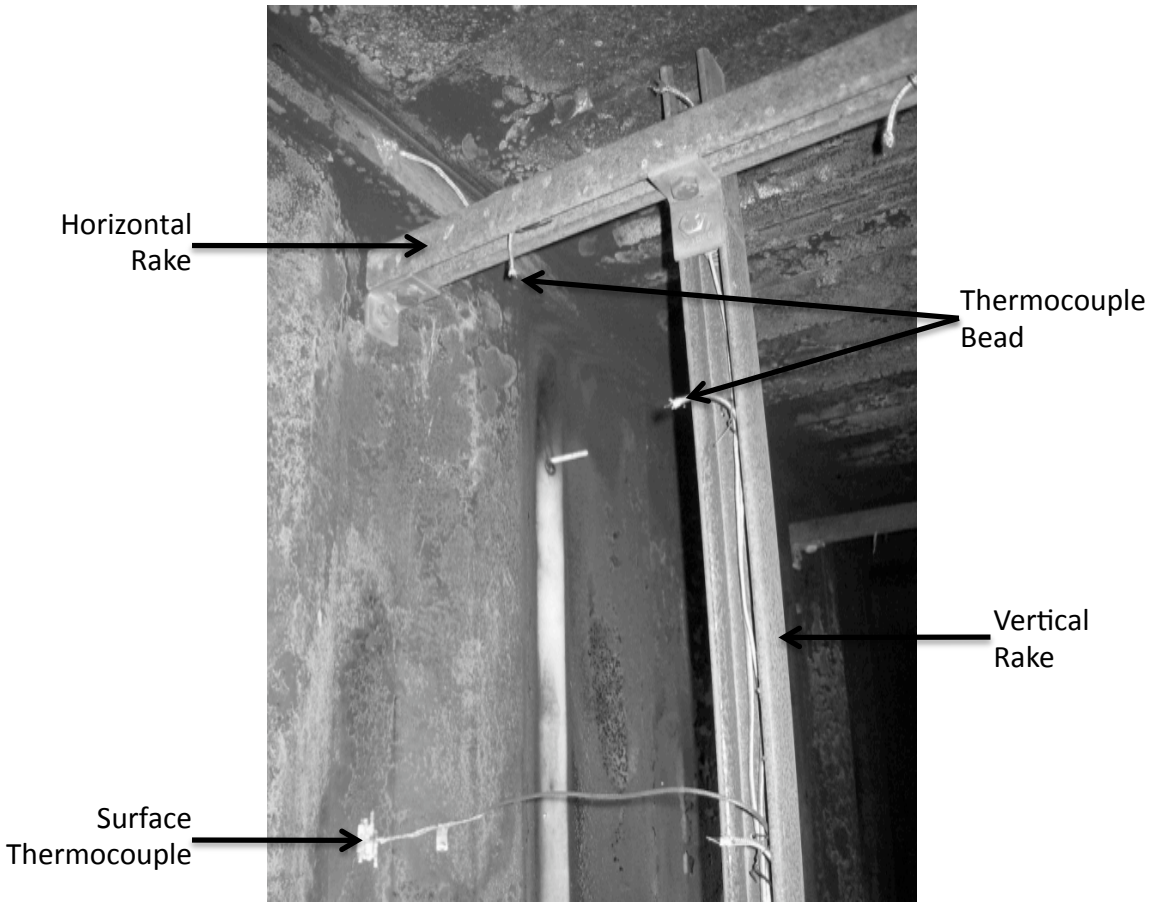

Figure 3.4. Picture showing the thermocouples mounted in the rakes and to the wall.

Three Gardon gauges, manufactured by Vatell Corporation, monitor heat flux in the compartment. Heat flux refers to the amount of heat transfer occurring to or from a surface per unit area, and includes contributions mainly from radiation, but also from convection and conduction [50]. Each gauge consists of a 4.7 mm diameter sensor on a 25.4 mm diameter face. The sensor itself is a thin circular constantan foil disk that is 0.013 mm thick with an emissivity of 0.95, and is centrally located on the sensor face [51]. Cooling water is supplied to the gauges via the domestic water supply which flows into the water-cooled cylindrical copper heat sink at a temperature of around 10°C [52]. The gauge body is then insulated during installation in the compartment. This keeps the gauge body at a constant temperature throughout each experiment. The temperature difference between the center and edge of the foil sensing element is measured using thermocouples, and the current output is related to the incident heat flux on the sensor using the manufacture supplied calibration constant, which has a ±3% accuracy [53]. Calibration of the Gardon gauges is conducted by the manufacturer, and rechecked before installation into the compartment using a known heat flux from a cone calorimeter. The values of the calibration

constant used to determine the heat flux [kW/m^2] from the measured voltage for each of the three heat flux gauges used in the experiment can be seen in Table 3.1.

Table 3.1. Heat flux gauge calibration data.

Gauge Location	Calibration Constant [kW/m^2•mV]
Wall	23810
Floor	10350
Door	10210

One heat flux gauge is mounted on the side wall of the compartment, 2.0 m from the opening and 0.85 m off the floor, oriented perpendicular to the floor and aimed at the center of the fire. The other two are mounted in the floor bricks, with the sensor surface flush with the top surface of the floor, one at a distance of 0.7 m from the side wall and 0.5 m from the opening, the other 0.5 m from the side wall and 2.4 m from the opening. The installation of the floor mounted heat flux gauges (with the protective cap on) can be seen in Figure 3.5 and Figure 3.6.

Figure 3.5. Uncovered floor mount heat flux gauge.

Figure 3.6. Covered floor mount heat flux gauge.

Along with the thermocouples and heat flux sensors placed inside the compartment, a number of sensors are placed external to the compartment to measure flow through the compartment door, as well as gas concentration, heat transfer, and other impacts of each suppression method at the position where a firefighter would be located in a real fire scenario.

A vertical rake consisting of eight bi-directional probes [54] is positioned along one side of the door opening to track the general movement and velocity of gases into and out of the compartment. Each bi-directional probe consists of a 19 mm internal diameter stainless steel cylinder measuring 38 mm long, open on both ends with a partition in the middle. Taps are drilled on each side of the partition [54], and a 2 mm internal diameter stainless steel line runs from each side of the partition to the positive and negative sides of a differential pressure transducer. When the axis of the probe is aligned with the flow, one side of the probe measures stagnation pressure, and the other measures static pressure [54]. The differential pressure transducer measures the difference between the two pressures acting on the attached probe.

The bi-directional probe is mounted in the apparatus so that the centerline of the cylinder is aligned with the flow. As the probes themselves behave as a bluff body, the wake regions they create cause the measured static pressure to be lower than the actual static pressure [55]. Through experiment, it has been found that the relationship between the measured and actual values of the dynamic pressure, which is determined by subtracting the static pressure from the stagnation pressure, is linear, and an average calibration constant of 1.08 can be used for these types of probes [54, 55].

The Setra model 267 differential pressure transducers were calibrated by the manufacturer, and included a calibration certificate. Each of the transducers were calibrated using eleven points over the full measurement range (±25 Pa), based on a dead weight tester [55]. The calibration equation used to determine the pressure from the measured voltage (V) for each of the eight transducers used in the experiment can be seen in Table 3.2.

Table 3.2. Calibration equations for the eight pressure transducers.

Transducer	Height above Floor in Experiment [m]	Equation [Pa]
463	0.15	4.9933(V) – 25.178
464	0.25	4.9933(V) – 25.272
467	0.60	5.0006(V) – 25.226
468	0.86	4.9873(V) – 25.216
472	1.01	5.0003(V) – 25.288
471	1.37	4.9992(V) – 25.183
476	1.62	4.9937(V) – 25.277
477	1.73	4.9965(V) – 25.254

The probes are placed with their centers at heights of 0.15, 0.25, 0.60, 0.86, 1.01, 1.37, 1.62, and 1.73 m off of the floor. The stagnation and static pressure taps of each bi-directional probe are connected to the two ports of a differential pressure transducer positioned at the same height as the corresponding probe. Based on the measured pressure difference across the probe, the velocity of the flowing fluid is determined using the 'Pitot Formula' [56]:

$$V \approx \left[2\frac{(p_o - p_s)}{\rho}\right]^{1/2} \tag{3.1}$$

where: V is the fluid velocity [m/s]
p_o is the stagnation pressure [kPa],
p_s is the static pressure [kPa], and
ρ is the density of the gas [kg/m^3].

In order to use Equation 3.1, the pressure transducer should be mounted with the line inlets at as close to the same elevation as the taps on the probe as possible to remove the effects of elevation changes on the fluid pressure [56].

In order to measure the temperature, and therefore gas density, in the vicinity of each bi-directional probe, a thermocouple is positioned directly above each one. Pictures showing one bi-directional probe and attached thermocouple and the full probe rake can be seen in Figure 3.7a and Figure 3.7b, respectively.

Figure 3.7. Bi-directional probe: (a) with attached thermocouple; (b) rake at the opening.

Concentrations of O_2, CO_2, and CO are measured during each test using a Novatech P-695 gas analysis system with Servomex Servopro 4900 infrared (IR) and paramagnetic analyzers. IR sensors are used to measure the concentrations of carbon monoxide and carbon dioxide in the sample, and operate by exciting the sampled gas with an IR laser, and measuring the laser absorption by the gas [57]. The absorption will occur to different degrees and at different wavelengths depending on the type and concentration of the gas. Paramagnetic sensors are used to measure oxygen, and operate by creating a magnetic field around the gas sample [58]. The oxygen in the sample will be drawn into the magnetic field because of its magnetic properties, changing the properties of the magnetic field by an amount proportional to the oxygen concentration in the sample [58].

The gases exiting the compartment are sampled via a probe located in the center of the upper opening. Samples are also taken (though not at the same time) of the gas in the area of the firefighter via a probe located along the compartment centerline at a distance of 0.2 m off the compartment floor.

To monitor overall heat transfer from the compartment to ambient, thirteen surface thermocouples are located on the exterior of the compartment. Five are on the bulkhead opposite those on the fireside, 0.10 m from the centerline at heights of 0.80, 1.40, 1.80, 2.00, and 2.20 m above the floor. Four are on the outside wall opposite the interior wall thermocouples at a distance of 1.7 m from the opening, and 0.50, 1.10, 1.70, and 2.30 m off the floor. Lastly, four additional thermocouples are mounted on the roof, two on the centerline, 2.9 and 3.3 m from the bulkhead, and two 2.9 m from the opening, 0.45 m off the centerline on either side. Pictures of thermocouples located on the external side of the side wall and bulkhead can be seen in Figure 3.8 and Figure 3.9, respectively.

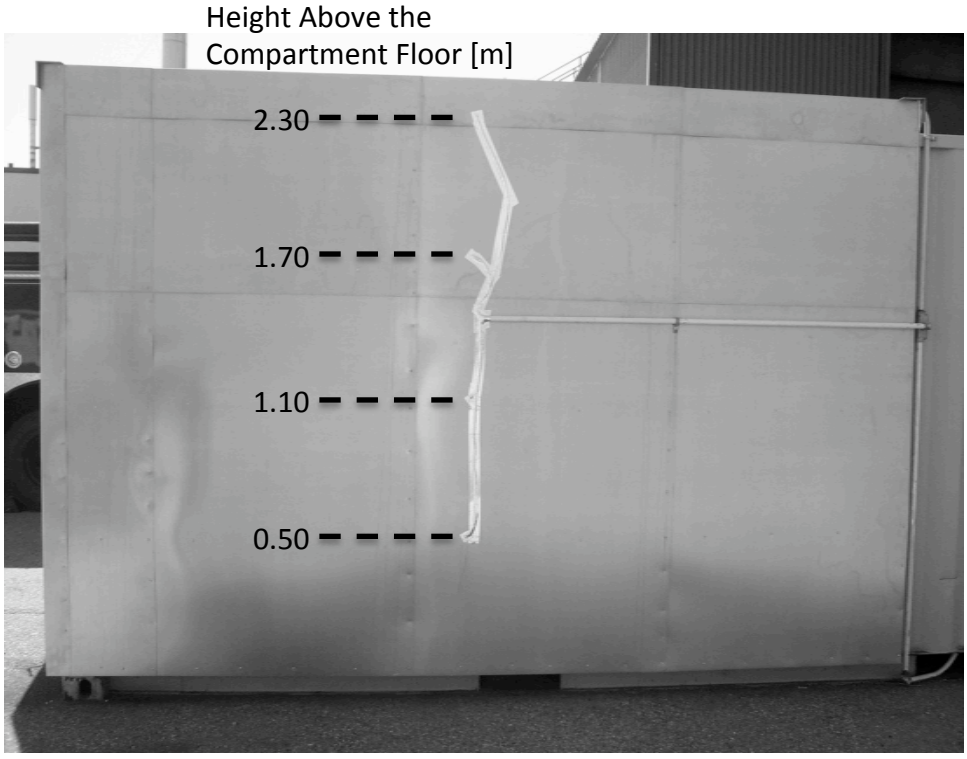

Figure 3.8. Thermocouples on the exterior wall of the compartment.

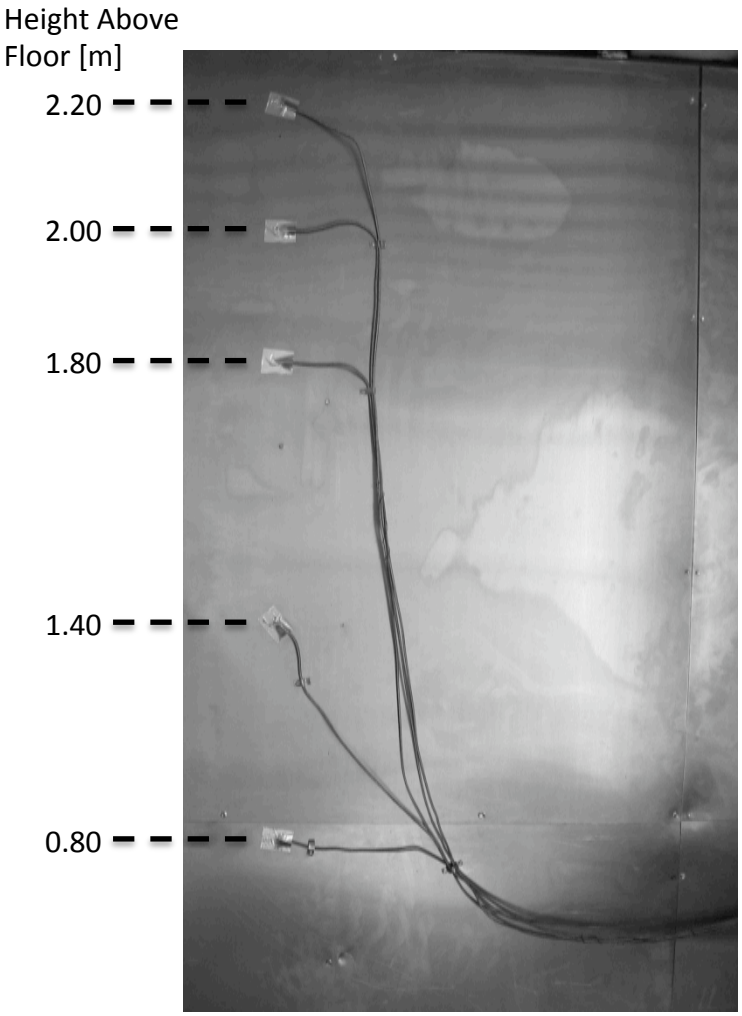

Figure 3.9. Bulkhead thermocouples on the backside of the compartment.

To further monitor interactions between the compartment and ambient environments, a 'firefighter' simulation board was designed and built. It is positioned a distance of 0.55 m outside the compartment opening. For this board, six thermocouples are positioned in the plane, four at 0.2 m from the compartment centerline at heights of 0.30, 0.45, 0.60, and 0.75 m above the floor, and two 0.2 m to the opposite of center at heights of 0.30 and 0.50 m above the floor. Four 'skin simulant' heat flux sensors designed to mimic skin response to fire radiation [59] are located in the same plane and adjacent to the thermocouples, at 0.30 and 0.50 m above the floor on one side, and at 0.50 and 0.75 m off the floor on the other side.

The skin simulant heat flux sensors are comprised of a Type-T (copper-constantan) thermocouple and a Colorceran cylinder measuring 23.0 mm in diameter, and 19.2 mm long. The thermocouple bead is rolled flat to around 0.1 mm thick, and attached to the face of the cylinder

using a high temperature epoxy [59]. The sensor face is then painted with Pyromark 2500 series flat black paint, giving it an emissivity of 0.95 [60].

Colorceran, which is made up of calcium, aluminum, silicate, asbestos fibers, and a binder, is used as the sensor body. As can be seen from the thermal properties listed in Table 3.3, Colorceran has a thermal inertia ($k\rho C$) similar to that of the dermis, which occupies about 96% of the thickness of the skin [58]. This results in the heat transfer through the Colorceran to be similar to that through human skin, making it possible to analyze the effect of the heat flux on human skin [61].

Table 3.3. Thermal properties of the Dermis and Colorceran.

Property	Dermis	Colorceran
k [W/mK]	0.523	0.97
ρ [kg/m^3]	1200	1877
C [J/kgK]	3222	1205
α [J^2/m^{4}K^{2}s]	2.0 x 10^6	2.2 x 10^6
$k\rho C$ [J/m^{2}Ks$^{1/2}$]	1414	1483

The heat flux (q) measured by each skin simulant heat flux sensor is obtained using the following equation:

$$q(t) = \frac{\Delta T}{\frac{2}{\sqrt{k\rho C\pi}}\sqrt{t}} \tag{3.2}$$

where ΔT is the temperature observed by the thermocouple above ambient [K],
$k\rho C$ is the thermal inertia of Colorceran (around 1483 J/m^{2}Ks$^{1/2}$), and
t is the time the heat flux is measured [s].

For this method to be valid, two assumptions must be satisfied over the course of each test. The first is that the sensors must initially be at a uniform temperature [61], and the second is that the unexposed side of the sensor must remain at that uniform temperature over the course of the measurement period [59]. If these are satisfied, then different skin burn analysis methods may be used to determine the damage that the imposed heat flux would inflict on the skin [62, 63].

The average thermal inertial of Colorceran is listed in Table 3.3; however, the sensors can measure more accurate values of the heat flux if the thermal inertia of each sensor is determined

through individual calibration. This is accomplished by subjecting each sensor to a known heat flux. The slope of the line produced by plotting the change in temperature over heat flux by the root of time is equal to $2/(k\rho C\pi)^{1/2}$ [59]. From this, a sensor-based value of thermal inertia is determined.

For this calibration, a cone calorimeter is used to apply a constant heat flux to each sensor. The heat flux from the calorimeter is itself calibrated using a 13 mm diameter Schmidt-Boelter gauge manufactured by Medtherm Corporation. Once the cone is calibrated, each skin simulant sensor is placed at the same distance from the heating element as the calibration gauge, and the temperature change of the sensor with time is recorded. All of the skin simulant sensors were calibrated at a constant heat flux of 15 kW/m^2. The slope of the calibration plots for each sensor as well as the corresponding values of thermal inertia can be seen in Table 3.4.

Table 3.4. Calibration 'slope' for each skin simulant sensor.

Sensor	Location and distance off floor [m]	Slope	$k\rho C$ [$J/m^2Ks^{1/2}$]
SS1	Right, 0.075	0.0291	1503.6
SS2	Right, 0.050	0.0306	1359.8
SS3	Left, 0.050	0.0294	1473.0
SS4	Left, 0.030	0.0314	1291.4

In the firefighter simulation board, six sensors are mounted on the same side of center (two skin simulant sensors and four thermocouples) under a Globe Firefighter Suits GX-7 Jacket, while the four on the other side (two skin simulant sensors and two thermocouples) are uncovered. This allows for examination of the temperatures and heat flux that might be encountered by an unprotected person or object, as well as a fully protected firefighter during each suppression activity. Pictures of the exposed and covered sensors in the area of the firefighter can be seen in Figure 3.10 and Figure 3.11.

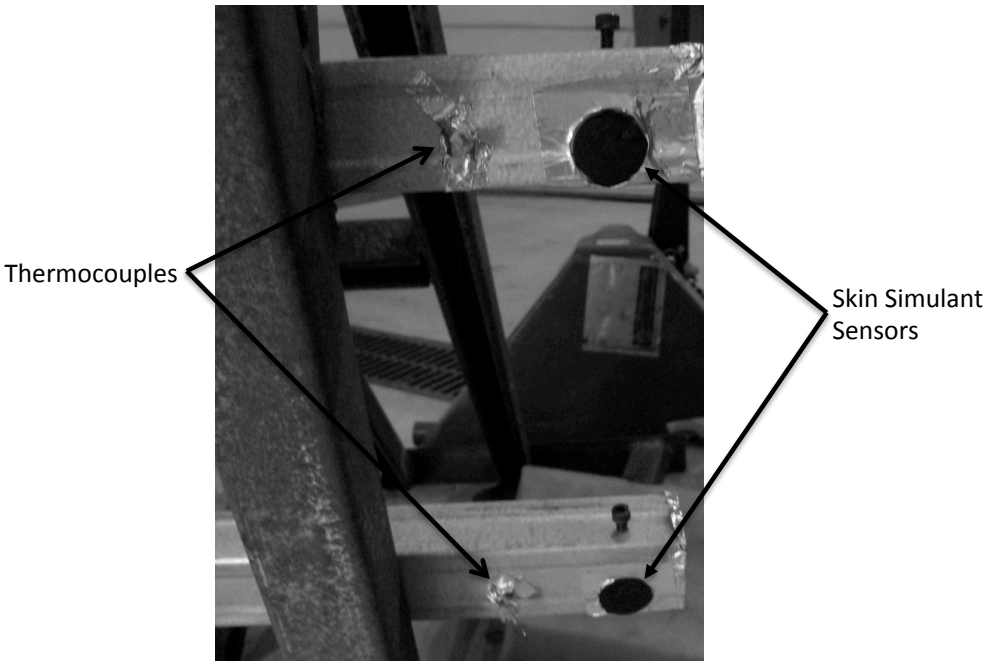

Figure 3.10. Firefighter sensors exposed to ambient.

Figure 3.11. Protected firefighter sensors: (a) covering removed; (b) covering in place.

3.3 Fuel Load

In order to keep the fuel loading and burning conditions in the compartment as similar as possible from test to test, a uniformly constructed wood crib was chosen as the fuel load. The cribs are constructed out of 0.61 m long, 38.1 mm square pieces of softwood lumber. Six pieces are place in each row of the crib, mounted perpendicular to the adjacent rows. Each crib contains six rows, which results in an average crib weight of around 15 kg. A picture showing two wood cribs placed side by side can be seen in Figure 3.12.

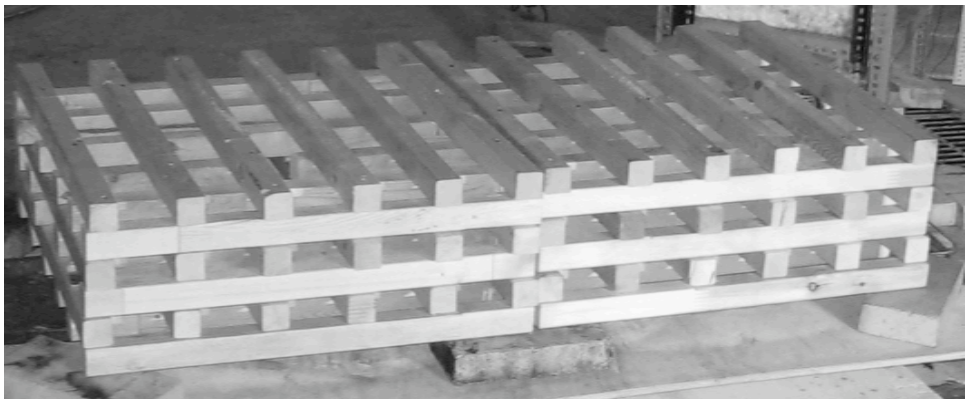

Figure 3.12. Two wood cribs placed side by side.

3.3.1 Free Burn Characteristics of the Wood Cribs

Three different wood crib configurations were tested in a furniture calorimeter in order to determine the free burn heat release rate of each crib configuration. These included one crib, two cribs side by side, and two cribs stacked. Larger crib configurations could not be tested in the calorimeter due to limitations of the apparatus. Free burn conditions were met in the calorimeter since there is no limit of oxygen available to the fire, and the exhaust gases do not collect in the area of the fuel [7].

The heat release rate of each configuration was determined using oxygen consumption calorimetry, in which measured concentrations of oxygen, carbon dioxide, and carbon monoxide during the burn test are used to determine the instantaneous heat release [18]. In the furniture calorimeter, the exhaust gas flow rate was set at 2.0 m^3/s for all three wood crib configurations. The exhaust gases were collected during each test, and CO, CO_2, and O_2 concentrations were measured in real time using a Servomex gas analyzer. Fire Testing Technology (FTT) software used the concentration data, along with the temperature and flow rate of the exhaust gas, to determine the time dependent heat release from each burning crib [64]. A second (independent) Servomex gas analyzer (the same as was used in the suppression experiment) was used to verify the accuracy of the gas concentrations measured using the FTT apparatus and software.

Prior to testing, all of the wood cribs were conditioned for 16 weeks in a fire laboratory room maintained at between 20 and 22°C, and 28 and 35% relative humidity. The furniture-scale oxygen depletion rig is located in the large fire test enclosure where the temperature and relative humidity are not controlled. Ambient temperature and relative humidity in the test enclosure were between 12 and 13°C, and 29 and 40%, respectively, over the course of the crib burns.

Each of the wood cribs was ignited by lighting a pan containing 200 ml of methanol, placed below and roughly in the center of the lowermost cribs. Therefore, one pan was used to ignite the single crib and stacked cribs, and two pans of methanol were used for the configuration composed of two side by side cribs.

3.3.1.1 Total Energy Released

In order to quantify the effects that the moisture content has on the fuel burning conditions, the measured total energy released during each test was determined. The total energy released could then be compared to the theoretical value, considering the heat of combustion of the fuel (14.1 kJ/g for dry wood [65]), and the mass and moisture content of the cribs.

The initial mass of each crib configuration was 14.52 kg, 28.96 kg, and 29.07 kg for the one crib, side by side cribs, and stacked cribs, respectively. The moisture content of the cribs, as determined using an oven drying method, was 7.2%, 6.9%, and 7.4%, respectively. Following the method outlined by Buchanan [66], the reduced heat of combustion due to the moisture content of the fuel for each crib is determined to be 12.98 MJ/kg, 13.03 MJ/kg, and 12.96 MJ/kg, respectively. Multiplying the reduced heat of combustion by the mass of each crib gives a theoretical total energy released by each crib of 188.5 MJ, 377.3 MJ, and 376.7 MJ.

From the calorimetry data collected during the crib burns, the measured total energy released in each test, after subtracting the heat released by the methanol, is 198.6 MJ, 391.1 MJ, and 420.6 MJ, respectively. These observed values are higher than the calculated ones, suggesting that in reality, a larger theoretical heat of combustion should be used to estimate total energy release for the uniformly constructed softwood cribs. The newly determined dry heat of combustion calculated from the analysis is 14.8 MJ/kg, and is used for subsequent wood crib tests when determining the total energy released.

3.3.1.2 Heat Release Rates

The heat release rate (HRR) data obtained using the oxygen consumption calorimetry method can be used to compare the burning characteristics of the crib configurations. In order to more effectively compare the results, the raw HRR data has been modified by removing that portion of the HRR arising from the burning methanol that was used to ignite the cribs, and by adjusting the

time axes on the plots so that the HRR time curves for all cribs were aligned to begin at time zero. The modified plots of the heat release rate for the three cribs tested are shown in Figure 3.13.

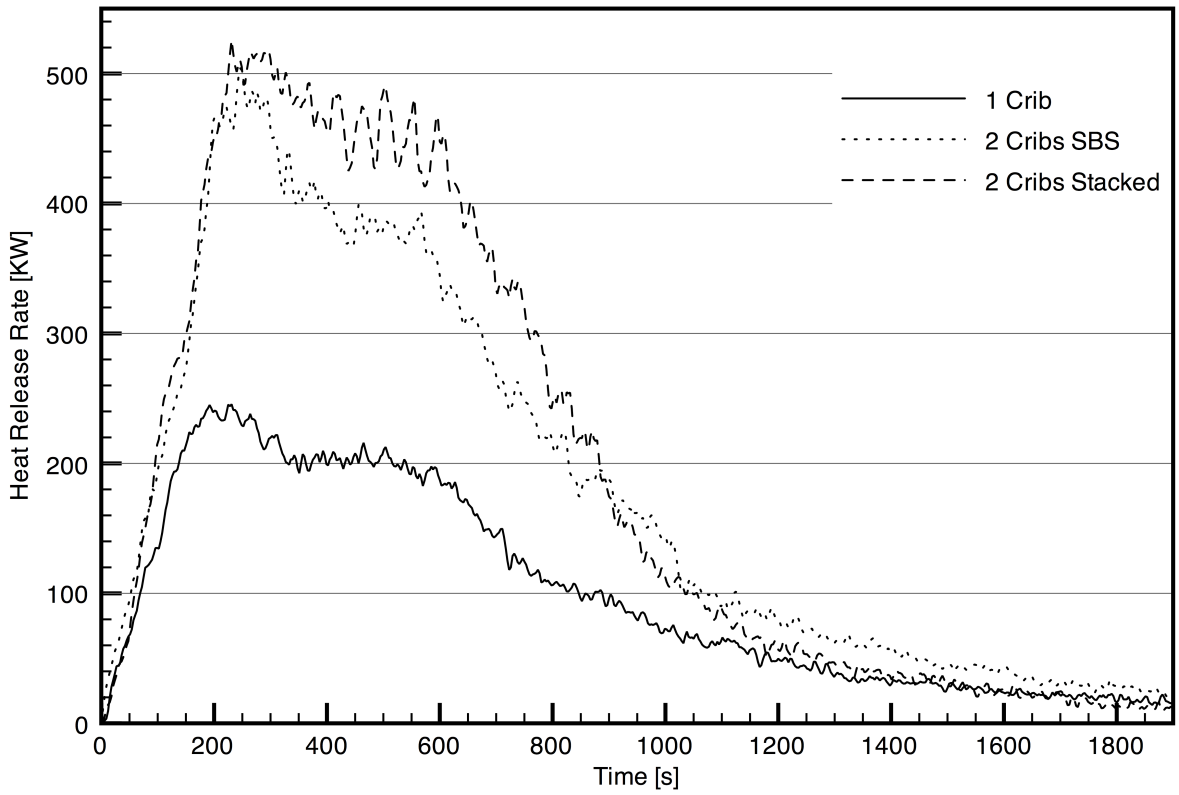

Figure 3.13. Heat release rate curves for the three crib configurations tested.

In Figure 3.13, it can be seen that the growth phase of the crib fires up to the peak HRR is very similar for all three configurations. Since fire growth is a function of the fuel and the configuration, this similarity suggests that the uniform crib construction results in uniform fire growth up to the steady burning phase. The peak and steady burning portions of the curves are also similar amongst the tests, although the decrease in HRR between the peak and steady burning portions for the side by side cribs appears more pronounced than for the other two crib configurations.

The peak heat release rates for the three configurations, as observed in Figure 3.13, are 246 kW for one crib, 504 kW for two cribs side by side, and 526 kW for two cribs stacked. In Figure 3.14, the measured HRR curve for two cribs placed side by side is compared to two times the measured HRR curve for a single crib.

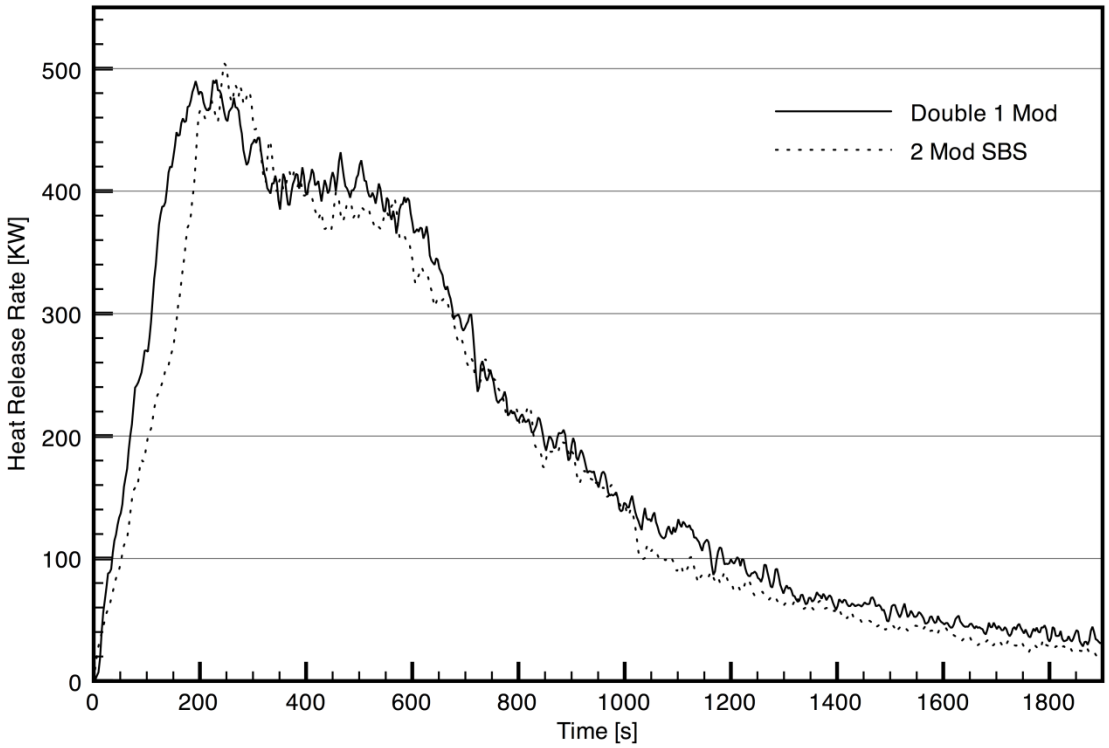

Figure 3.14. Double the heat release rate for one module compared to two modules side by side

The similarity of the two curves demonstrates that a fuel load consisting of 2 cribs stacked side by side can be modeled by doubling the HRR curve measured for a single crib. It appears that the HRR derived from cribs placed side by side is additive, most likely limited only by the free entrainment of air into the centre of the configuration. The difference in shape between the HRR curves for two side by side cribs and two stacked cribs suggests that the same rule does not hold for estimating HRR from stacked cribs; doubling the HRR from one crib under-predicts the HRR measured for two stacked cribs. It appears possible, therefore, to predict the heat release rate curve for a 4 crib configuration consisting of two sets of two stacked cribs (a configuration too large to test in the calorimeter), by doubling the HRR curve produced by the configuration consisting of one set of two stacked cribs. Even though the results for stacked cribs may be under-predicted, it should also be possible to at least estimate the HRR from configurations with more than two stacked cribs following the same method. From the data, it is estimated that the under-prediction would be on the order of less than 10%.

3.3.2 Compartment Loading

A number of trial burns were required to determine a fuel loading which is consistent from test to test, while providing the desired temperature conditions within the compartment. Various configurations of three, four, and six wood cribs were burned, with and without polyurethane foam slabs on top (0.61 m^2 x 0.2 m thick). For combinations of three and four cribs alone the hot

layer temperatures produced are too low (around 750 K peak). The addition of a foam slab to the four crib configuration leads to a more rapid increase in heat release rate (HRR) than that seen for the wood alone; however, the temperatures in the compartment cannot be sustained at high enough values throughout the test period. For the six wood crib configuration tested, fire HRR and compartment temperatures fall within a range representative of fully developed compartment fire behaviour [6], and remain consistent from suppression test to suppression test.

Therefore, the fuel loading for each test is six softwood cribs stacked two side by side and three cribs high. The fuel load is 1.22 m wide by 0.69 m high by 0.61 m deep, with an average weight of 85.16 kg. The average moisture content of the cribs measured at the time of each test was 12.3%. The fuel load is centered in the compartment side to side, with the back of the fuel placed 0.30 m from the bulkhead wall. The fuel is ignited using 200 ml of methanol in each of two 0.384 m by 0.26 m pans, one centered under each stack of three wood cribs. The compartment schematic with the entire fuel load included can be seen in Figure 3.15.

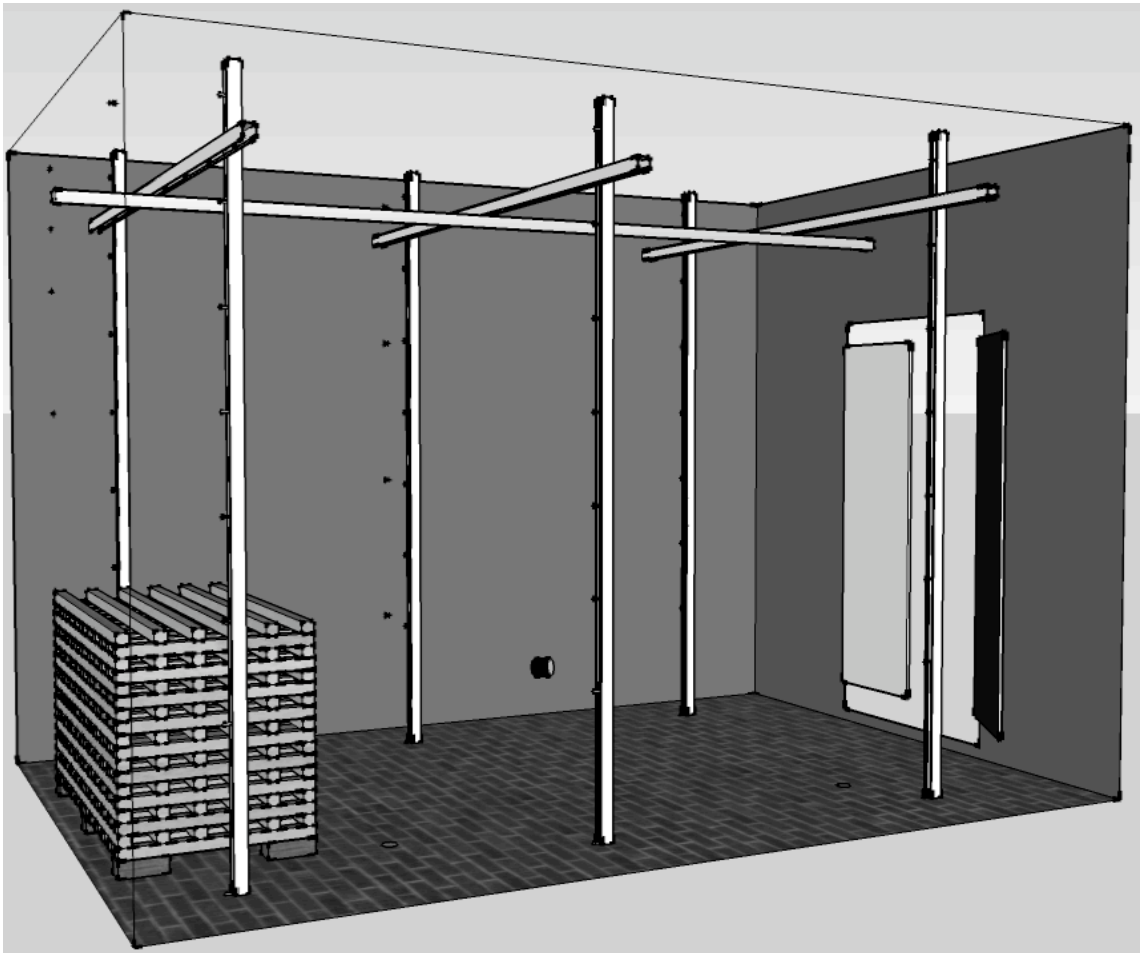

Figure 3.15. Compartment schematic with fuel load included.

The burning characteristic of the fuel load in the compartment is compared to that of the fuel under free burn conditions by comparing the measured heat release rates in each condition. The HRR curve for the six crib configuration is estimated by adding the curve for three sets of two stacked cribs. As discussed above, this may under-predict the HRR produced by two sets of three stacked cribs, but the under-prediction should not have a large impact in the analysis.

The HRR curve for the six crib fire in the compartment is also calculated based on the theory for oxygen consumption calorimetry, using values of velocity and CO, CO_2, and O_2 concentrations measured in the gases flowing out of the compartment during each test [18]. The velocity of the gases is determined using the temperature and pressure difference measured on the top three bi-directional probes during each burn. The area of the flow opening is estimated taking into account the upper ventilation opening, and the opening area of the doors observed in each test (recorded via video camera). The area of the ventilation openings for the three zones used, one for each of the top three probes, is summarized in Table 3.5.

Table 3.5. Ventilation openings used for oxygen consumption calorimetry analysis in the compartment.

Probe		Opening		
#	Height [m]	Width [m]	Height [m]	Area [m^2]
8	1.73	0.914	0.102	0.0929
7	1.62	0.3	0.25	0.075
6	1.37	0.3	0.25	0.075

Along with the velocity and area data, a duct calibration factor is required in the analysis. The duct calibration factor estimated for the compartment is 0.09, based on comparison of the heat release rate curves for a trial burn conducted in the compartment with four cribs configured as two stacks of two cribs, and the estimated HRR curve developed by doubling the free burn curve from two stacks of two cribs in the calorimeter.

Once the calibration factor and other variables are included in the oxygen consumption analysis, the HRR of the crib burn in the compartment can be analyzed. The two heat release rate curves for the six module cribs (free burn and compartment burn) can be seen in Figure 3.16.

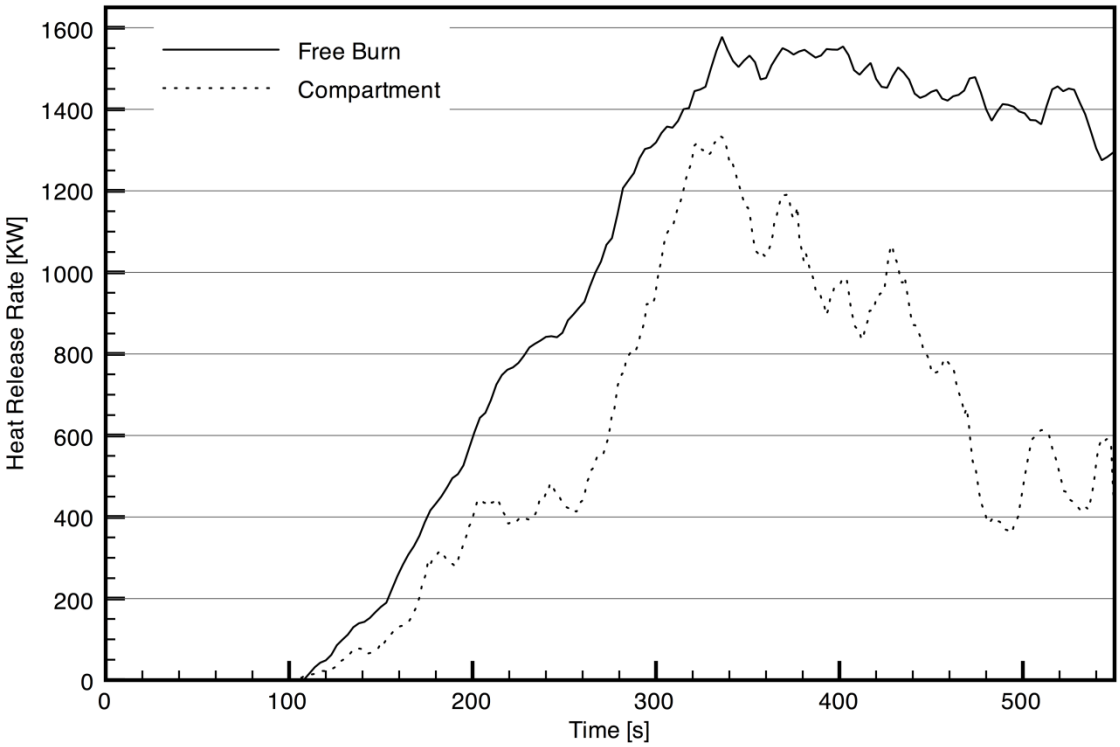

Figure 3.16. Heat release rate curves for the six crib configuration.

Comparison of the traces in Figure 3.16 indicates that the peak heat release rate of the two burns occur at roughly the same time after ignition (approximately 225 s after ignition, or at approximately 325 s on the plot), although, as expected, the peak HRR in the compartment fire is less than that in the well-ventilated calorimeter test. After reaching the peak, the fuel continues to burn at a constant HRR for some time in the calorimeter, while the crib fire in the compartment is under ventilated, causing the heat release rate to decrease, and eventually cycle in value dependent on ventilation and availability of air. The effects caused by the different ventilation in the two tests, then, explain the differences between the two traces, while the agreement in peak values of HRR suggests consistency in fuel loading versus HRR between tests.

The heat flux measured in the compartment using the wall mounted Gardon gauges can also be compared to heat flux data obtained during the calorimeter burns at the same distance off the floor and from the center of the crib configuration. Unlike the heat release rate, the fact that the fire is in a free burn or compartment condition should not have a large impact on the heat flux, until the fire becomes under-ventilated. The heat flux traces for a compartment fire test, along with the traces for a two crib test and estimated four crib test can be seen in Figure 3.17.

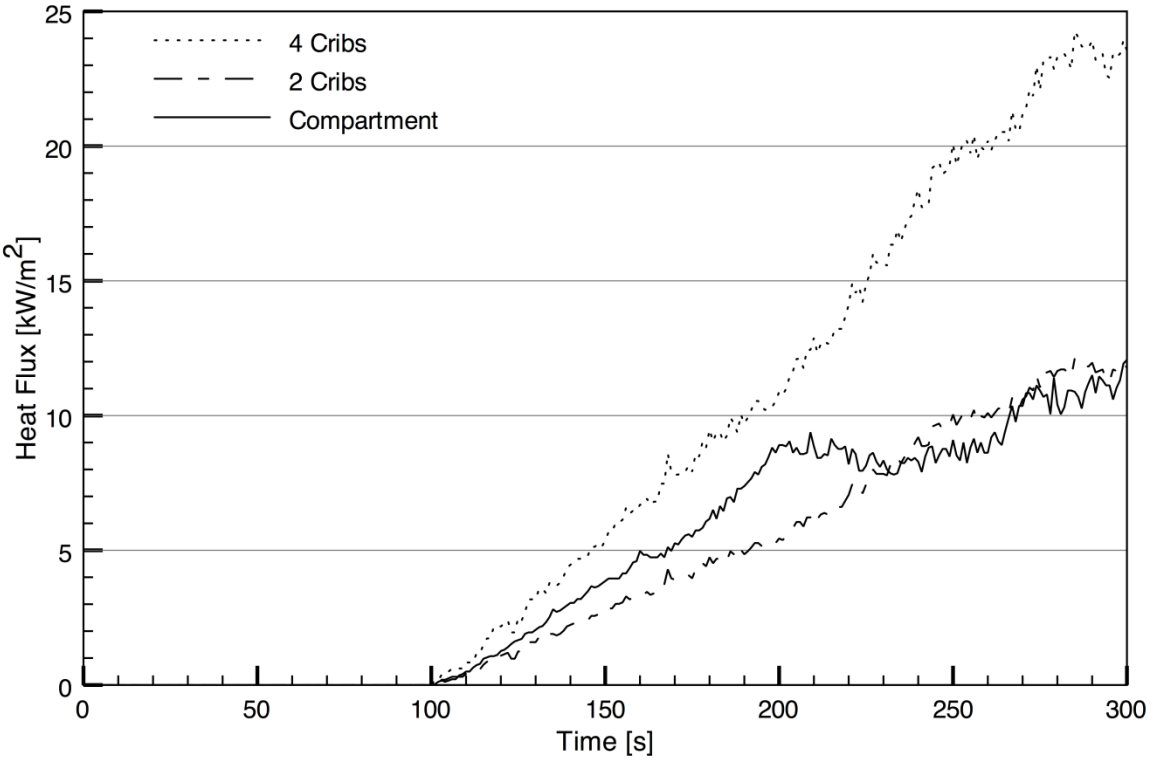

Figure 3.17. Heat flux measured for different crib configurations in the compartment and calorimeter during the initial burning phase.

It can be seen in Figure 3.17 that the heat flux in the compartment test rises in value until around 100 s after ignition at which time it decreases slightly, levels off for a period of time, and then begins to rise again, a trend consistent with that seen in Figure 3.16 for the HRR measured in these fires. Further, the measured heat flux follows that expected for a three crib test, as it lies approximately halfway between the two and four crib values. Since the heat flux gauge is on the side wall, it records heat flux from one stack of cribs in the compartment. These figures indicate that the heat flux and HRR data obtained in the tests is consistent, and captures the overall fire behavior in the compartment.

3.4 Suppression

3.4.1 Equipment and Set-Up

A 38.1 mm (1 ½ inch) internal diameter Akron 1720 Pyrolite Turbojet variable pattern nozzle with five different flow rate settings is used in all suppression tests. The nozzle is rigidly mounted to a stand such that, when horizontal, the nozzle exit is centered on the lateral centerline of the compartment, 0.75 m above the floor and 0.3 m outside the compartment opening. This positioning simulates a firefighter crouched on one knee holding the nozzle centered in the door opening. The angle of suppression application is then adjusted at the stand. A picture showing the suppression stand with the nozzle attached can be seen in Figure 3.18a, along with a picture showing the stand at the compartment entrance in Figure 3.18b.

Figure 3.18. Suppression stand used in the experiments: (a) before instrumentation; (b) at the door.

In previous suppression experiments conducted at the University of Waterloo Live Fire Research Facility and by others, an experienced firefighter was positioned at the door to execute fire suppression [43, 44]. It was found, however, that suppression could not be delivered as consistently as desired to a given location in the compartment. Introducing the suppression stand into the experiment removes any uncertainty inherent in having a human operator holding the nozzle and activating/deactivating the water during suppression. Using the stand, the angle of suppression can be set once, and will remain consistent not only during the test, but in subsequent tests as well, greatly reducing the variability introduced by having a human operator.

Suppression water is supplied to the nozzle via a standard 38.1 mm diameter, 15.24 m long fire hose from the reservoir of a Mack 600 pumper truck with a 4000 liter per minute pump. This allows operation at various pressure/flow rate combinations, whilst removing pressure fluctuations often encountered when using a fire hydrant. The pressure at the pumper is set based on the desired flow rate and discharge pressure at the nozzle, accounting for the pressure loss due to friction in the hoseline and elevation changes, as discussed in section 2.2.1.2.

3.4.2 Energy Balance

In order to estimate an acceptable maximum volume of water to inject into the compartment during one suppression activity, a theoretical energy balance is conducted on the compartment during suppression. A maximum water volume for the present tests is determined via an overall energy balance to ensure discernible results from the suppression experiments. If the heat absorption capacity of the water is much greater than the heat energy built up in the compartment fire, all of the suppression methods will appear to have the same effect, that of total cooling of the compartment. Conversely, if too little water is used, the compartment fire environment will only be cooled by a small amount and the resolution in the experiment will be poor, making it difficult to notice any effect at all due to suppression. For these reasons, it is desired to have an amount of cooling capacity enter the compartment via the water over the longest duration test that is similar, but not greater than, the amount of heat energy stored in the compartment.

The energy contained in the compartment at a given time can be estimated by combining the heat energy stored in the hot fire gases with that in the walls of the compartment. Assuming the hot layer is 1.5 m thick, the volume of hot gases in the compartment (V) is 13.365 m^3. As the desired hot layer temperature at the time of suppression is 900 K, and ambient air temperature is around 300 K, a maximum temperature difference of 600 K is assumed. Using the density (ρ) and specific heat (cp) of air at 900 K as 0.404 kg/m^3 and 1.1 kJ/kgK [50], respectively, the energy stored in the gas volume can be found using Equation (3.3):

$$E_i = \rho_i \cdot cp_i \cdot V_i \cdot \Delta T_i \tag{3.3}$$

Using Equation (3.3) and the data presented, the total estimated energy in the compartment gases is 3.6 MJ.

The energy in the compartment walls can be determined much the same way. As the suppression only lasts for around 5 seconds, and the steel walls are wrapped in insulation, it is assumed that energy will only be removed from the steel portion of the walls, and not the insulation. Under the assumption of a 1.5 m deep hot layer, the volume of steel in the walls and ceiling that can be cooled is 0.0762 m^3. It is also assumed that the steel will not reach as high a temperature as the gases throughout the test (assumed to be around 600 - 700 K), and will also not be cooled as effectively. An average temperature decrease due to suppression of 100 K is estimated for the steel, as some areas will drop to the water temperature (surfaces in direct contact with the suppression water), but others may be only slightly affected by suppression (such as the ceiling by the door). Using an estimated density and specific heat for steel at 650 K of 7774 kg/m^3 and 0.56 kJ/kgK [49], the estimated energy stored in the walls and ceiling is determined using Equation (3) as 33.2 MJ. Therefore, the estimated total amount of energy in the compartment at the time of suppression is around 37 MJ.

The potential capacity of the water to cool the compartment environment can be estimated by taking into account the energy required to heat the water from ambient to 373 K (E_h [kJ]), and the energy required to evaporate the water (E_{ev} [kJ]). These quantities can be determined using the following two equations [67]:

$$E_h = 4.186 M_w (373 - T_{in}), \text{ and} \tag{3.4}$$

$$E_{ev} = 2261 M_w, \tag{3.5}$$

where M_w is the mass of water supplied [kg], and
T_{in} is the temperature of the water supplied [K].

As the incoming water is supplied at approximately 283 K, a mass of 14 kg of water would be required to cool the compartment fire (absorb the estimated 37 MJ of stored energy discussed above). While this assumes 100% conversion of the water for cooling, which would not be the case, it does provide an upper bound on the possible level of cooling by a specified amount of suppression water. This analysis suggests that a volume of suppression water up to but not greater than 14 ℓ is sufficient to achieve an appropriate level of cooling in the compartment for analysis of the different initial fire attack suppression methods.

3.4.3 Flow Properties

In order to determine the most appropriate flow rate for the tests, the flow through the nozzle is characterized at a number of different nozzle and pressure settings. The mass of water output by the nozzle/pump configuration as used in the suppression experiments was measured as a function of duration of flow. The results of these tests are summarized in Table 3.6, along with the calculated flow rate, the estimated friction loss in the line, and the calculated nozzle discharge pressure for each pump pressure and nozzle setting.

Along with the nozzle discharge pressure, Table 3.6 also shows the volume of water discharged in 5 seconds for each combination of settings. As 5 seconds is the desired maximum suppression duration for each test, the volume of water discharged in this time can be used along with the theoretical energy balance to determine the most appropriate nozzle and pressure settings. Based on the energy balance discussed above, the maximum desired volume of water delivered via the nozzle is 14 ℓ. From the flow rate data for the nozzle, the most appropriate settings to meet that volume of water are a nozzle setting of 230, and a pump discharge pressure of 425 kPa. The resultant nozzle pressure during the suppression tests with these settings is 411 kPa.

Table 3.6. Nozzle calibration test data.

Pump Pressure [kPa]	Setting	Measured Flow Rate [kg/s]	[lpm]	Friction Loss [kPa]	Nozzle Pressure [kPa]	5 s Flow Volume [ℓ]
425	115	1.5	87.46	4.4	420.6	7.29
425	115	1.4	86.88	4.4	420.6	7.24
425	230	2.6	155.46	14.0	411.0	12.95
425	360	3.7	219.58	27.9	397.1	18.30
425	475	4.7	284.83	47.0	378.0	23.74
570	115	1.8	105.85	6.5	563.5	8.82
570	230	3.2	192.00	21.3	548.7	16.00
570	360	4.8	285.41	47.2	522.8	23.78
570	360	4.8	285.48	47.2	522.8	23.79
570	475	5.8	348.27	70.2	499.8	29.02
650	115	1.9	112.48	7.3	642.7	9.37
650	230	3.5	208.78	25.2	624.8	17.40
650	360	5.1	304.59	53.7	596.3	25.38
650	475	6.3	379.05	83.2	566.8	31.59
775	115					
775	230					
775	360	6.00	360.00	75.0	700.0	30.00
775	475					

NOTE: Due to experimental constraints, the calibration could not be performed at the highest pressure, however, as this is the original calibration point for the nozzle, some values are known.

Comparison suppression tests are also to be conducted at higher pressures. For the higher pressure experiments, the optimal nozzle discharge pressure and setting is used, as specified by the manufacturer [39]. These settings are what municipal fire departments in the area use when attacking compartment fires [38]. In this case, the optimal nozzle discharge pressure is 700 kPa, and nozzle setting is 360. This requires a pump discharge pressure of 775 kPa, and results in a 5 second flow of 30 ℓ of water.

In order to compare different suppression tactics, three different nozzle discharge patterns are used: straight stream, narrow fog, and wide fog. As a combination nozzle is used for the suppression tests, the three patterns are achievable by adjusting the exit valve, while leaving the body in place. The three flow patterns can be seen in Figure 3.19.

Figure 3.19. Nozzle flow patterns. L-R: straight stream, narrow fog, wide fog.

The average cone angle (angle of water discharge) for each setting is measured at 0°, 16.6°, and 110.0°, for the straight stream, narrow fog, and wide fog settings, respectively. The water flow rate for each pattern is also independently measured for each of the desired tactics under test flow conditions. The flow rate for each flow pattern and tactic determined at the nozzle setting of 230 and discharge pressure of 411 kPa can be seen in Table 3.7.

Table 3.7. Flow rate determined for each flow pattern and flow tactic.

Tactic	Mass Flow Rate [kg/s]		
	Straight Stream	Narrow Fog	Wide Fog
5 second flow	2.81	2.69	2.75
2 x 2 bursts	2.55	2.63	2.70
Short bursts	2.04	2.38	2.44

From the data in Table 3.7, it can be seen that as the tactic changes from a continuous 5 second flow to a short burst, the flow rate through the nozzle decreases due to a slight pressure drop at the pumper each time the nozzle is opened. Therefore, these flow rates are used along with video data from each suppression test in order to more accurately determine the amount of water actually introduced into the compartment during each suppression activity.

3.5 Test Procedure

3.5.1 Pre-Test Conditions

All of the suppression tests were conducted during days when the ambient temperature ranged from 15 to 29°C, and the average wind speed was never greater than 11 km/h. As suppression did not start until the temperature at points in the upper layer of the compartment reached 900 K (around 630°C), it is assumed that the variation in ambient temperature had little effect on the experiment.

The wood cribs were conditioned for at least 8 weeks in a room where the temperature is maintained between 20 and 22°C, and the relative humidity was held below 35%. The average moisture content of the wood cribs determined on the day of each suppression test is 12.3% ±2.2% standard deviation. In order to retain the effectiveness of the conditioning, the cribs are not positioned in the compartment until just prior to ignition.

3.5.2 Test Procedure

The methanol in the pans below the wood cribs is ignited using a butane lighter, and the doors are left open to allow the fire to build. When the temperature at points in the hot layer in the area of the fire reaches 700 K, the doors are adjusted (opening is reduced) to allow the hot layer to build further and the thermal profile to homogenize throughout the compartment. Using feedback from the real-time data acquisition system, the doors are adjusted as necessary until the desired temperature of 900 K is reached at points in the hot layer. At this time, the doors are opened fully, and suppression is carried out within 10 to 20 s. After suppression, the doors are left open for around 15 s to allow the fire to rebuild, and the process is repeated by adjusting the door opening until the target hot layer temperature is again reached. Depending on the suppression methods under investigation, as many as nine consecutive tests are carried out using one fuel load.

3.6 Measurement Uncertainty and Sources of Error

Measurement uncertainty involves estimating the difference between the measured value and a true value, or error in a measurement [48]. As expected, the true value of any variable being measured is rarely, if ever, known in an experiment, so the measurement error is specified as an uncertainty interval, whether it be a range of values, or a percent of the measured or full-scale value [48].

The uncertainty in a measurement, like the measurement itself, cannot be determined exactly. Instead, both bias and precision errors in each measurement device are combined to determine the overall uncertainty in that measurement. Bias errors are offset errors that are constant for the device throughout the experiment, for example, the difference in the value measured by the device used in the experiment and a more accurate device used for calibration. Precision errors are random errors that occur from undesired variations in the measurement, the response of the device, or the measurement system. The two types of uncertainties, bias and precision, are added to determine the overall uncertainty using the following equation [48]:

$$u = \sqrt{b^2 + p^2} \tag{3.6}$$

where u is the overall measurement uncertainty,
b is the bias error, and
p is the precision error.

The bias and precision errors can be determined using the following two equations, which assumes a student t value of 2 for 95% convergence [48, 51]:

$$b = \left(\sum_{k=1}^{K} b_k^2 \right)^{1/2} \tag{3.7}$$

$$p = \left(\sum_{k=1}^{K} p_k^2 \right)^{1/2} \tag{3.8}$$

where b_k and p_k are the individual bias and precision errors.

The individual bias and precision errors are used to calculate the overall bias and precision error, b and p using Equations 3.7 and 3.8, respectively, for each measurement. Equation 3.6 can then be used to determine the overall uncertainty in the measurement.

The measurement uncertainty related to all of the measurement instruments used in the experiment, as discussed previously in this chapter, is determined below. This includes uncertainties for the temperature measurements made via the Type-K thermocouples, the heat flux measurements made by the Gardon and skin simulant heat flux gauges, the gas velocity measured by the bi-directional probes and pressure transducers, and the uncertainty in the gas concentration measured by the Servomex analyzer.

3.6.1 Temperature Measurement

As mentioned in the experimental set-up, the thermocouples consist of a length of high temperature inconel sheathed thermocouple wire, typically connected to a length of thermocouple extension wire. The extension wire is then connected to the data acquisition system. In order to determine the bias error in the temperature measurements, the error in each of these three components needs to be considered. The standard bias error for Type-K thermocouple wire for a 95% level of confidence is the larger of either ±1.5°C, or ±0.5% of the measured temperature above 0°C [68]. As the maximum recorded temperature over all of the experiments was 930°C, a maximum bias error for the thermocouple wire of ±4.65°C is used. For the thermocouple extension wire, a calibration error of ±1.5°C is specified [68], and for the Fieldpoint data acquisition system, a bias error of no more than ±1.2°C for the maximum measured temperature of 930°C is specified by the manufacturer, which takes into account a number of uncertainties, including the uncertainty in the cold junction compensation [69]. Combining all of these errors as per Equation 3.7, the estimated bias error for the temperature measurements becomes ±5.03°C, or 0.54%.

The largest precision error in thermocouple measurements in compartment fires is due to radiation effects to and from the thermocouple [70]. If a thermocouple is placed in the upper regions of the compartment but not in direct flame contact, the temperature measured may be lower than the actual temperature, as the thermocouple bead radiates energy to the cooler compartment below [71]. The opposite may occur in the lower region of the compartment, as the thermocouple bead absorbs radiation from the fire and heated upper wall surfaces. The precision error due to radiation has been estimated to be around 10% for thermocouples in compartment fires [72].

The total measurement uncertainty for the thermocouple measurements is therefore determined using Equation 3.6, and the bias and precision uncertainties determined. As the precision error greatly outweighs the bias error, the total measurement uncertainty in the thermocouple measurements is around 10%.

3.6.2 Heat Flux Measurement

3.6.2.1 Gardon Gauges

The accuracy of the calibration of the Gardon gauges, as supplied by the manufacturer, is 3% [52]. The gauges also had a repeatability uncertainty of 1%. The total bias uncertainty for the Gardon gauges therefore becomes 3.16%. Work has been done previously at the University of Waterloo Fire Research Lab to quantify the effect that a forced convective flow over a heat flux gauge has on the heat flux measurement which suggests an additional contribution to the uncertainty of the Gardon gauges should be included [51]. Although the only phenomenon forcing the convection in the compartment is the buoyancy of the heated exhaust gases, the velocity into the compartment measured in the area of the floor is as high as 3.5 m/s during the experiment, which is similar to the 4.6 m/s windspeed tested previously [51]. When a heat flux was imposed on the gauge from a 600°C source with forced convection over the gauge present, the measured heat flux was around 8% lower than that of a more accurate gauge [51]. This suggests that a precision error of 8% should also be included for the gauges due to the convective flow in the compartment. Therefore, the maximum total uncertainty in the heat flux measured by the Gardon gauges in the compartment is 8.6%.

3.6.2.2 Skin Simulant Sensors

Unfortunately, the two assumptions discussed in Section 1.2 of this chapter that must be met in order to effectively use the Colorceran sensors to model the heat transfer into human skin cannot be verified for this experiment. The assumption that the sensor behaves like a semi-infinite slab, or that the back surface of the sensor does not have an appreciable temperature rise,

is valid for a short time during suppression, but cannot be verified over the entire action. It is also observed that the skin sensors did not have time to cool between each suppression action, so they would not have been at a uniform temperature before each measurement.

As a result of the above two assumptions not being met, the quantitative (magnitude) values of heat flux obtained from the sensors are likely not accurate over the entire test. The values for heat flux are included in the discussion of the results, however, as the relative trends and comparisons among different tests are still valid and useful. As no significant changes are expected over the course of the tests, the skin simulant sensors will behave in a similar fashion from test to test, allowing for a comparison of the values measured. The uncertainty in the calibration of the skin simulant heat flux gauges, as discussed by the manufacturer, is around 10% [59].

3.6.3 Velocity Measurement

Velocity measurements are conducted using the bi-directional probes and pressure transducers. The transducers are set with a full-scale pressure output of ±25 Pa. The manufacture specified accuracy of the transducers is 1% of full-scale, and the errors due to non-linearity, hysteresis, and non-repeatability are specified at 0.98%, 0.2%, and 0.1% of the full-scale value [73]. From these values, the maximum bias uncertainty in the velocity measurements is calculated to be ±0.35 Pa.

The pressure transducers also have precision errors associated with zero and span shifts of 0.033% and 0.06% of the full-scale value, and a setting specific error of 2.1% of full-scale when the ±25 Pa measurement range is selected [73]. The precision error associated with the transducer is ±0.525 Pa, resulting in an overall maximum uncertainty for the transducer of ±0.63 Pa, or 2.5%.

The bi-directional probes themselves also have a calibration uncertainty associated with them of 10% [54]. The total uncertainty in the velocity measurements is therefore the combination of these two uncertainties. The uncertainties can be added in the same way as adding the precision and bias uncertainties in Equation 3.6, resulting in a maximum total uncertainty in the velocity measurements of 10.3%.

3.6.4 Gas Concentration Measurement

The parametric oxygen sensor has a maximum intrinsic error of 0.05%, a maximum linearity error or 0.05%, and a maximum repeatability error of 0.05% of the oxygen reading [74]. There is also a drift value associated with the span and zero calibration of the instruments of 0.05% per week, but since the analyzer is calibrated each day, it is assumed this error is negligible for this experiment [74]. The maximum oxygen concentration measured during any test was 20.95%; therefore, the maximum repeatability error becomes ±0.0105, or 1.05%. Using Equation 3.7, the total bias error associated with the oxygen measurement is 1.05%.

The precision errors associated with the oxygen measurement are made up of the noise in the measurement, and the error due to temperature increases of the incoming gas. The noise produces an error of 0.01%, and the error due to temperature is either 0.1% for every 10°C increase above ambient, or 1% of the reading, whichever is greater [74]. The maximum temperature of the gas sampled is around 600°C, but it took approximately 45 seconds for the gas to go from the sampling port to the analyzer. Over this time, the gas stream cools considerably, as the stainless steel and nylon gas sampling tubes were exposed to the atmosphere (30°C). Conservatively, assuming the gas would cool to half of the sampling temperature, or 300°C, a maximum error of 3% would be observed. The total precision error determined using Equation 3.8 is therefore 3%. The total uncertainty in the measurement of the oxygen concentration in the gas stream, using Equation 3.6, is 3.2%.

The infrared carbon dioxide sensor has a full-scale measurement range of 25%, and an intrinsic error, linearity error, and repeatability error of 1% of the full-scale, or 0.25% for each [74]. The total bias error for the carbon dioxide measurement is calculated to be 0.43%. The span drift of the analyzer is 1% of the reading per day, which means it is not negligible if the instrument is only calibrated once a day [74]. The error due to instrument noise is 1% of the reading or 0.5% of the range, and the error due to increased temperature is 2% of the reading or 1% of the range. The precision errors due to the noise and temperature increase therefore become 0.125% and 0.25%. The total precision error and total uncertainty in the measured carbon dioxide concentrations become 1.04% and 1.125%, respectively.

The infrared carbon monoxide sensor has a full-scale measurement range of 3000 ppm, and the maximum measured value was around that of the full-scale. The errors due to accuracy, linearity, and repeatability for the analyzer are all ±0.5 ppm [74]. The bias error in the carbon monoxide measurement is therefore ±0.866 ppm. The zero and span drifts are negligible for the carbon monoxide sensor if it is calibrated once a day, and the errors from noise and increased temperature are ±0.5 ppm, and either 3% of the reading or ±1 ppm, whichever is greater [74]. The precision error for the instrument is therefore ±90 ppm, and the maximum total uncertainty in the carbon monoxide measurement is ±90 ppm, or 3%.

3.7 Summary

Suppression tests are conducted in the instrumented fire compartment using the suppression stand described in this chapter. The measurement instruments, with their estimated measurement uncertainty, are used to examine the effects of 5 different suppression actions on the compartment fire environment at different nozzle discharge pressures and angles. The repeatability of the experiments, as well as the results of the suppression tests, can be found in the following chapters outlining the details of the final experimental results.

Chapter 4

CHARACTERIZATION OF THE COMPARTMENT FIRE ENVIRONMENT

As mentioned in Chapter 2, one key indicator of a fully developed compartment fire is an upper layer temperature of around 600°C. As such, the upper layer temperature in the compartment must be above 600°C (875 K) before suppression (above 900 K desired), in order to successfully test the different suppression methods in a simulated, yet realistic, compartment fire environment. Upper and lower layer temperatures in the compartment should be relatively uniform axially, and should be representative of actual conditions laterally, in order to verify that the desired compartment environment is achieved throughout the tests.

In this chapter, the estimated interface height determined during testing, the temperature profile in the compartment, and the average temperature in the upper layer during fire growth are discussed in order to confirm that the fuel load produced consistent conditions in what was classified as the upper layer. The lateral and axial temperatures are also presented, along with the upper layer temperature before suppression, and the heat flux out of the compartment door. The results from all of these measurements are used to assess the suitability of the compartment, fuel load, and test procedure for the proposed suppression study.

The origin for the measurement grid is located at the door opening looking into the compartment, with three measurement planes containing thermocouples located at 0.55, 1.7, and 3.1 m from the door. These are numbered as planes 1, 2, and 3, respectively. Vertical rakes are located 0.9 m on each side of the compartment centerline, and labeled by plane number and lateral location, for example, as 1L and 1R for the left and right rakes closest to the door, respectively. The horizontal rake at each plane is located 2.15 m off the floor, and denoted by an H, so 1H is

the horizontal rake in the plane closest to the door. Lastly, the horizontal rake running from the door to the bulkhead along the center axis of the compartment is located 1.4 m off the floor, and denoted as H4.

4.1 Interface Height

The interface height in a compartment fire is defined in the second chapter as the boundary between the upper and lower layers in the compartment. The upper layer consists of the heated compartment gases and products of combustion, and can be distinguished from the lower layer by observing the height of the smoky layer in the compartment, or by observing the temperature difference between the two layers. As the upper layer was determined visually during testing, the height of the smoke layer in the compartment is considered to be the interface height, with the upper layer existing above the interface.

The interface height in the compartment prior to suppression can be considered by examining the video of the compartment fire and observing the height of the smoke layer. One frame of the crib fire in the compartment with a clearly defined smoke layer is shown in Figure 4.1.

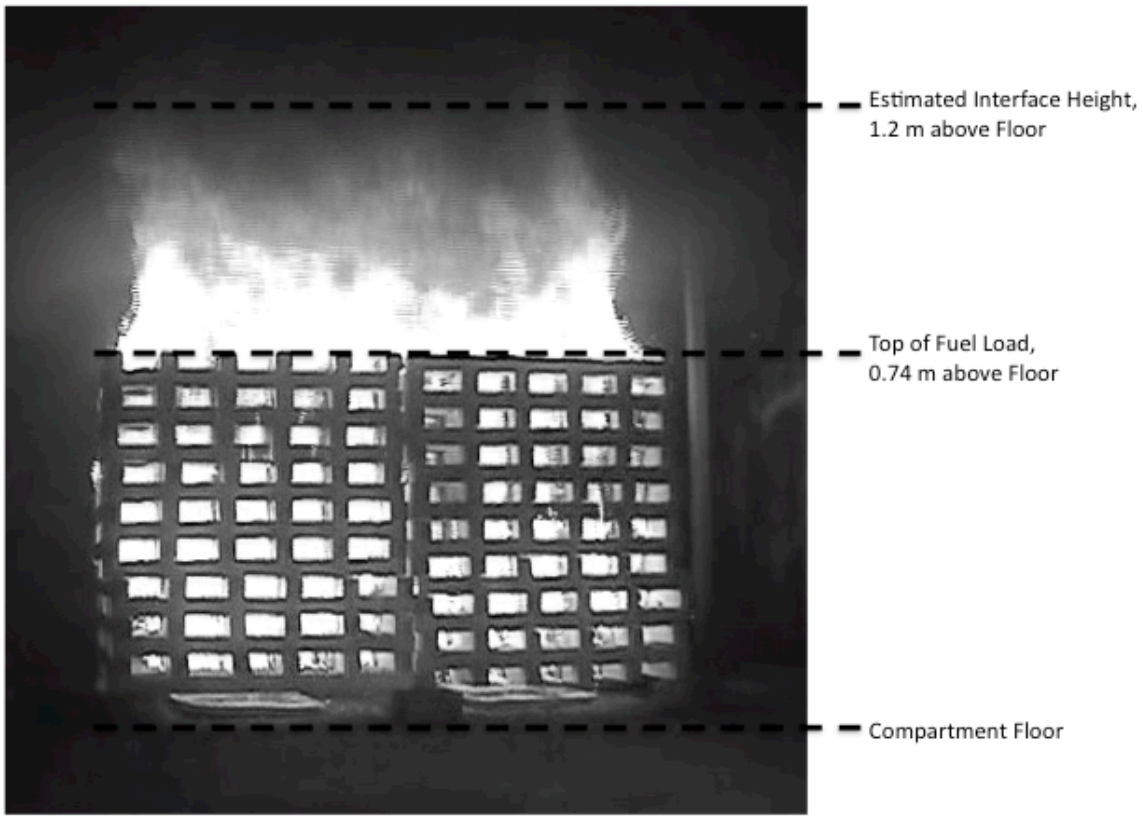

Figure 4.1. Frame from the compartment video just prior to suppression.

Although it is not visible in the picture, the flames extend well above the crib shown in the photo, and almost reach the ceiling of the compartment. The flames cannot be seen because they are shielded by the smoke in the upper layer. Using an estimation of where the flames are obscured by the smoke as a guide, the estimated interface height is determined.

In the picture, it can be seen that the smoke layer (interface height) is roughly 2/3 again as high as the stack of wood cribs. As the fuel load stack is around 0.69 m high and placed on 0.05 m high fireclay bricks, the wood crib stack is around 0.74 m off the ground. From this, the estimated interface height is therefore around 1.2 m above the floor.

The temperature profile in the compartment taken from thermocouple rake 2L at the same time as the captured frame in Figure 4.1 is shown in Figure 4.2. The figure shows that the temperature is very uniform over the bottom 0.5 m in the compartment, and then rises by about 100 K between the next two thermocouples, which are each spaced 0.4 m apart. The largest temperature increase is observed between the thermocouple at 1.1 m and the one at 1.4 m above the floor, followed by a relatively small temperature increase over the next 3 thermocouples, suggesting that the temperature of the upper four thermocouples is fairly uniform.

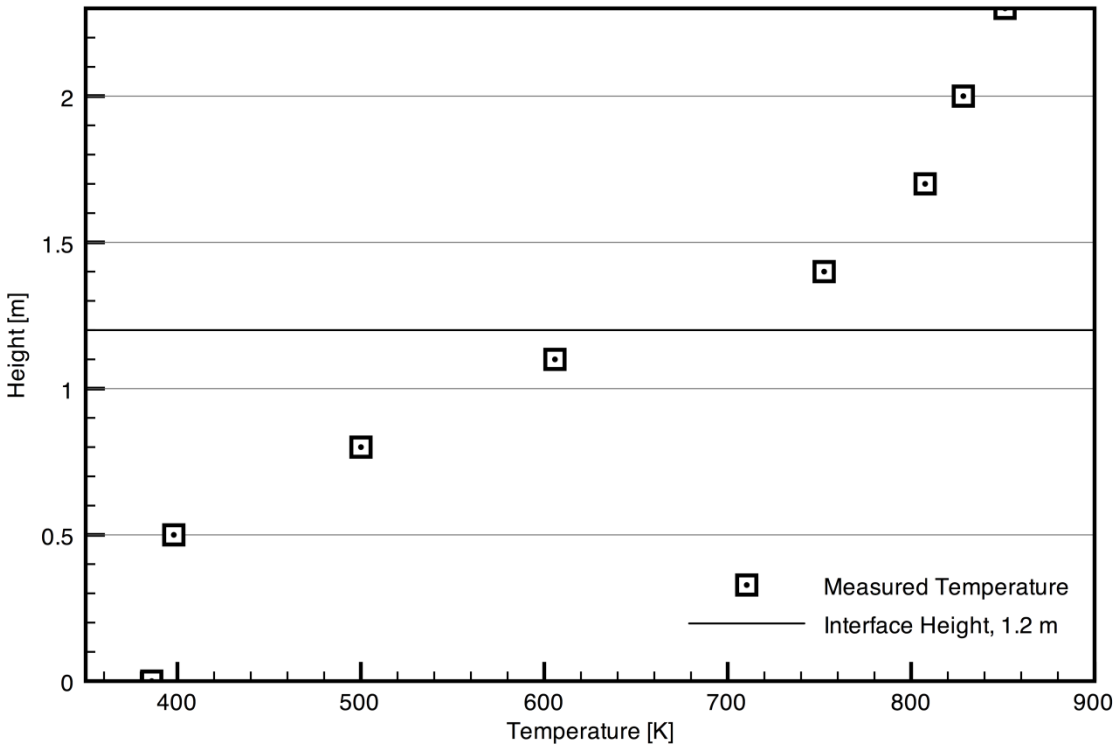

Figure 4.2. Temperature and interface height before suppression.

Along with the temperature at each thermocouple height, the interface height estimated from the video is plotted. As seen in the figure, the interface height determined during testing is located

between the 4th and 5th thermocouples from the bottom. There is some debate among researchers, however, as to whether the interface height would be in the location presented, or at the first inflection of the temperature profile, i.e. around 0.5 m above the compartment floor.

As the height of 1.2 m was determined during testing, this height is used as the interface for this research and the following results, thus defining which thermocouples are in the upper and lower layers. As per Figure 4.2, the thermocouples in the lower layer are located at heights of 0.0, 0.5, 0.8, and 1.1 m off the floor. All of the thermocouples above that, located at heights of 1.4, 1.7, 2.0, and 2.3 m off the floor, as well as all of the thermocouples in the horizontal rakes, are taken to be in the hot upper layer.

4.2 Upper Layer Average Temperature

The average upper layer temperature is determined by averaging the temperature measured on all of the thermocouples in the vertical rakes above the interface height of 1.2 m. As there are four thermocouples on each rake above the interface height and six vertical rakes in the compartment, the average upper layer temperature is calculated from the temperatures measured by 24 individual thermocouples. The average and standard deviation of the upper layer temperature in the compartment during the fire growth phase of one test fire is shown in Figure 4.3.

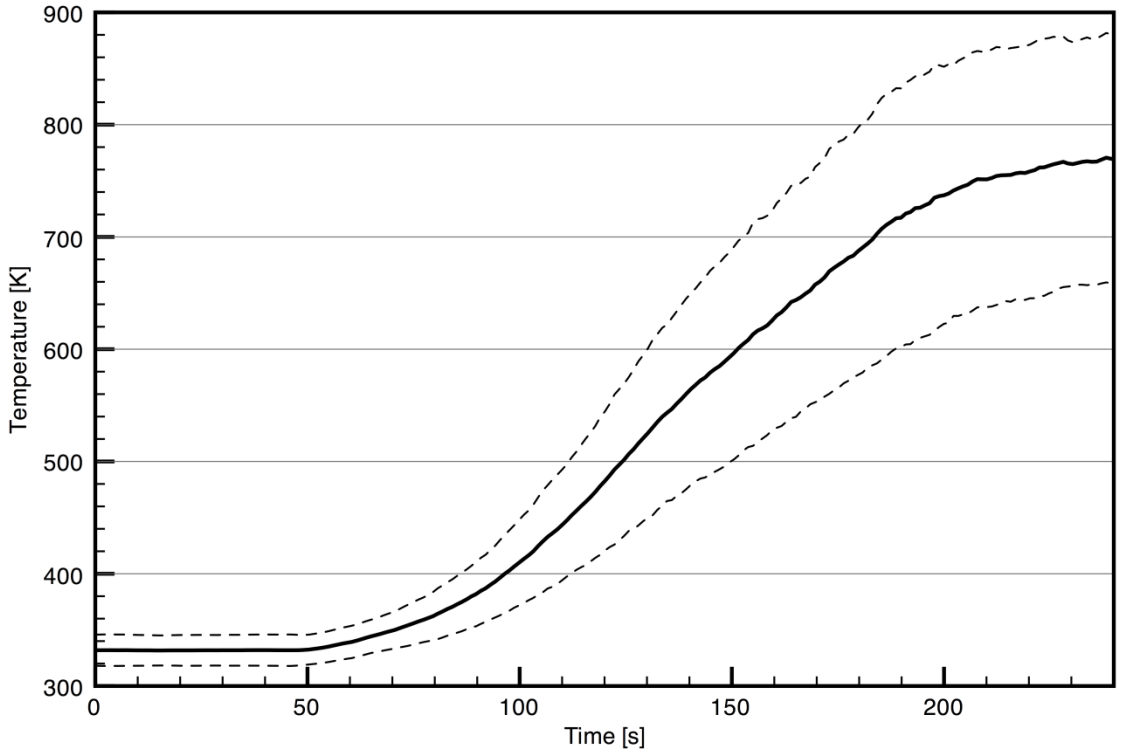

Figure 4.3. Average upper layer temperature during a fire growth phase.

The solid dark line in Figure 4.3 is the average upper layer temperature in the compartment, which is initially around 330 K before ignition occurs, at about 50 seconds. As the test continues, the upper layer temperature rises as the fire grows, reaching an average upper layer temperature of around 770 K at 200 seconds after ignition.

Along with the average upper layer temperature, the two dashed lines in Figure 4.3 represent the maximum and minimum values based on the standard deviation of the data. Before ignition, from 0 to 50 seconds, the standard deviation is around ±5%, which is due to the natural temperature stratification in the compartment. This stratification occurs because there is very little air flowing into or out of the compartment when there is no fire burning, so the compartment stratifies based on ambient temperature and incident sunlight. As the fire grows, the standard deviation reaches around ±15% at 100 seconds after ignition, and remains at that value throughout the rest of the fire growth phase. Some of this deviation in average temperature is due to buoyant stratification in the compartment, since even though the hot layer is fairly uniform, the temperature will still stratify in the layer. This can clearly be seen in Figure 4.2, where the temperature measured by the thermocouples above the interface height ranged from 750 K to 850 K with increasing in height in the compartment. Some stratification also exists from the front to the back of the compartment. This effect accounts for an additional portion of the deviation seen in the average upper layer temperature.

4.3 Lateral and Axial Uniformity

The instantaneous temperature measured from the same fire test used in Figure 4.3 by each of the thermocouples on the six vertical rakes in the upper layer at 200 seconds after ignition is shown in Figure 4.4. The symbols in the figure indicate the rake on which the thermocouple is located, and the lines indicate at which plane the measurement was made, i.e. the two dashed lines correspond to the 1-plane, which is closest to the door. In the figure, it can be seen that the temperature measured at the same height off the floor in each plane is quite similar, aside from one outlying point at a height of 1.7 m on rake 1R. When the singular outlier point is removed, the maximum temperature difference between two points at the same height on the same plane is 79 K, and the average temperature difference is 33 K. An average temperature difference between two points at the same height on the same plane of 33 K suggests very uniform upper layer conditions moving laterally across the compartment.

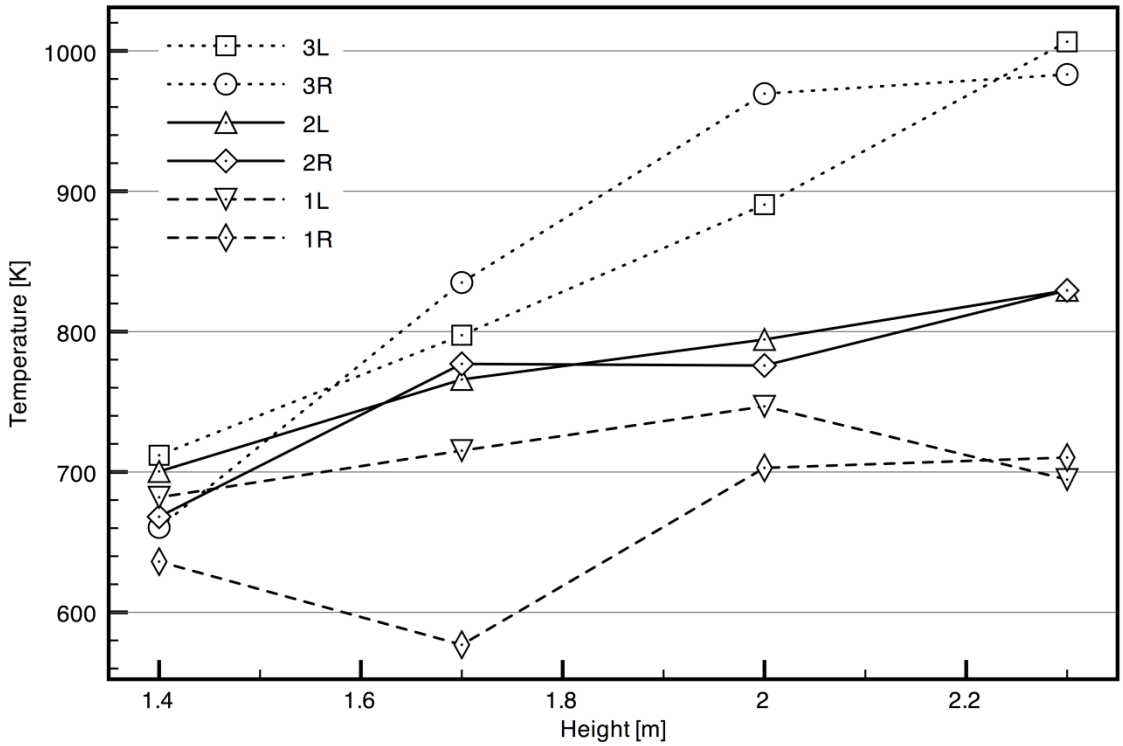

Figure 4.4. Instantaneous temperature measured by each upper layer thermocouple on the six vertical rakes at 200 seconds after ignition.

As expected, conditions are not as uniform from front to back as they are laterally in the compartment. The temperatures in the plane closest to the door are expected to be lower than those at the other two measurement planes. This is observed in Figure 4.4, where the temperature varies from 636 K to 746 K as the height increases on the 1-plane (again not taking into account the outlying point on the 1R rake). On the middle plane, the temperatures range from 668 K to 829 K, and on the plane closest to the fire, the temperatures range from 660 K to 1006 K. The temperatures are expected to be lower closest to the door because the gases have more time to cool as they travel away from the fire, and mix with the cool air coming in through the door. On the other hand, the plane closest to the fire is expected to be the hottest and exhibit the largest vertical stratification due to buoyancy of the hot gases. This result is seen in the large temperatures and temperature gradient measured in the 3-plane.

The same phenomenon is observed when considering the temperature measured on the horizontal rake running from the door to the bulkhead along the center axis of the compartment (H4). The temperatures measured by the thermocouples on H4 at 200 seconds after ignition for the same test as above, along with the temperatures measured on the centerline plane of H1, H2, and H3, are shown in Figure 4.5.

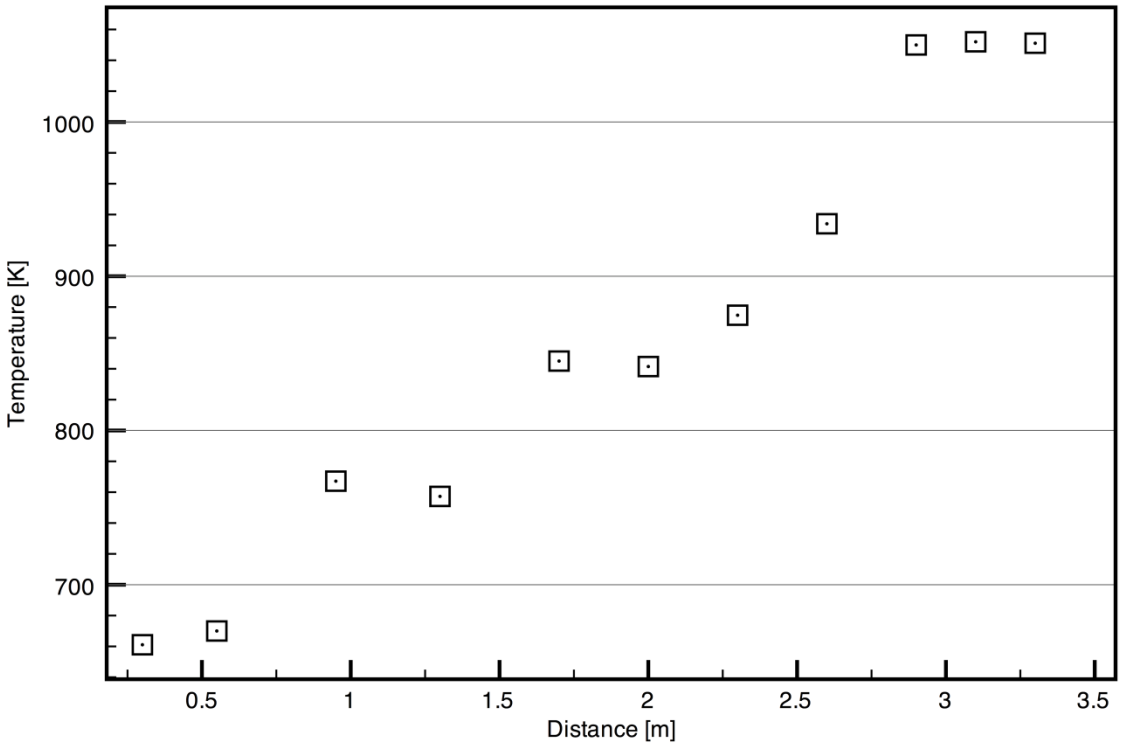

Figure 4.5. Temperature measured by the thermocouples on the centerline axis of the compartment at 200 seconds after ignition.

In Figure 4.5, it can be seen that the temperature rises steadily from 660 K measured by the thermocouple closest to the door (0.3 m away) to a temperature of 934 K measured by the thermocouple 2.6 m inside the door, located just in front of the wood cribs. The three thermocouples located further into the compartment than 2.6 m, which are above the fuel load, measure higher temperatures, around 1050 K. The uniform and high temperature across all three thermocouples suggests that they are being directly impacted by flaming gases. As a result, there is a temperature variation of approximately 390 K in the upper layer between the front and the back of the compartment.

From the plots of measured upper layer temperature in Figure 4.4, and the temperature measured on the centerline axis of the compartment, Figure 4.5, it can be concluded that the compartment environment is fairly uniform during a crib burn. The average lateral variation in temperature on each of the three planes is approximately 33 K ±22 K, a very small difference considering the large temperatures measured in the compartment. The variation from the front to the back of the compartment is much larger, estimated at 390 K, while acknowledging that three thermocouples are positioned in direct contact with the flames. The lateral variation in temperature speaks to the uniformity of the hot layer in a given plane. On the other hand, there is a larger temperature gradient from front to back of the compartment (along the length of the compartment) since, as expected during a real fire, the heated upper layer gases cool as they move

from the fire towards the door of a compartment, while also entraining more cool air from the lower layer. Therefore, the compartment temperatures are relatively uniform laterally, and representative of a real compartment upper layer during the wood crib burns used in the present research.

4.4 Upper Layer Temperature Repeatability

Discussions in the previous section indicate that the compartment conditions in the upper layer are relatively uniform and representative of actual conditions during a crib burn. Another aspect of the compartment conditions to consider is the repeatability of the fire growth and upper layer temperature distributions among subsequent crib burns. To assess this repeatability, the time series of the upper layer temperature during the growth phase for all seven crib burns is shown in Figure 4.6.

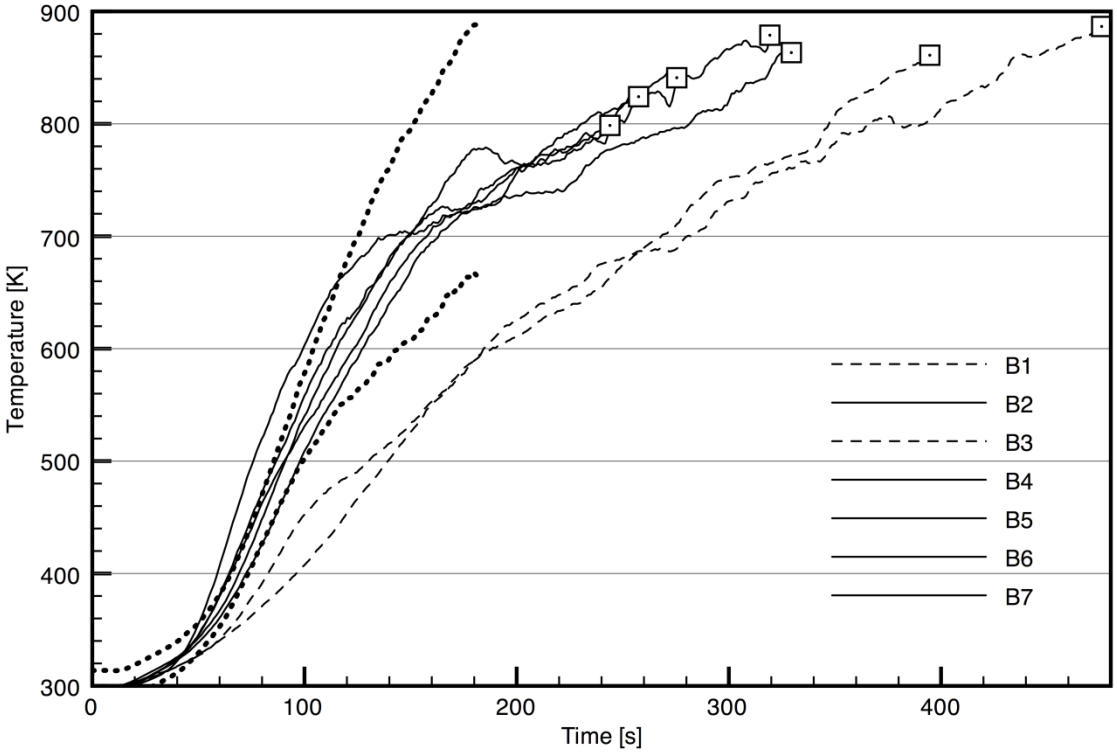

Figure 4.6. Average upper layer temperature during the fire growth phase for all crib burns.

Along with the average upper layer temperature plotted for each burn in the above figure, the maximum and minimum standard deviation lines for one of the burns, B5, are plotted as the two dotted lines. It can be seen that the majority of the curves, B2, and B4 to B7, lie within or very close to these two bounds. On the other hand, curves B1 and B3 in the figure do not fall within the two bounds, but are similar to one another.

The amount of ventilation in the compartment influences the fire growth curve more than any other factor. If the compartment is underventilated, not enough oxygen is getting to the fire, and the temperature grows more slowly, as was the case in B1 and B3. The impact of the amount of ventilation was considered while planning the experiment, and the adjustable doors were incorporated into the compartment to allow the ventilation to be varied during a burn. After the first three burns, the temperature growth data was analyzed and it was discovered that the fire was underventilated. To remediate the situation, the doors were opened wider during the growth phase of subsequent burns to provide more ventilation in the compartment, and raise the temperatures more quickly. Underventilating the fire does not cause problems with the test itself, it simply increases the time required for the test, and reduces the available fuel load once suppression starts. It can be seen that once the ventilation problem was addressed, the upper layer temperature in the compartment during the growth phase was quite constant from test to test.

4.5 Compartment Environment Prior to Suppression

4.5.1 Upper Layer Average Temperature

In Figure 4.6, the square symbols at the end of each temperature curve indicate the average upper layer temperature in the compartment when the first suppression test was initiated for each crib burn. The combined average upper layer temperature over all seven burns at this time was 850 K, with a standard deviation of 30 K. This relatively small standard deviation suggests that the compartment conditions during the fire growth to initial suppression stage were sufficiently repeatable for all seven burns, even though two took longer to reach the desired upper layer temperatures. However, the average upper layer temperature of 850 K is slightly lower than the desired value of 900 K discussed in the objectives for this research. The main reason for this is that the average temperature in the upper layer is not determined until after a test is completed, as the only real time-temperature data observable during a test is from individual thermocouples in the hot layer. Considering that the temperature data from a few individual thermocouples was used to determine the appropriate time to start suppression, very repeatable average upper layer temperatures are achieved, with a very small variance from test to test.

The average upper layer temperature just prior to suppression for all of the 52 different suppression tests conducted in the seven different compartment burns is 910 K, with a standard deviation of 38 K. Therefore, average upper layer temperatures over all of the tests are above the 875 K upper layer temperature considered typical of compartment fires, and above the 900 K desired. The small standard deviation in these temperatures is further confirmation of the uniformity of conditions in the compartment during the experiment.

4.5.2 Heat Flux out of the Compartment

The heat flux values measured by the skin simulant sensors located in ambient conditions just outside the compartment door confirm that uniform conditions are achieved with the test fuel loads and experimental procedures. A plot showing the heat flux measured by the same sensor, 0.5 m above the floor, in five different tests can be seen in Figure 4.7.

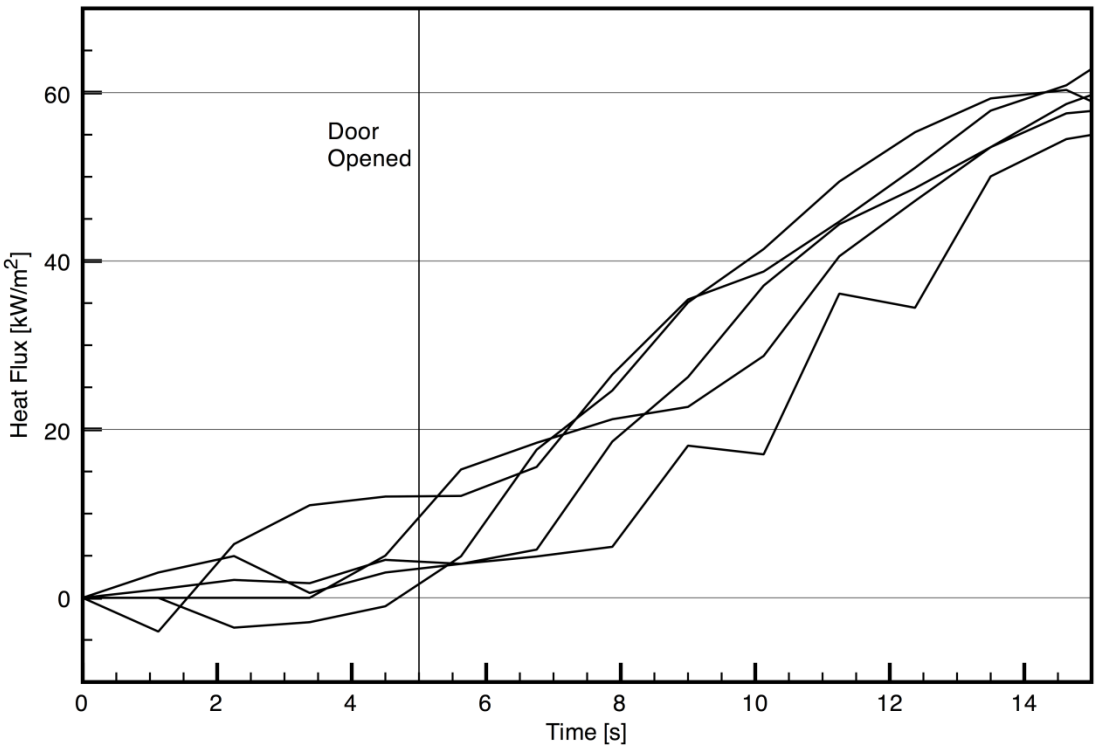

Figure 4.7. Heat flux measured just outside the compartment in ambient conditions for five tests.

In the plot, it can be seen that the heat flux is relatively uniform and low in all of the tests before the door is opened, which occurs at the 5 s mark. This is expected, as the door is somewhat blocking the sensor, so little heat flux is imposed on it. After 5 seconds, the measured heat flux increases relatively uniformly throughout all of the tests to a value around 60 kW/m^2 at 15 s, 10 seconds after opening the door. Once the door is opened, heat flux from the fire is imposed on the sensor. The fact that the measured heat flux is similar in all of the tests suggests the fuel load and fire conditions are establishing consistent conditions in the compartment throughout the experiment. The heat flux plot also confirms that the operation of the doors is consistent from test to test, speaking to the repeatability of the test procedure.

4.6 Summary

The consistent upper layer temperature curves developed during the fire growth phase in these experiments, along with the uniformity of the compartment environment, suggest that both the fuel load and the compartment set-up enable repeatable fire tests to be conducted in the compartment, as long as the doors are set to ensure appropriate ventilation conditions within the compartment during the fire growth phase. The average upper layer temperature achieved just prior to suppression in all of the 52 suppression tests conducted was 910 K ±38 K, and is above the target upper layer temperature of 900 K. Overall, the uniformity of the compartment conditions, the high and repeatable upper layer temperatures achieved, and the uniformity of the heat flux out the compartment opening indicate that the present experimental set-up is very well suited for studying the effects of different initial attack suppression methods on the compartment environment and firefighter.

Chapter 5

RESULTS

5.1 Repeatability

The repeatability of the compartment fire environment and any other features of the experiment, such as the methods of suppression, are key issues in conducting large-scale experiments to study fire suppression. The repeatability of the fuel load has been discussed in terms of heat release rate in section 3.3.2, in terms of upper layer temperatures in sections 4.3 and 4.4, and in terms of heat flux inside and out of the compartment in sections 3.3.2, and 4.5.2, respectively. These measured results have shown that the fuel load produces both repeatable heat fluxes and temperatures in the compartment, and consistent heat fluxes out of the compartment door. Therefore, the only other significant feature of the experiment where repeatability needs to be considered, is that of the suppression methods themselves.

5.1.1 Characteristics of Suppression

Repeatability of the suppression experiments is determined by examining the effect of each suppression activity on the vertical profile of compartment temperature across a series of repeat tests. Data are compared by determining differences in average temperature before and during suppression for various heights above the compartment floor as measured using the vertical thermocouple rakes. The average temperature at a given vertical height in the compartment before suppression is taken as the average of temperatures measured on all six thermocouple rakes at that height recorded 10 seconds before suppression begins, i.e., before the compartment doors are opened. The temperature during suppression is taken as the lowest average temperature over the six thermocouples at the corresponding height during a suppression activity. By way of example, Figure 5.1 shows the difference in average temperature in the compartment before and during suppression for three straight stream penciling tests using 10.03 kg, 11.52 kg, and 10.58 kg of water for tests T1, T2, and T3, respectively.

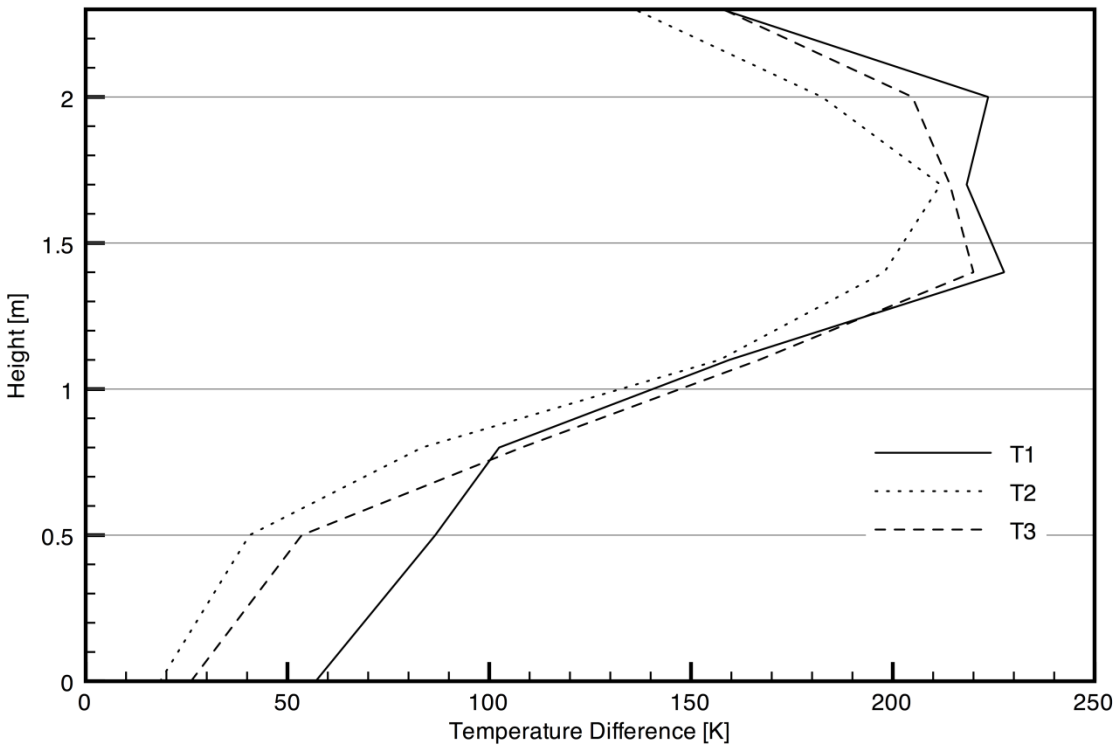

Figure 5.1. Average compartment temperature difference for three penciling tests.

All three curves in the figure follow the same trend, with a small amount of cooling occurring from the floor to 0.7 m, followed by a linear increase in cooling occurring past the interface height at 1.2 m, to around 200 K at 1.4 m above the floor. The peak cooling occurs between 1.4 and 2.0 m above the floor, where temperature reductions between around 200 and 230 K are achieved for all three tests. Between the 2.0 m mark and the ceiling (2.3 m), the reduction in temperature decreases to around 150 to 160 K for the three tests.

The similarity among the three curves over the entire compartment indicates that the cooling effect on the compartment is very similar across the three penciling tests. It is interesting to note, however, that the largest temperature reduction, at 1.4 and 2.0 m, is seen for the test using the smallest amount of water, T1. This can perhaps be explained by examination of bulkhead temperatures measured 2.2 m above the floor during each suppression test, as plotted in Figure 5.2.

Figure 5.2 shows that the measured bulkhead wall temperature increases slightly from 0 to 15 seconds for all tests, which is before suppression occurs. This temperature rise is caused because the fire is continuing to heat the wall, as temperatures between 550 and 563 K are measured during the three tests just prior to suppression. As suppression occurs, the temperature drops rapidly for all of the tests to a minimum value of between 480 and 500 K (depending on the test), at around 2 seconds after suppression, which is at the end of the first 2 second penciling spray.

During the two second break between suppression applications, the bulkhead temperature rises to between 525 and 540 K, after which it is lowered further to around 410 K for all three tests at the end of the second 2 second suppression application. After all of the suppression has ceased, at around the 21 s mark, the temperature of the bulkhead rises to between 460 and 480 K in approximately 2 s, and then rises more slowly to between 500 and 514 K at 45 s, depending on the test.

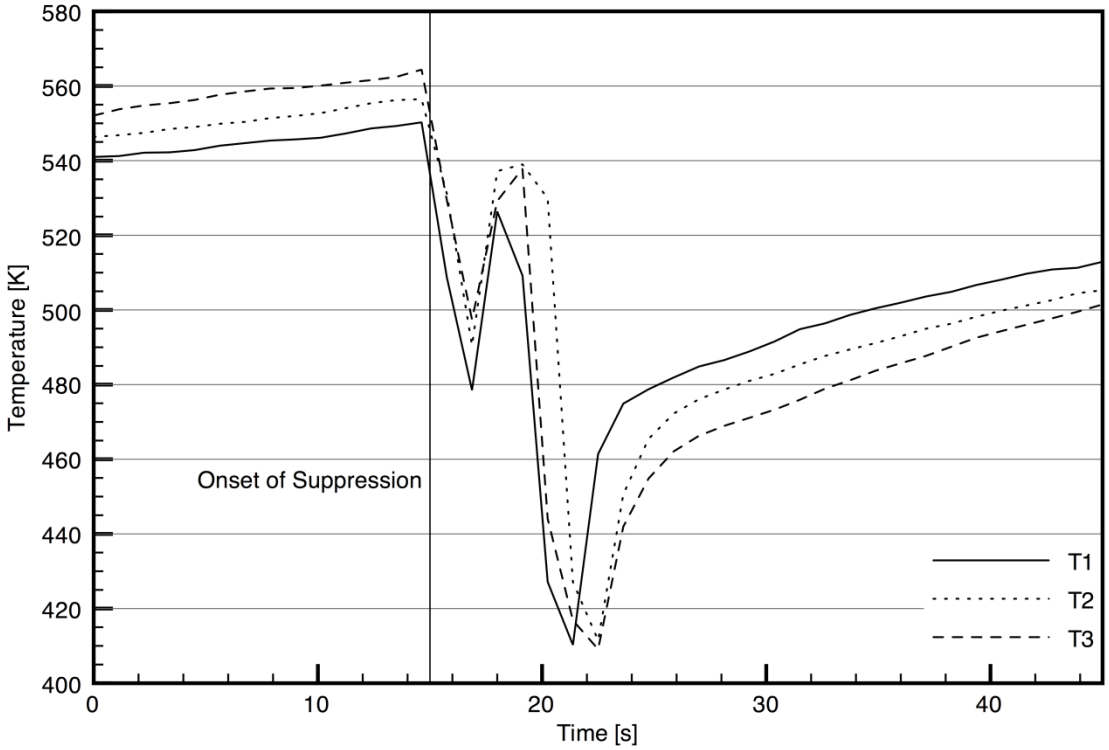

Figure 5.2. Upper bulkhead wall temperature for the three penciling tests.

The measured bulkhead wall temperature increases as the tests progress from T1 to T3, with initial measured bulkhead temperatures of 540 K for T1, 546 K for T2, and 552 K for T3, while the lowest temperature recorded during suppression remains fairly constant. Referring to the energy balance discussed in the background section, this suggests that, since the suppression water is directed at the bulkhead wall in all tests, even though more water is used in tests T2 and T3 than in T1, additional energy (water) goes to cool the bulkhead in the latter two tests. As additional water is cooling the bulkhead, less is available to cool the compartment gases, resulting in the apparently reduced cooling of the compartment gases in tests T2 and T3 compared to T1, even though less water is used in T1. These consistent trends suggest that the cooling of the compartment by water suppression is reasonably similar when the same suppression method is employed in repeated tests.

Along with the straight stream penciling tactic, the repeatability of the suppression can be examined by looking at similar suppression tests for the narrow fog and wide angle fog methods. The average temperature difference in the compartment between times before and during suppression for two narrow fog settings where two 2 second bursts are applied can be seen in Figure 5.3, and average temperature difference in the compartment before and during suppression for two continuous wide angle fog tests can be seen in Figure 5.4.

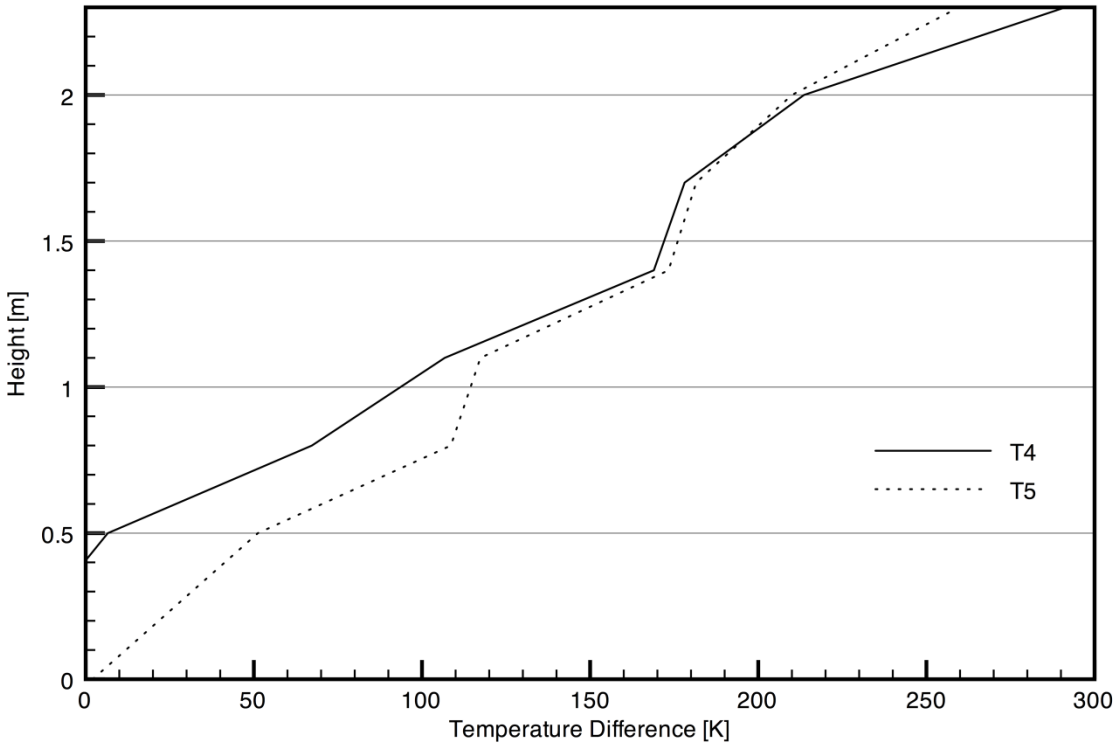

Figure 5.3. Average compartment temperature difference for two narrow fog applications.

Figure 5.3 shows that the reduction in temperature during suppression follows a reasonably linear trend from the top of the compartment, where the largest amount of cooling is observed, to the bottom of the compartment, where no cooling is observed. A similar volume of water was applied in these two narrow fog applications (13.05 kg and 12.87 kg for T4 and T5, respectively), which is consistent with the similarity of the compartment cooling.

The compartment cooling achieved in the two wide angle fog tests (Figure 5.4) follows the same trend as shown for the penciling tests in Figure 5.1. The maximum cooling in these tests is observed between 1.4 and 2.0 m. Lower amounts of temperature reduction are observed between 2.0 m and the ceiling, and below 1.4 m to the floor. A relatively linear decrease in temperature reduction is observed as height in the compartment decreases for both the tests.

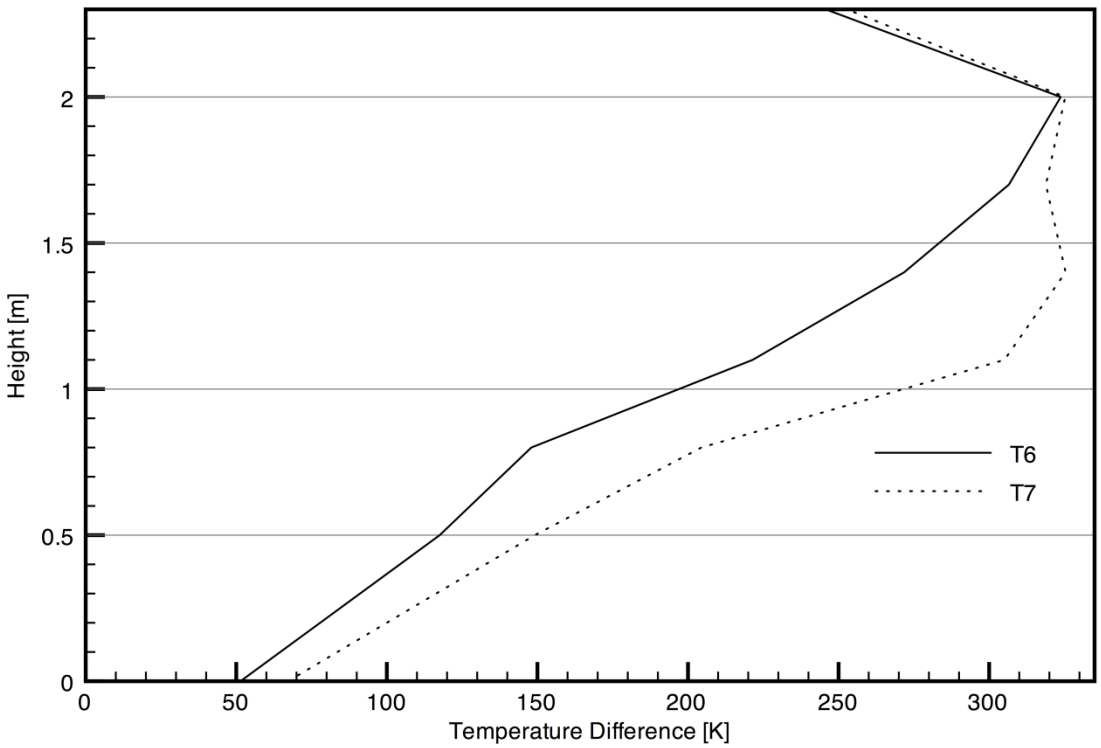

Figure 5.4. Average compartment temperature difference for two wide angle fog applications.

For the two wide angle fog suppression attacks shown in Figure 5.4, a larger amount of water was used in test T7 (14.03 kg) compared to T6 (11.41 kg). This difference was due to slightly varying application times induced by the human operator. Figure 5.4 shows that the suppression action involving more water, T7, leads to a greater cooling of the compartment that test T6, which is consistent with the theory on the amount of water used.

The comparison of these three sets of tests indicates that the suppression can be considered both consistent and repeatable for each of the different suppression stream angles used. Even though the average compartment cooling is not exactly repeatable for very similar quantities of water, the results correlate very well considering the scale of, and inherent variability in, such large fire experiments.

5.2 Suppression Impact on the Compartment and Firefighter Environments

Once all aspects of the repeatability of the experiments are confirmed, the overall impact of each suppression method on the compartment environment can be assessed. From this, measures of the effectiveness of each of the different methods can be made. To compare the different methods in terms of compartment cooling, the average cooling at different heights in the compartment is determined by averaging the temperatures recorded on all six vertical rakes at each

height in the compartment, i.e. averaging temperatures across each of eight horizontal slices in the compartment and recombining them into a single vertical temperature profile. The temperature difference due to suppression is determined by subtracting the vertical profile exhibiting the lowest temperatures from the temperature profile recorded 10 seconds before suppression begins. This temperature difference is used because the initial compartment temperature varies from test to test. Further, the average temperature at 10 seconds before suppression is taken as the initial temperature to ensure that the compartment doors have not been opened, therefore, ensuring similar temperature conditions in the compartment for the analysis of each test. The lowest average recorded temperature profile is used to characterize compartment cooling independent of the time after suppression because the different suppression actions occur over different durations of time, causing the lowest recorded temperature to occur at different times for different methods.

Along with the overall cooling of the compartment, the temperatures observed by the 'firefigher' are also compared. These temperatures were measured by the thermocouples located outside the compartment. Both of the thermocouples on the uncovered side of the firefighter followed the same trends, and since the upper one, at 0.5 m above the ground, always measured a higher temperature than the lower one, only the upper one is included in the subsequent analysis.

Five different suppression methods are compared in this section. The five methods considered are a full straight stream for 5 seconds, a 'penciling' method which involves two 2 second bursts using a straight stream with a 2 second break in between, a full narrow fog application for 5 seconds, a full wide angle fog application for 5 seconds, and a wide angle fog burst application. The primary wide angle fog burst application involved four 0.5 – 1 second bursts with a 2 second break in between each one. The four burst method was used to keep the water quantity similar for all five methods.

All suppression methods were initially applied at an angle of 20° from horizontal, which directs the water at the common seam between the back wall and ceiling of the compartment. The pump discharge pressure was set at 425 kPa and the nozzle was set to 230, resulting in a 411 kPa nozzle discharge pressure for the tests. Further tests were run with the water applied at an angle of 30° to assess any differences resulting from a change in the angle of attack. Tests were also conducted at a nozzle discharge pressure of 700 kPa to assess the effects of increased nozzle pressure on the results. The influence of the variation in angle of attack and nozzle pressure are discussed after the initial comparison of the five suppression methods.

5.2.1 Initial Impact of the Suppression Methods

The average temperature differences observed in the compartment for each of the five suppression methods, straight stream (SS), penciling (P), narrow fog (NF), wide angle fog (WF), and burst (B), can be seen in Figure 5.5.

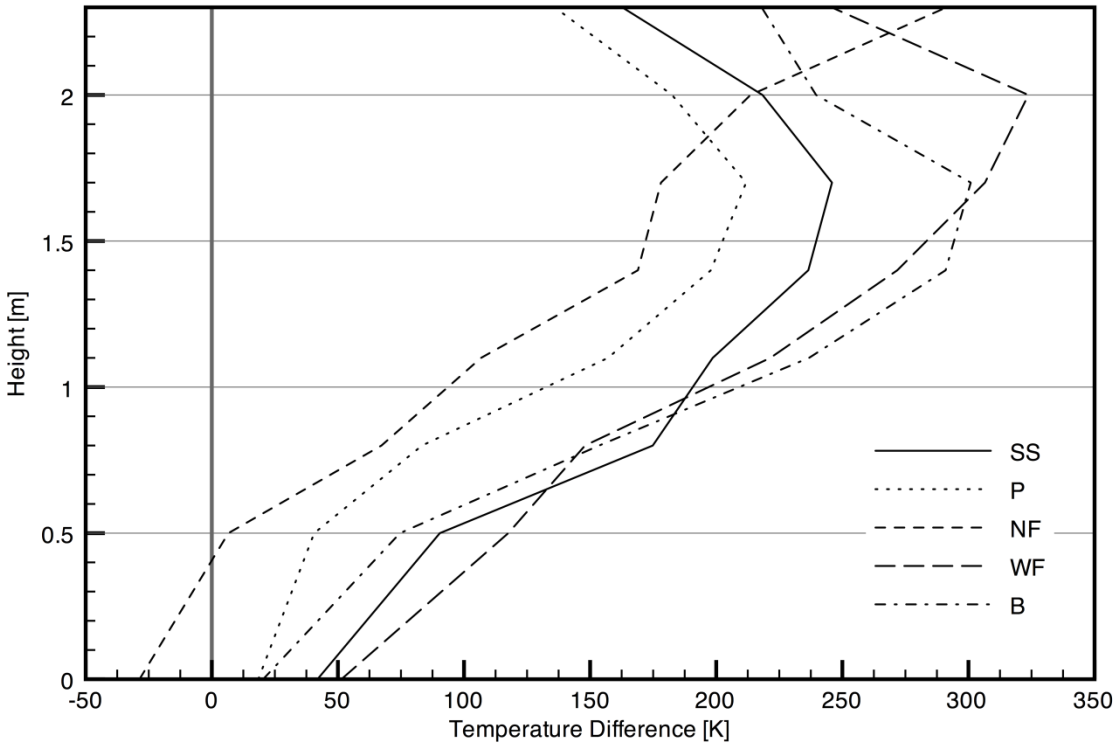

Figure 5.5. Average compartment temperature difference for each suppression method.

The total water used in these tests ranged from 11.5 to 13.5 kg, depending on the method used. Figure 5.5 shows that the greatest reduction in compartment temperature is observed for the wide fog test, particularly near the ceiling. The minimum temperature reduction near the ceiling is observed for the penciling method of attack, while the least effective method from the floor up to 1.8 m is the narrow fog attack.

The results for all methods except narrow fog follow similar trends, with maximum cooling seen between 1.5 to 2.0 m above the floor. Maximum cooling of both the air and products of combustion in the compartment is observed at this height because of the initial temperatures, angle of suppression, and compartment ceiling material. Before suppression, the hot layer exists in the compartment above the 1.2 m mark, as shown in section 4.1. As such, with the angle of the suppression attack directed into the upper layer, more significant reductions in temperature occur relative to the initially cooler lower layer. However, as mentioned previously, the maximum cooling occurs below the ceiling for 4 of 5 suppression methods, at 2.0 m above the floor instead

of 2.3 m, which can partially be attributed to the properties of the ceiling. The temperature of the insulated steel ceiling above the fire load can exceed 1000 K during the tests. As the suppression water is directed at the location where the wall and ceiling meet, it will interact with and directly cool gases in the upper layer, but less water will be directly applied to the ceiling. The hot ceiling will continue to radiate heat to the gases near it, increasing their temperature during suppression, as observed in Figure 5.5.

The cooling observed for both the wide angle fog and the burst method are very similar in the lower layer (below 1.2 m). In the upper layer, the continuous wide angle fog method cools the gases at the 2.0 m height more than the burst method. The straight stream method again cools the lower layer in a fashion similar to the two wide fog methods, but is less effective in the upper layer, with 50 to 100 K less cooling, than either fog method. Throughout the entire compartment, cooling induced by the penciling tactic is constantly 50 to 150 K less than that of the wide fog and burst methods, but follows the same overall trend in cooling with vertical height as the other three wide fog and straight stream initial attack methods.

In contrast to the other methods, the narrow fog suppression curve shows maximum cooling at the top of the compartment around 300 K, with a quasi-linear reduction in cooling with decrease in height ending with a negative temperature difference in the lower layer. This suggests that the narrow fog tactic created an imbalance in the compartment environment leading to an increase in temperature in the lower layer. The temperature imbalance (increase in the lower layer) is most likely caused by the suppression water from the narrow fog essentially 'pushing' the hot layer down towards the floor in the area of the fuel load (where the largest increase was observed). This phenomenon is only observed for the narrow fog suppression because of the nature of the spray compared to the others. The straight stream tactic penetrates the hot layer gases, and therefore does not have a displacing effect. The wide fog tactic displaces gases in both the upper and lower layers because of the wide spray and rapid production of steam. The narrow fog spray does not penetrate the upper layer because there is some width to the stream, but it apparently does displace the upper layer as shown by the temperature increase in the lower layer in Figure 5.5.

The velocity of the gases exiting the compartment measured by the bi-directional probes also support this theory. During straight stream suppression, no change to the velocity outflow is measured, suggesting the stream penetrates the layer and does not disrupt gas movement to a large extent. During wide fog suppression, gas is flowing out of the compartment through the entire opening except right at the nozzle height, suggesting the rapidly expanding gases and steam overwhelm the compartment volume. Lastly, during narrow fog suppression, an increased amount of gas is exiting the compartment at times in the upper portion of the lower layer during suppression, suggesting the increased steam or the spray may be forcing the upper layer out of the compartment.

The temperatures measured just outside the door of the compartment can be used to determine the effect that each suppression method discussed in Figure 5.5 has on the firefighter. The temperature measured by the uncovered thermocouple positioned at 0.5 m off the floor for the five tests is plotted in Figure 5.6, along with the vertical line indicating the start of suppression for each test.

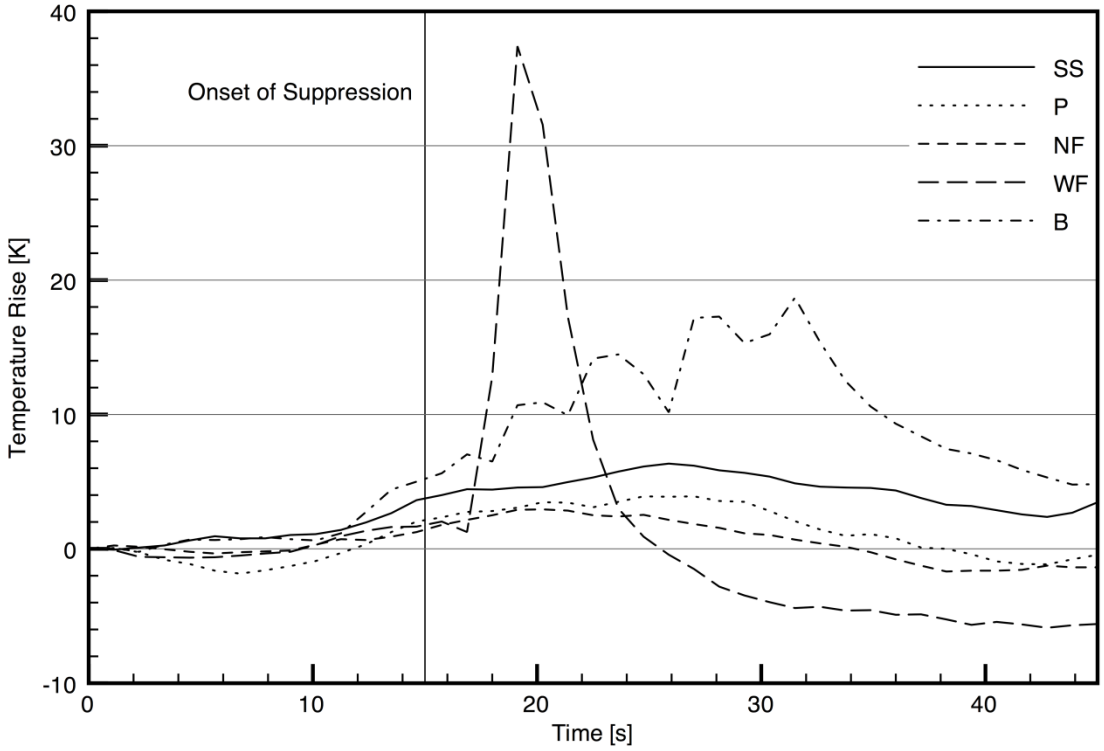

Figure 5.6. Typical temperature increase at the firefighter measured using five different suppression methods.

Figure 5.6 shows that for straight stream, penciling, and narrow fog suppression, the temperature measured just outside the compartment door does not change by an appreciable amount, with only a 5 to 7 K increase observed. In contrast, when a wide angle water spray pattern is used, whether applied in a continuous or burst mode, temperature increases of almost 40 K and 20 K are measured, respectively.

The wide angle methods show such a marked increase in temperature at the firefighter in comparison to the other methods because of the rapid expansion of the steam created in the compartment. No increase in lower layer temperature was observed for the two wide angle methods, suggesting that the created steam exits the compartment. The same increase in temperature at the firefighter was not observed for the straight stream methods because much of

the water penetrates the upper layer and does not form steam as quickly. No temperature increase was observed for the narrow fog method because the upper layer gases were displaced to the lower layer of the compartment in the area of the fuel load. The lower layer gases then flowed out of the compartment door, and less steam was created.

The rapid increase and decrease of the temperature observed for the continuous wide angle fog suppression method (approximately 8 s of elevated temperature) suggests that not as much steam is created compared to the burst method, which shows an increased temperature at the firefighter for over 25 s. The continuous method may be producing enough steam to saturate the compartment, while when using the burst method, the temperature is able to re-establish somewhat before the next burst, and so more steam can be generated. This, combined with the larger peak temperature observed, suggests that the continuous method initially cools and removes the gases and steam more quickly than the burst method, but after the suppression action has ceased (5 s), there is no more gas movement out of the compartment, as expected. The burst method continues to apply water into the compartment up until the time of the last burst, around the 32 s mark, indicated by the last temperature increase at the firefighter at that time. Therefore, as shown in Figure 5.6, the burst method does not create as high a temperature at the firefighter at any time compared to the continuous method, but it does cause the increased temperature to be sustained for a longer period of time.

5.2.2 Impact of Varying the Burst Method

Figure 5.5 shows that the burst suppression method produces similar, although lower, levels of cooling in the compartment compared to that observed for the continuous wide angle fog method, while producing half as much peak temperature increase at the firefighter (Figure 5.6). In order to examine this more closely, and to determine if a different number of bursts would be more apt to cool the compartment while producing little effect at the firefighter, a number of tests were run using different numbers of 0.5 to 1 second bursts. The average compartment cooling for tests involving 2, 3, 4, 5, and 6 bursts, in comparison to the continuous wide angle fog application (WF), can be seen in Figure 5.7. Temperature increases just outside the compartment door for the burst and continuous methods are shown in Figure 5.8.

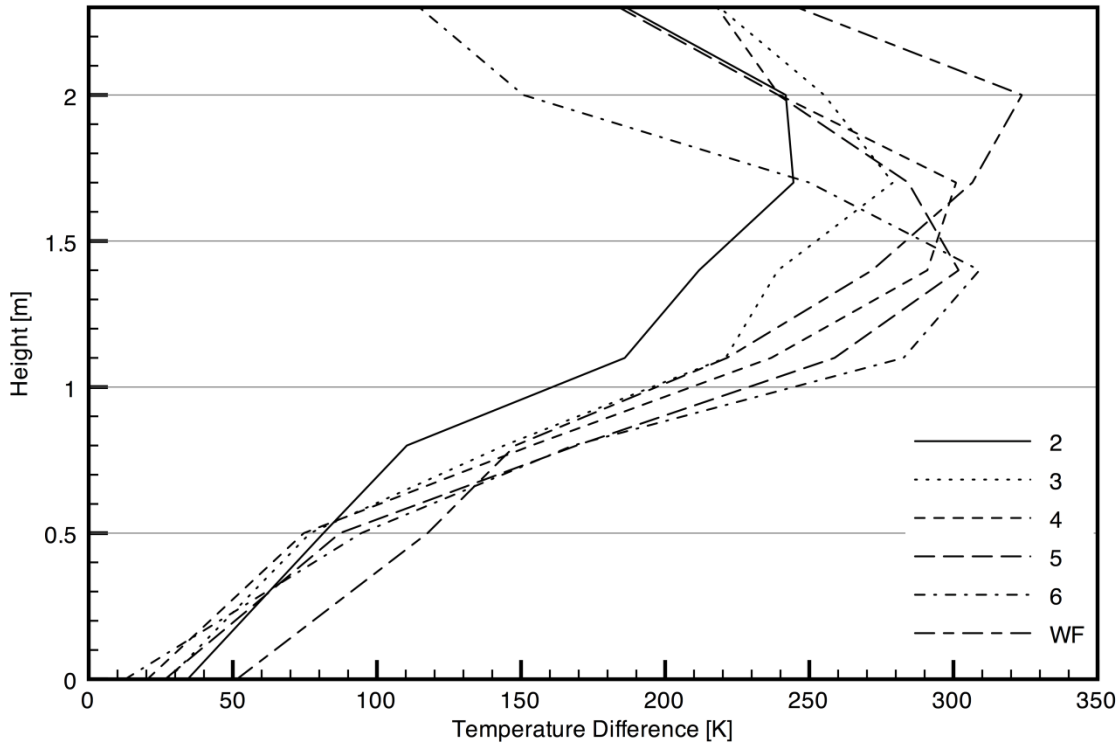

Figure 5.7. Average compartment temperature difference for different numbers of bursts.

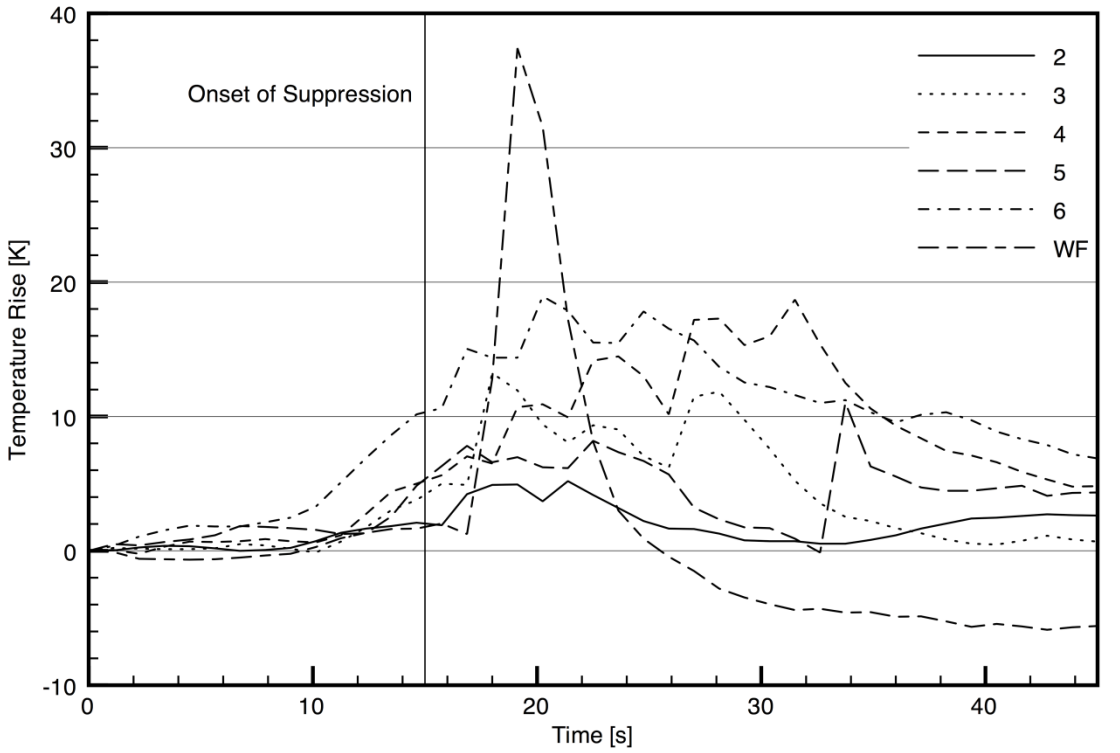

Figure 5.8. Temperature increase at the firefighter observed from suppression using different number of bursts.

Figure 5.7 shows that all methods achieved maximum cooling between 1.2 to 2.0 m above the floor of the compartment. All of the burst methods and the continuous method show a similar level of compartment cooling in the lower layer (below 1.2 m). As the lower layer is cooler than the upper layer, less temperature reduction is expected in that region. All of the methods use the wide angle fog setting, which applies water to both the upper and lower layers. The water applied to the lower layer, especially below 0.7 m, is able to cool to the same degree for each method, even when more water is applied.

In the upper layer, especially in heights ranging from 1.2 to 2.0 m, increasingly greater temperature reductions are observed as the number of bursts (and hence amount of water) increases from 2 to 4, which translates into water quantities of 7.20, 10.49, and 12.77 kg for 2, 3, and 4 bursts, respectively. As the number of bursts increases to 5 and 6 bursts, however (water quantities of 16.06 and 19.60 kg, respectively), the degree of cooling in the upper layer of the compartment is not increased, and even decreases above 1.5 m when 6 bursts are applied. This might be explained by considering the duration of the suppression, 20 s for 6 bursts compared to 6s for 2 bursts, as the longer duration test allows the fire to re-establish as additional oxygen is forced into the compartment via suppression. Another possible reason is that as more and more mist is added to the compartment, the water droplets start to collect in the air, come into contact, and grow so they are no longer as effective at cooling the gases in the compartment.

Lastly, it can be seen in Figure 5.7 that none of the burst methods are able to produce as much cooling as the continuous method, in which 11.41 kg of water is applied to the compartment, which is less than the quantities of water applied in the methods using 4, 5, and 6 bursts. This suggests that even though more water is added when more bursts are used, the overall cooling is not as substantial, possibly because the fire is still generating heated gases in the compartment throughout the bursting methods (longer duration of suppression), and possibly because the burst methods are not generating the same quantity of steam in the hot layer of the compartment. The latter possibility can be examined by considering the temperature just outside the compartment door for the six methods, as shown in Figure 5.8.

In Figure 5.8, it can be seen that as each burst is applied to the compartment for the different methods, a spike in temperature at the firefighter is observed, i.e. two spikes are observed when two bursts are applied. As the number of bursts increases from 2 to 6 bursts, the temperature increase at the firefighter also increases, except for the 5 burst test. In this test, the temperature increase at the firefighter is between those for the 2 and 3 burst methods until around 34 seconds, where it spikes to near what was seen for the 4 and 6 burst methods. A review of the data for the 5 burst test revealed no explanation for this apparently anomalous behaviour.

None of the burst methods tested display as large and as sudden of a temperature increase at the firefighter as the continuous wide angle fog test, suggesting that this method creates relatively more steam in the compartment which is forced through the door opening, impacting directly on the firefighter. By not creating as much steam as the continuous wide fog method, the bursts are not able to cool the compartment as much; however, they also do not produce as high a temperature spike at the firefighter.

5.2.3 Impact of Increased Discharge Pressure

For the comparison of the five attack methods and the burst amount comparison discussed above, a nozzle discharge pressure of 410 kPa was used. This discharge pressure was chosen in order to maximize the effectiveness of the experiment, by introducing an amount of water that would still cool the compartment while not introducing so much suppression water that the compartment was essentially flooded. In North America, however, nozzle discharge pressures are more typically set at around 700 kPa, which is the discharge pressure for which nozzle performance is optimized [39]. For this reason, one set of suppression tests were conducted at a nozzle discharge pressure of 700 kPa, and a nozzle setting of 360. These settings result in a 1.4 to 2.2 times increase in the volume of water applied during each suppression test, depending on the flow pattern setting of the nozzle and the variation in application time over each method. The temperature difference in the compartment for all five of the initial attack suppression methods at the two different discharge pressures is presented in Figure 5.9.

For the straight stream method, the higher discharge pressure produces a 1.9 times increase in the amount of water. Figure 5.9 shows that this resulted in a similar amount of cooling in the lower part of the lower layer, up to a height of 0.7 m, and a much larger increase in cooling above that point. The maximum temperature difference of 150 K occurred at the ceiling of the compartment, with a nearly 100 K difference in temperature occurring throughout the rest of the upper layer. The increased cooling is due to the increase in water applied to the compartment. As the suppression is aimed towards the ceiling, the increased amount of water hits the ceiling and disperses, cooling the upper layer and ceiling more than the lower pressure stream.

A similar trend is noticed for the penciling method at the higher discharge pressure, with very little difference occurring below 0.7 m, and a large difference in cooling of the upper layer. However, at the higher pressure, the penciling tactic shows a greater amount of cooling at 1.4 m, with an increase of around 115 K. Throughout the rest of the upper layer, an increased amount of cooling is evident, but only at around 50 K difference, even though 2.14 times more water was applied than at the lower pressure.

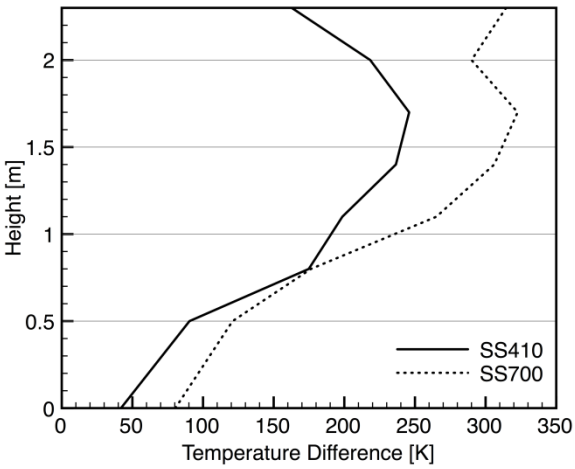

Straight Stream

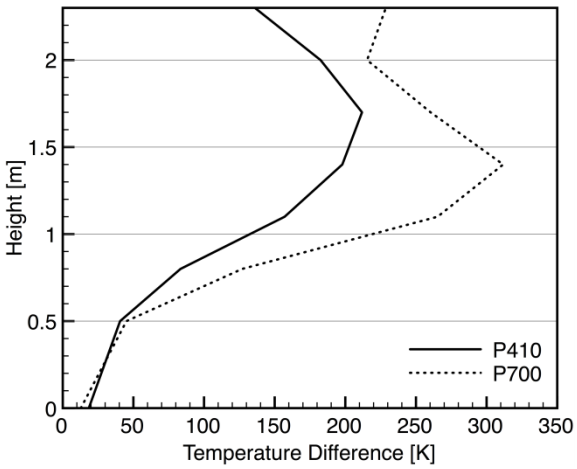

Penciling

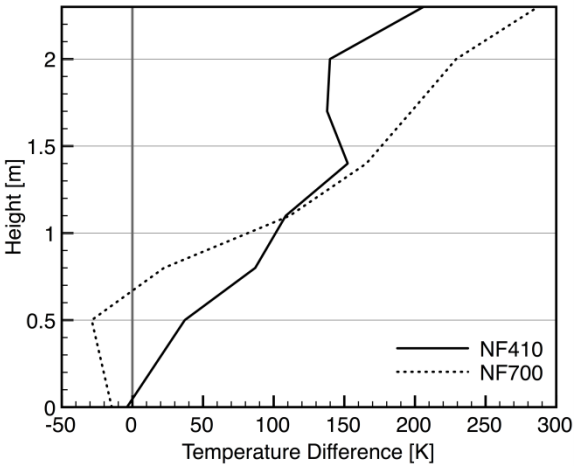

Narrow Fog

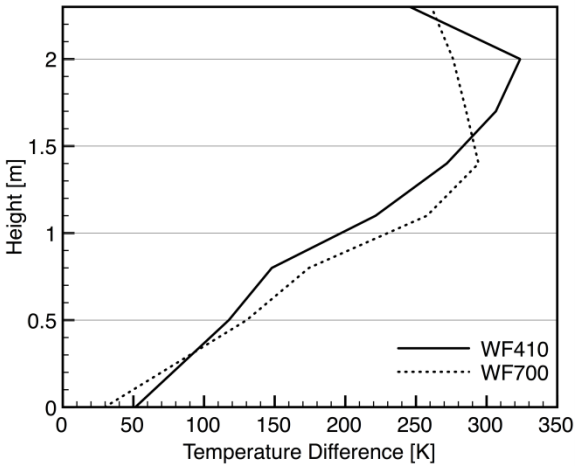

Wide Fog

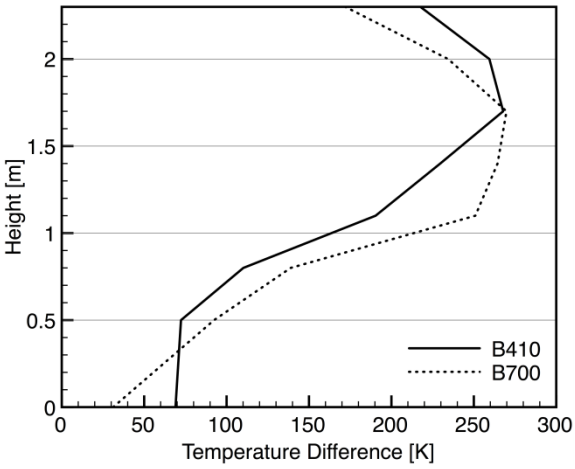

Burst

Figure 5.9. Temperature reduction in the compartment observed for the five suppression methods at two different discharge pressures, 410 and 700 kPa.

The narrow fog method shows an increase in the level of cooling in the upper layer of the compartment at the higher pressure, but a marked decrease in the level of cooling of the lower layer. This suggests that at the higher pressure, the narrow fog method is even more likely to displace the hot upper layer gases into the lower layer of the compartment, as highlighted by the 30 K increase at 0.50 m above the compartment floor shown in Figure 5.9. In the upper layer (above 1.4 m), a fairly consistent temperature increase of around 80 K is observed for the high pressure narrow fog application over the lower pressure application. In these two tests, 1.41 times more water was applied during suppression at the higher pressure. The fact that this amount is lower than that applied in the two straight stream methods could explain why only the upper layer above 1.4 m displays an increase in the amount of cooling, and not more of the upper layer.

Unlike the other methods, both wide angle fog methods show very little increase in the amount of cooling achieved at the higher water pressure. For the two tests, one using the continuous and one the burst method, increases in water quantity of 1.7 and 2.2 times were measured, respectively. The fact that no increased cooling was observed suggests the wide angle fog application was already saturating the compartment such that additional water was simply 'wasted', whether it is getting pushed back out of the compartment, or simply falling to the compartment floor. There may also be a difference in droplet formation, depending on the discharge pressure, which could influence the cooling process.

The temperature measured 0.5 m above the floor just outside the compartment is also compared for the tests at the two discharge pressures to help quantify possible impacts of the various suppression methods on a firefighter situated at the door. Of all the methods, the only one showing a marked difference at the firefighter is the narrow fog test. In this case, the temperature profiles measured just outside the door at the two different discharge pressures, as shown in Figure 5.10, indicate a marked increase in temperature at the firefighter at 20 s, for the high-pressure suppression only. Apparently, the narrow fog suppression method is very sensitive to discharge pressure, with the higher pressure producing significantly more thermal imbalance in the compartment. This results in much higher temperature in the lower layer that exit through the door and impinge on the firefighter.

It is not unexpected that the straight stream and wide angle fog methods do not show an increased temperature at the firefighter. Both straight stream methods do not displace the compartment gases, so no temperature increase is noticed at the firefighter. In the tests using the wide fog methods at the lower and upper nozzle pressures, no noticeable amount of increased compartment cooling was observed. As the level of compartment cooling is not increased, it is reasonable that there is no increase or decrease in temperature observed at the firefighter.

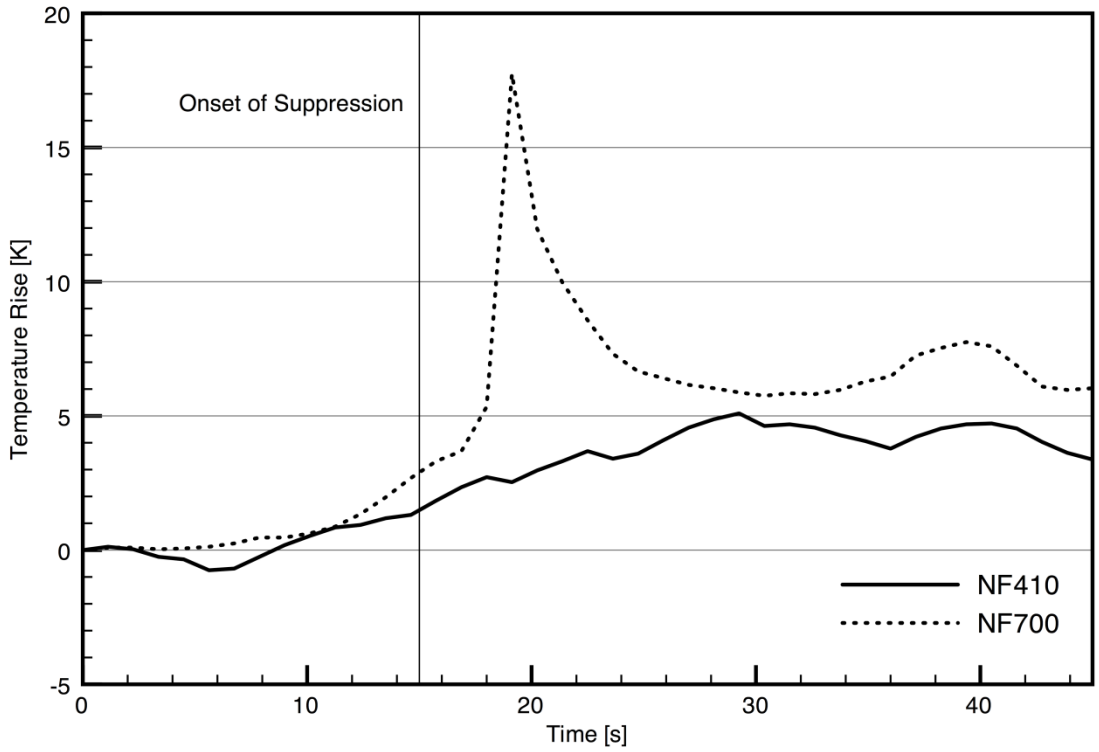

Figure 5.10. Temperature increase at the firefighter for the narrow fog suppression method at two pressures.

5.2.4 Impact of Increased Discharge Angle

In order to investigate the effect of the nozzle angle on the suppression effectiveness, a second set of tests using approximately the same methods and quantities of water (410 kPa nozzle discharge pressure) is conducted with the nozzle angle set at 30° above horizontal. In contrast to the test data for suppression with a nozzle angle of 20° above horizontal shown in the previous plots, the 30° angle results in the nozzle being aimed at the center of the ceiling of the compartment. The temperature reduction in the compartment achieved by each suppression method at the two different nozzle angles can be seen in Figure 5.11.

For tests involving the wide angle fog in both the continuous and burst application methods, very little change in compartment cooling was observed due to the greater angle. Since the same quantity of water was used for both sets of tests, this result suggests that the cooling effectiveness of the wide angle fog methods are not sensitive to the discharge angle. Apparently, as long as the nozzle is located at the door entrance and aimed into the compartment at some form of positive angle (towards some part of the ceiling), the mist from the wide angle fog will enter relatively evenly into both the upper and lower layers of the compartment. This results in very little change in the temperature observed in the compartment.

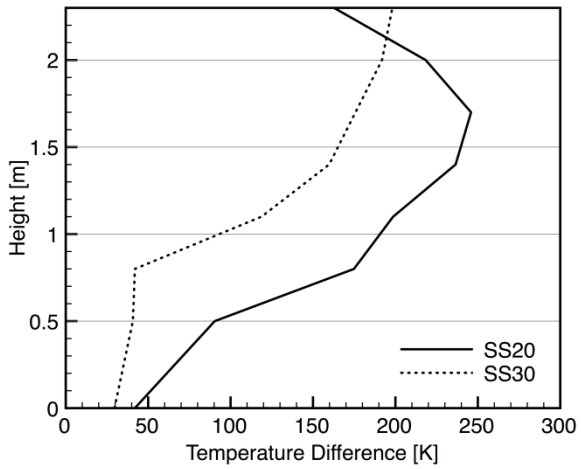

Straight Stream

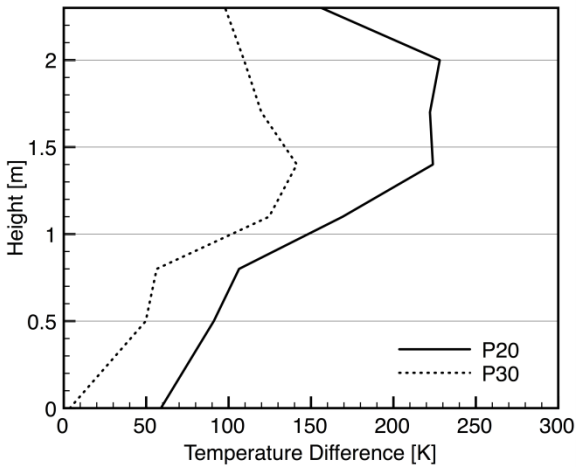

Penciling

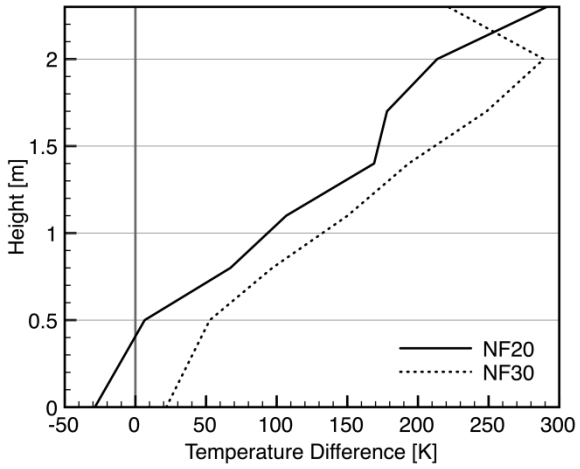

Narrow Fog

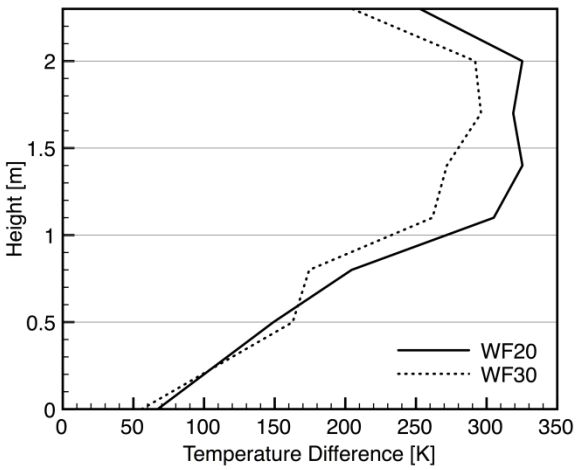

Wide Fog

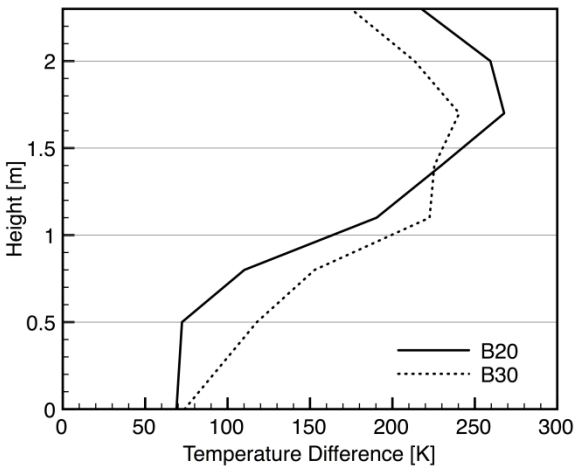

Burst

Figure 5.11. Average compartment temperature difference for the five suppression methods at two different application angles, 20 and 30° above horizontal.

For the narrow fog case, a slight increase in cooling (around 50 K) in the compartment up to the ceiling was observed, with a decrease in cooling at the ceiling. It is also noted in tests involving the narrow fog method that a temperature inversion is no longer observed at the greater application angle. This may result from the fact that as the suppression water is aimed towards the middle of the compartment, it is less effective at pushing the hot layer down, and essentially pushes it into the top of the compartment, resulting in a decrease in effectiveness of the suppression near the ceiling.

The straight stream methods, when applied both continuously and using the penciling tactic, show a decrease in the amount of cooling throughout all heights in the compartment, except at the ceiling for the continuous method. The decrease in temperature reduction likely occurs because the straight stream is no longer aimed at the hottest part of the compartment, directly over the fire. Unlike the wide angle fog method, the straight stream methods do not spread water everywhere in the compartment, but instead produce a more limited dispersal by bouncing the water off the ceiling. When aimed at the middle of the compartment ceiling, this dispersion makes the straight stream methods less effective at cooling those hot gases immediately above the fire.

The temperature measured just outside the door at 0.5 m above the floor for the two narrow fog suppression methods conducted at the two different nozzle angles is shown in Figure 5.12.

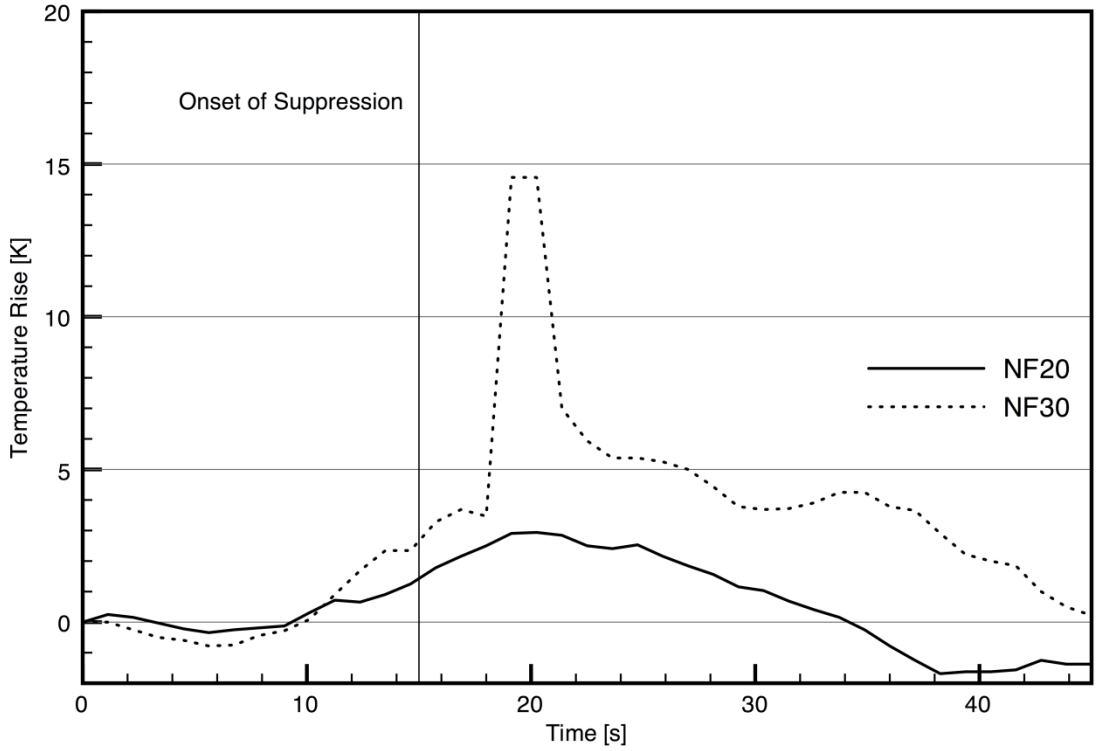

Figure 5.12. Temperature increase at the firefighter using two narrow fog tests, one at each angle.

Similar to the tests conducted at the higher discharge pressure, the narrow fog suppression method is the only one that shows a marked difference in temperature at the firefighter at the greater discharge angle. The increase observed when using the narrow fog method is surprising, as no thermal imbalance was observed at the greater angle. The wide angle fog methods produced similar temperature spikes at the firefighter because of the similar level of compartment cooling, and the fact that water is sprayed everywhere in the compartment when the wide cone angle is used. The straight stream methods both produced very little temperature increase at the firefighter because they penetrate the upper layer, do not disturb the hot gases, and do not push anything out the door.

5.3 Protected vs. Ambient Environment at the Firefighter

5.3.1 Temperature

Temperature profiles on either side of the firefighter sensor board can be examined to investigate the effects of each suppression method as measured by the exposed thermocouples just outside the compartment door, as well as the thermocouples under the firefighter turnout gear. The two exposed thermocouples were on the left side of center, and are denoted in following plots as either L0.30 or L0.50, where the 0.30 and 0.50 specify the height above the floor in meters. The thermocouples under the firefighter gear were on the right side of center, and are described as R0.30, R0.45, R0.60, and R0.75, where the number is again the height above the floor in meters.

A typical plot of the temperatures recorded during suppression under the firefighter gear can be seen in Figure 5.13. The results show that the temperature under the firefighter gear begins to rise even before suppression, as the environment outside the compartment is exposed to the radiation from the fire. The temperature under the firefighter gear continues to rise until the end of the test at a rate similar to that before suppression. The curves show no temperature spikes during suppression, suggesting that the primary cause of the modest increase under the firefighter gear over the 45 seconds is the radiation on the suit. This is not unexpected as the turnout gear moderates the temperature underneath, protecting from short-term temperature spikes. This trend is consistent for all of the suppression tests conducted, with the peak values of temperature rise measured under the firefighter gear ranging from 3.4 to 7.1 K, as shown in Table 5.1.

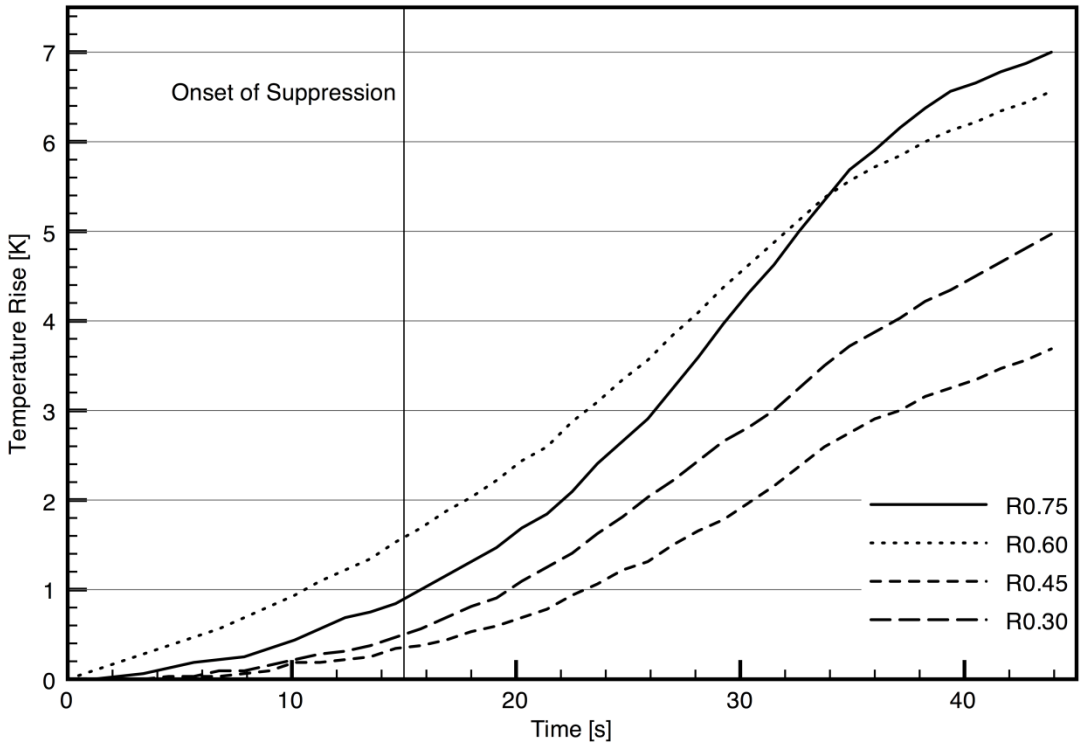

Figure 5.13. Typical temperature profile of the thermocouples under the firefighter gear for one suppression test.

Table 5.1. Typical peak temperature rise under the firefighter gear for each suppression method.

	Peak Temperature [K]		
	Baseline Test	Increased Pressure	Increased Angle
Straight Stream	6.1	3.9	3.4
Penciling	7.1	5.5	6.2
Narrow Fog	6.6	5.1	5.8
Wide Fog	4.8	5.9	6.5
Burst	7.0	4.4	3.6

Two plots typical of the temperature measured by the exposed thermocouples located in the firefighter environment can be seen in Figure 5.14 and Figure 5.15. Since these thermocouples respond better to the instantaneous changes in the ambient air, it is not surprising that the trends shown in Figure 5.14 and Figure 5.15 are different than those in Figure 5.13, which are moderated by the firefighter suit.

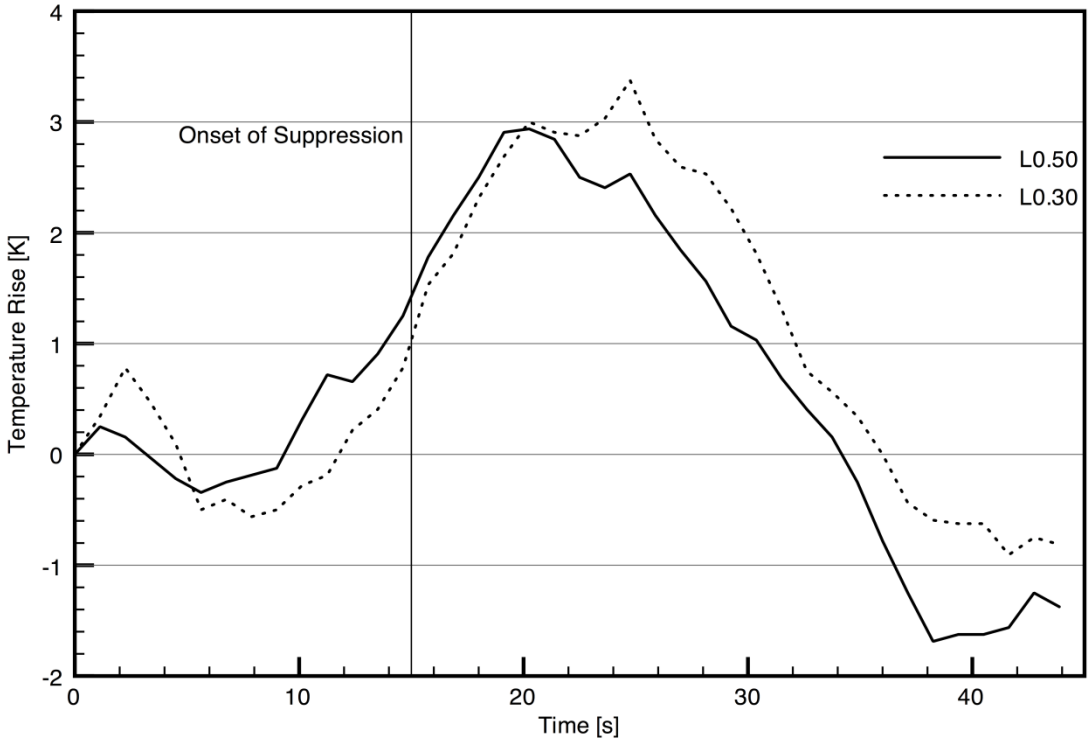

Figure 5.14. Typical ambient temperatures measured just outside the compartment using straight stream suppression.

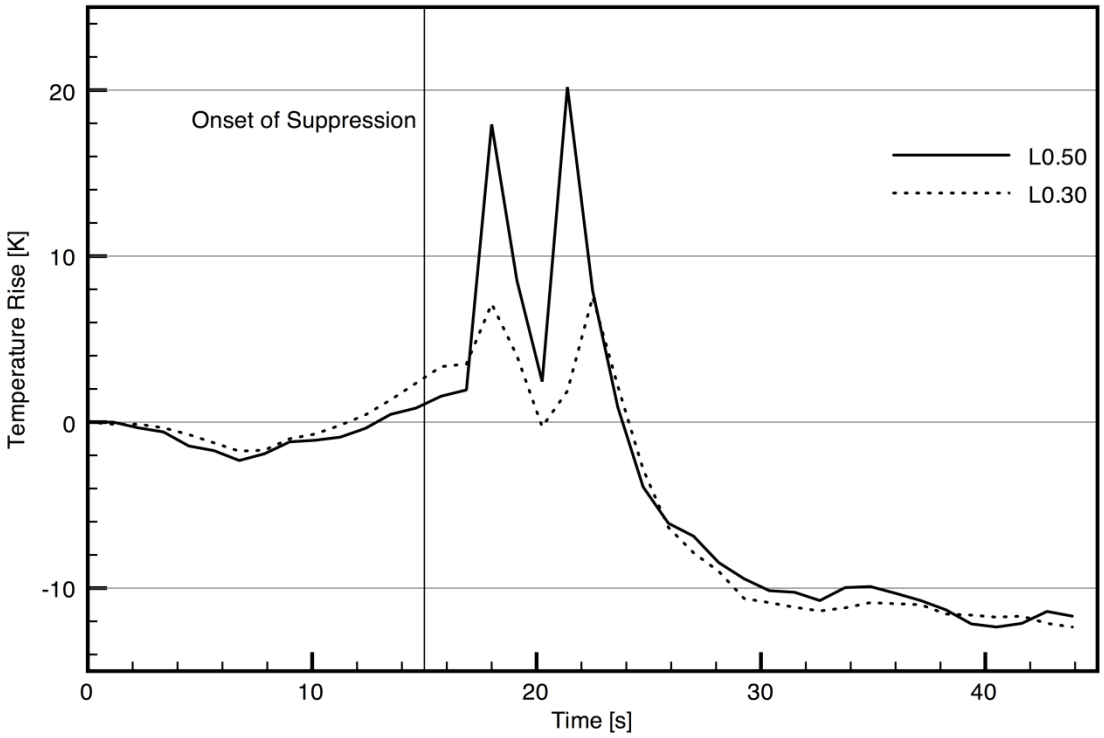

Figure 5.15. Typical ambient temperatures measured just outside the compartment using burst suppression.

Figure 5.15 shows that the effect of the straight stream attack on the ambient temperature just outside the door is minimal over the 45 second period. The increase in temperature is less than 1 K after the doors are opened and before suppression (5 to 15 s), and only 2 K higher to the peak at around 25 s. After this time, the temperature gradually reduces to, or just below, the initial level. The reason the temperature returns to a value below the original is that after suppression, there is more moisture in the air around the nozzle which is cooler than the air temperature, and reduces the ambient value to less than at the start of the test. This trend is seen in all of the suppression tests, regardless of the spray pattern used.

In Figure 5.15, a similar trend is noticed before suppression begins, with a small temperature increase from 5 to 15 s. This is followed by two spikes of nearly 20 K measured at the top thermocouple at around 18 and 23 s. Subsequently, the temperature rapidly decreases to a value over 10 K below the initial value. The two observed spikes are caused by the two wide fog bursts creating steam and forcing the heated gases and steam out of the door.

The typical peak temperature rise of the ambient air just outside the door measured for each suppression method and its variation is summarized in Table 5.2.

Table 5.2. Typical peak temperature rise of the ambient gases just outside the door for each suppression method.

	Peak Temperature [K]		
	Baseline Test	Increased Pressure	Increased Angle
Straight Stream	6.5	3.1	15.3
Penciling	7.1	3.8	5.0
Narrow Fog	3.4	17.7	14.5
Wide Fog	37.4	31.9	41.2
Burst	21.5	27.8	20.2

The tests involving the straight stream application, except the continuous method at the greater angle, show peak temperature rises similar to those under the firefighter gear (3 to 7 K). The narrow and wide fog methods, on the other hand, produce larger peak temperature rises, except for the initial narrow fog test. The larger peak temperature rises measured for the narrow fog, wide fog, and burst tests results from the steam created, which is forced out the door by expansion within the compartment. It should be noted, however, that even though increased peak temperatures of the ambient gases were noted, the temperature rise under the firefighter jacket was similar for all the tests, whether the straight stream, narrow for, or wide fog was used.

5.3.2 Heat Flux

The plots of the heat flux measured by the skin simulant sensors follow much the same trend as those of temperature measured at the firefighter, except in the case of the sensors exposed to ambient air, in which a heat flux peak is measured when the door is first opened. This initial peak was discussed in the previous chapter, and an example plot is shown in Figure 5.16.

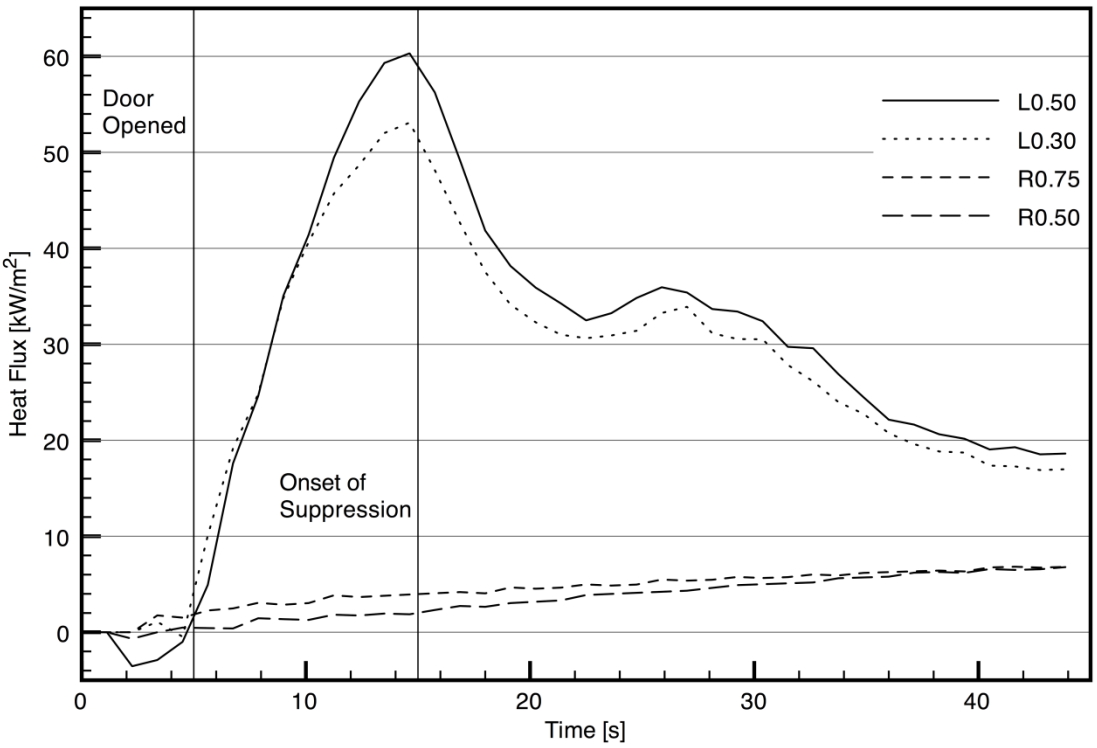

Figure 5.16. Typical heat flux measured by the skin simulant sensors for one suppression test.

In Figure 5.16, the results for the two sensors exposed to ambient conditions (L0.50 and L0.30), show that heat flux starts to increase when the door is opened (at 5 s), which exposes the sensor to the radiant heat flux from the compartment. The heat flux increases to its peak value before suppression (at 15 s), and then begins to decrease during suppression. A second, much smaller rise in heat flux is observed between 26 and 30 s. This peak is likely a result of the applied suppression, which moves more hot gases out of the compartment. All of the heat flux profiles for the sensors exposed to ambient follow this trend, where an initial peak is observed prior to suppression (caused by opening the door), and a second peak, sometimes much larger than that shown here, occurs as a result of the suppression action.

Figure 5.16 also presents typical profiles of heat flux measured by sensors that are underneath the firefighter gear. The heat flux measured by the two protected sensors, R0.75 and R0.50,

begins to rise as soon as the door is opened, and proceeds linearly as the test progresses. This trend is seen in all of the recorded heat flux data. The firefighter suit moderates the rise in heat flux such that no peaks are observed. Typical values of the peak heat flux measured during each suppression test for the sensors in the ambient are summarized in Table 5.3, and for the sensors under the firefighter gear in Table 5.4. It should again be noted that for the sensors exposed to ambient conditions, the heat flux peak that occurs when the door is opened is not considered in the table. Rather, values in the table are restricted to those measured as a result of the suppression activity itself. Also, since the assumptions required to validate the data measured by the skin simulant sensors cannot be verified, it is important to remember that the values presented may not represent actual magnitudes of heat flux, but can be used for comparison of incident heat flux among methods of suppression.

Table 5.3. Typical peak heat flux rise measured by the sensors exposed to ambient for each suppression method.

	Peak Heat Flux [kW/m^2]		
	Baseline Test	Increased Pressure	Increased Angle
Straight Stream	35.9	36.5	45.5
Penciling	42.9	31.6	42.9
Narrow Fog	24.0	40.4	24.6
Wide Fog	117.1	66.7	104.0
Burst	46.0	44.1	50.8

Table 5.4. Typical peak heat flux rise under the firefighter gear for each suppression method.

	Peak Heat Flux [kW/m^2]		
	Baseline Test	Increased Pressure	Increased Angle
Straight Stream	6.8	2.0	3.4
Penciling	5.6	4.7	4.5
Narrow Fog	5.0	5.5	4.9
Wide Fog	4.7	9.1	9.1
Burst	4.6	6.3	6.3

The values of heat flux measured by the sensors exposed to ambient suggest that very little change in incident heat flux is observed for the methods involving straight stream or narrow fog suppression. The wide angle fog burst method produces heat flux values slightly above those for the straight stream and narrow fog methods in all three tests, but only by 20 to 25%. In contrast, the wide angle fog continuous method produces very large peak heat flux values at the sensors exposed to ambient conditions, with heat fluxes that are 3 and 4 times larger than those of the straight stream and narrow fog methods for both the baseline test and the test at the greater nozzle angle.

This increase in heat flux may in part be caused by the continuous wide angle fog creating steam that flows out of the compartment, and in part by the change in the characteristics of the fire as the wide angle fog spray reaches the fuel load. Higher heat flux is also observed for the continuous wide angle fog method at higher pressure, but not as large as that observed for the other two wide angle fog methods. In the former, the heat flux may not be as large because the extra water added to the compartment at the increased pressure may absorb more heat before hot gases are pushed out of the compartment.

The heat flux measured by the sensors that are protected by the firefighter jacket are reasonably similar for nearly all tests. The exceptions were the continuous wide angle fog methods at higher pressure and greater angle, which produced noticeably larger heat fluxes (almost twice that of the average of the other methods). This apparent inconsistency might merit further investigation in future experiments.

5.4 Gas Concentration

The concentration of carbon monoxide (CO) exiting the compartment was measured in all of the suppression tests. The gas stream was sampled along the centerline of the opening at a position 0.3 m outside the door and 0.3 m above the compartment floor, to yield the concentration of carbon monoxide in the area of the firefighter. This data, in conjunction with temperature data measured at the firefighter sensor board, helps confirm whether or not any hot layer gases are pushed out the bottom of the door opening during each suppression test. The advantage of using the gas concentration along with the measured temperature is that the upper layer gases may be sufficiently cooled by the suppression water before being pushed out the door, with no appreciable increase in temperature measured near the firefighter. Sampling the concentration of CO, on the other hand, might determine if any hot layer gases reach the firefighter, even if they are cooled. A plot of the carbon monoxide concentration measured in the area of the firefighter for one entire set of suppression tests, i.e. one compartment burn containing 6 independent suppression tests, is given in Figure 5.17.

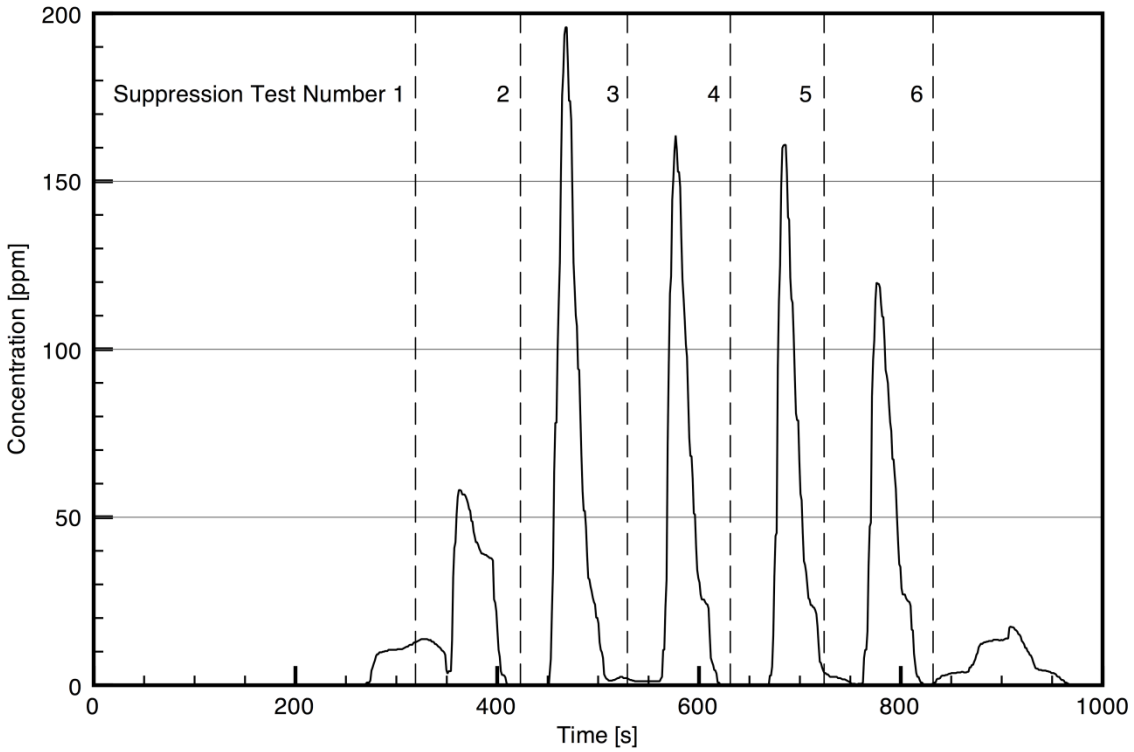

Figure 5.17. Carbon monoxide levels measured near the firefighter for the suppression tests conducted during one compartment burn.

From the start of the compartment burn until 260 s, there is no CO measured in the area of the firefighter. No measurable value of CO is expected during this fire growth phase, as ambient air is entering the compartment through the lower part of the door where the measurement is made. The first rise in CO is a small amount at less than 15 ppm, occurring from 260 to 350 s. This rise occurs because prior to suppression, the valves on the gas sampling line are opened and closed to ensure proper sampling. When the top line is opened, CO from the upper layer is sampled until the line is closed again, and the CO returns to almost zero just prior to the first spike due to suppression.

The first spike in CO due to the first suppression test occurs at 375 s into the plot, with a peak CO value of approximately 60 ppm. After the peak, the measured value of CO goes back to zero until a second peak in CO (of 195 ppm) due to suppression occurs at 475 s. This trend continues with the CO concentration returning to zero between peaks, in sequence with the third, fourth, and fifth tests at times of 590, 690, and 790 s, and peak CO values of 165, 160, and 125 ppm, respectively. At the end of the plot, a final, although much smaller peak in CO concentration is measured at 910 s with a value of 20 ppm, which is a result of the final suppression test conducted on the fuel load.

Along with the measured value of CO during the compartment burn, dashed lines indicating the time at which suppression started for each test in the compartment can be seen in Figure 5.17. These lines are numbered as 1 to 6, and the timing for each was determined via video data of the test. From these lines, it can be seen that the measurement of carbon monoxide by the sensor has a lag time on the order of 30 to 40 s in the experiment.

Instead of trying to analyze time dependent CO concentration, the peak CO concentration measured after a suppression test is used as an indicator of CO concentration for that method. The peak carbon monoxide concentration measured in all of the suppression tests can be seen in Figure 5.18.

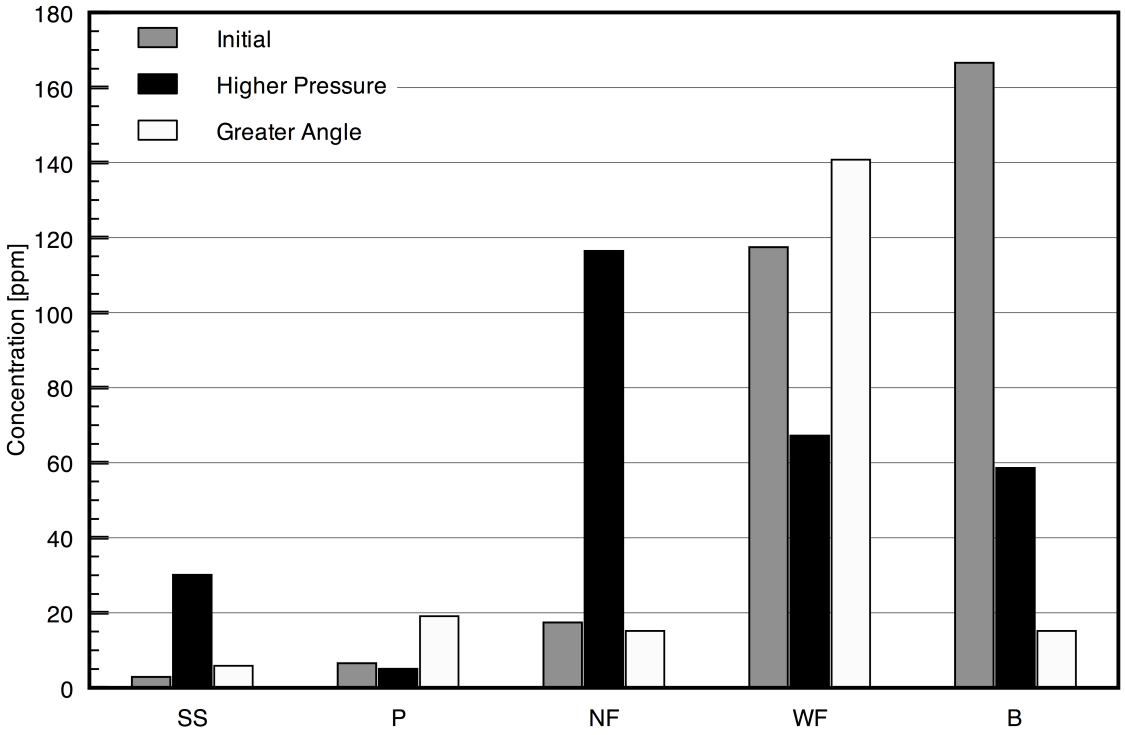

Figure 5.18. Peak carbon monoxide levels measured during each suppression method.

The level of CO measured during the straight stream and penciling tests is much less than for the other suppression methods. CO concentrations measured during the narrow fog test are also low for suppression at low pressure, but increase dramatically at the higher nozzle pressure. Conversely, the value of CO measured during the wide angle fog continuous and burst methods was very high for the low nozzle pressure, but lower when the high nozzle discharge pressure was used. The fact that very little CO was measured during burst suppression at the greater angle of attack is interesting, as an increase in temperature at the firefighter was recorded. This is also true

for narrow fog suppression at the greater angle of attack, where temperatures observed at the firefighter were similar to those at the higher pressure, and these temperatures were both much greater than those measured at the low angle and low pressure for narrow fog suppression.

5.5 Overall Suppression Effectiveness

As a final stage of analysis, data recorded for all tactics at all conditions are compared to assess global measures of suppression effectiveness, specifically maximum and integrated values of compartment cooling, as well as temperature and carbon monoxide levels at the firefighter during suppression. Vertical profiles of temperature difference for the four tactics that produced the largest levels of compartment cooling are shown in Figure 5.19.

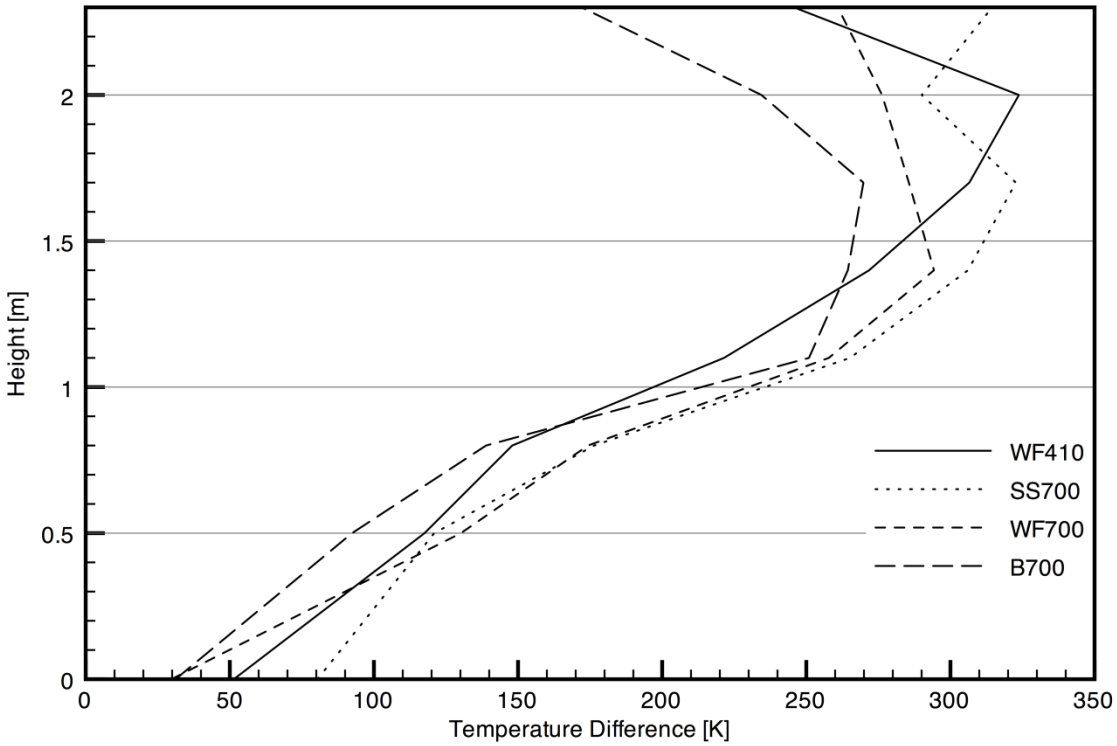

Figure 5.19. Average compartment temperature difference caused by the four most effective suppression methods.

These four methods include the continuous wide angle fog methods discharged at 410 and 700 kPa, the straight stream method discharged at 700 kPa, and the wide angle burst method (2 bursts) discharged at 700 kPa. All of these methods were applied at the lower angle of attack of 20°. Figure 5.19 shows that these methods produce similar cooling trends from the floor to the ceiling in the compartment, with 50 to 150 K decrease in temperature up to 0.7 m above the floor. Greater decreases in temperature, from 150 to 250 K, are typical in the range from 0.7 m to 1.2 m

above the floor. The maximum decrease in temperature is observed at heights between 1.4 to 2.0 m above the floor, depending on the method. Finally there is a slight reduction in the level of cooling right at the ceiling. The figure shows that the low pressure continuous wide angle fog method (WF410) provides the highest peak in cooling, followed by the high pressure straight stream method (SS700), high pressure continuous wide fog method (WF700), and high pressure burst method (B700).

Overall, the high pressure straight stream method appears to be the most effective at cooling the entire compartment, even though the peak temperature reduction is lower than that for the low pressure continuous wide angle fog method. To assess this further, the four temperature profiles are integrated using trapezoidal integration to estimate the total amount of cooling (area under each curve). Results are summarized in Table 5.5, and confirm that the high pressure straight stream method is the most effective at cooling the entire compartment, followed by the high pressure wide fog, low pressure wide fog, and burst methods.

Table 5.5. Integrated compartment cooling by the four methods.

Method	Estimated Total Cooling [m•K]
WF 410	560
SS 700	730
WF 700	640
B 700	390

The temperatures measured by the exposed thermocouples and those under the firefighter suit for each of the four most effective suppression methods are reviewed to check for any potentially negative influences on the firefighter environment. The temperatures measured by the highest thermocouple on the exposed and protected side of the firefighter can be seen in Figure 5.20 and Figure 5.21, respectively. The data at only one thermocouple height is sufficient for the comparison here, since the trends at all heights of the sensor board are similar on each side of the nozzle.

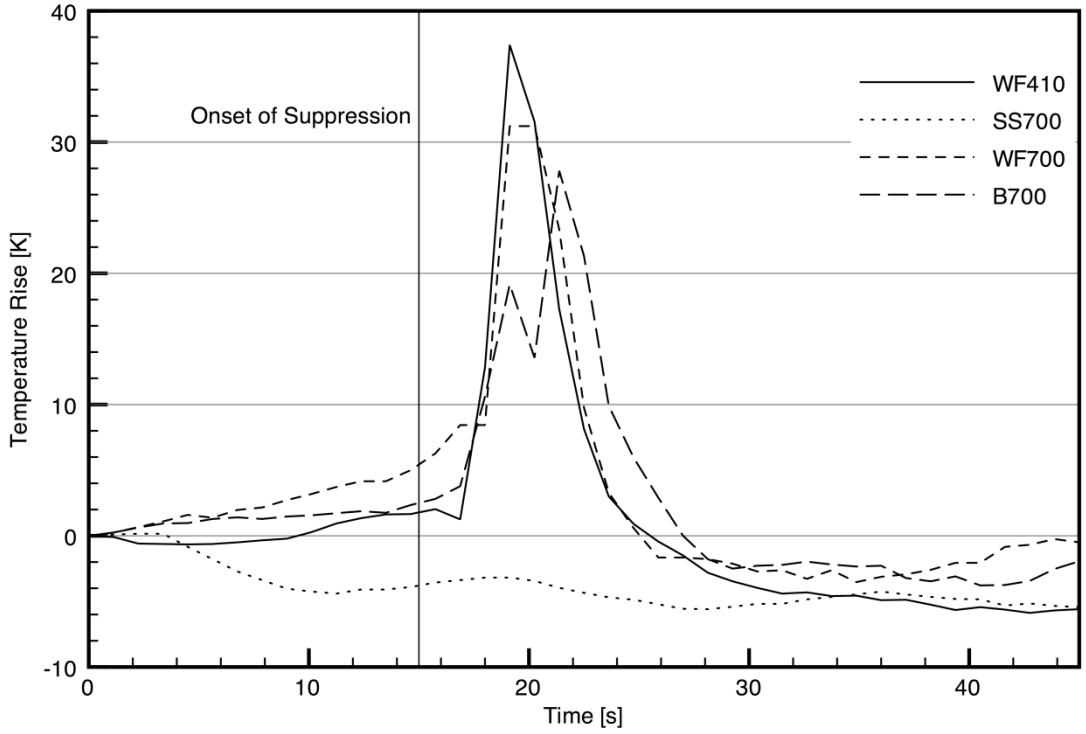

Figure 5.20. Temperature increase of the ambient air measured just outside the door for each of the four methods that provided the greatest amount of compartment cooling.

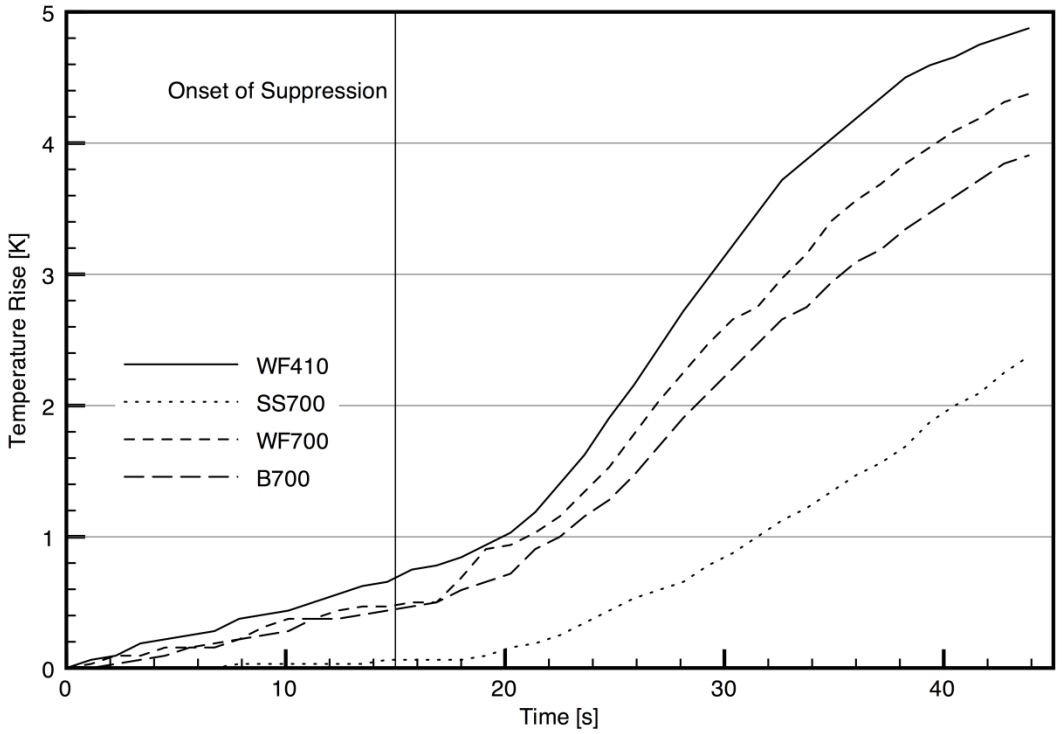

Figure 5.21. Temperature increase measured under the firefighter suit for each of the four methods that produced the greatest amount of compartment cooling.

Figure 5.20 shows that the ambient temperature measured at the firefighter for the three attack methods involving the wide angle nozzle setting starts to rise between 2 to 3 s after the onset of suppression, and peaks 5 to 7 s later, depending on the method. The largest peak is observed for the low pressure wide angle fog method, followed by the high pressure wide angle fog method, and then the burst method. In contrast, the straight stream method has no effect on the firefighter environment. This again suggests that the straight stream method penetrates the hot layer, while the other methods create more steam and displace the hot layer, forcing some hot gases and steam out the door.

The temperature measured by the thermocouples under the firefighter gear all follow the same trend as described earlier in this thesis, with the temperature rise starting as the doors are opened, and continuing until the end of the 45 s measurement time. Although the trends are the same for all methods, there is a significant separation in temperature between the three wide angle methods and the straight stream method. The observed temperature for the three wide angle fog methods rises much more steeply from 20 to 30 s, and reach a final temperature of between 4 and 5 K above ambient. The straight stream method, on the other hand, produces temperature that rises more slowly, to just 2.4 K above ambient.

Lastly, the peak carbon monoxide concentrations observed at the firefighter are compared for the four most effective suppression methods, as shown in Figure 5.22.

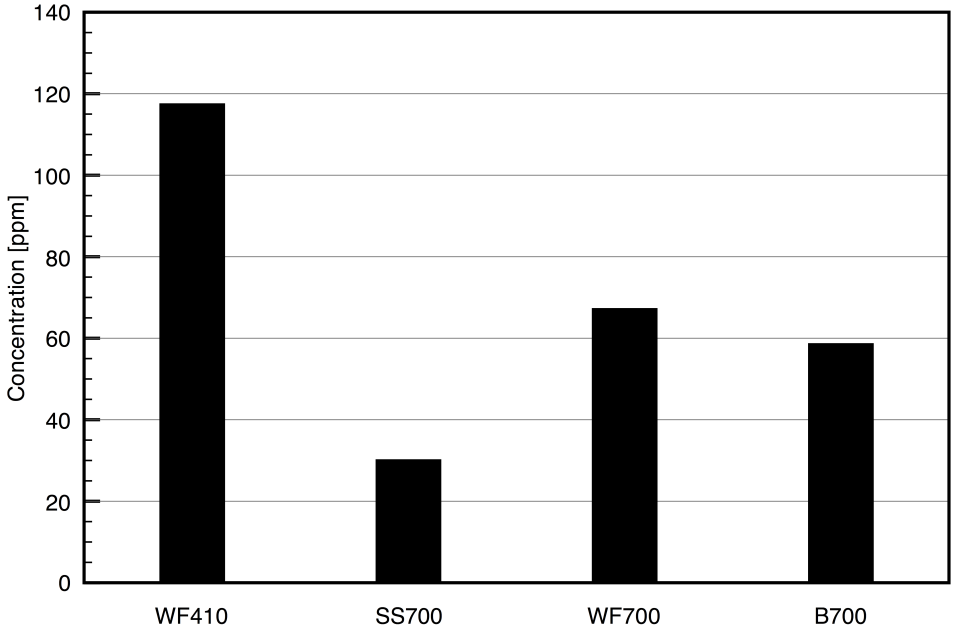

Figure 5.22. Peak carbon monoxide levels measured at the firefighter.

The largest CO concentration is measured for the low pressure wide angle fog method, at almost twice that of the high-pressure wide angle fog and burst methods, and over three times that of the straight stream method. This again supports the previous conclusion that the wide angle fog methods create steam that forces the upper layer out of the door, whereas the straight stream method has a limited impact on the area of the firefighter.

5.6 Summary

It was demonstrated at the start of this chapter that the suppression experiments conducted in the instrumented compartment behave in a repeatable manner when considering the scale and complexity of the fire scenario. Therefore, the results obtained from the different suppression tests are valid for this fire situation. The consistency of the temperature and heat flux results just outside the compartment door on both the ambient and protected side of the nozzle also validates the results.

In terms of overall suppression effectiveness, it is important to consider both the impact of the suppression method on the compartment environment as well as on the environment around the firefighter. The measurements reported here have shown that the continuous straight stream suppression method delivered at high pressure for 5 seconds into the upper rear of the compartment (20° angle of attack) produces the greatest amount of total compartment cooling of all those tested. This method also produced the lowest temperature increases both in the ambient environment around the firefighter and beneath the firefighter gear. In addition, the carbon monoxide levels measured in the area of the firefighter are the lowest for the straight stream method delivered at high pressure, suggesting that overall, the straight stream method has the least impact on the firefighter.

Chapter 6

CLOSURE

6.1 Conclusions

A number of conclusions can be drawn from the results obtained from the large-scale suppression experiments conducted in this research. It is important to remember that any conclusions made from these results are only confirmed for the situation presented, i.e. compartment conditions similar to those that would be observed in a fully developed fire but with a single fuel load. The size of the compartment and the ventilation conditions are also important when comparing different fire scenarios and suppression methods, as well as the length of the suppression, which was a maximum of 5 seconds here.

6.1.1 Compartment Environment and Repeatability

During all of the compartment burns, a well-defined interface height was present at 1.2 m above the floor. Above this, a relatively uniform hot layer existed laterally in the compartment, with axial variations typical of a compartment fire. Average upper layer temperatures of 910 K were achieved with a 38 K standard deviation over the 52 tests, which is within the range desired to resemble upper layer compartment conditions that would exist during a fully developed compartment fire. Along with the uniform upper layer temperatures that were established for each test, similar heat flux profiles were observed outside the open compartment door before suppression began. These consistent and repeatable results suggest that the experimental set-up and procedure were well suited to the study of the impact of suppression on the compartment and firefighter environments.

Along with the consistent compartment fire conditions described above, excellent repeatability of each method of suppression was observed for all three nozzle patterns under the same discharge pressure and application angle, particularly considering the scale of the experiment. Any variation observed in the compartment cooling can be explained by the slightly different amounts of water volume used in the different tests, and the relative amount of surface cooling in the

compartment. Therefore, the experiment was well suited to study the effect of different suppression tactics on the compartment fire environment.

6.1.2 Methods of Suppression

When comparing the average compartment cooling for all five suppression methods, the same general curve of temperature reduction with height in the compartment was observed, except for the narrow fog tests. The continuous wide angle fog suppression method produced the largest temperature reduction in the compartment, followed by the wide angle burst method, then the continuous straight stream method, when similar water quantities were used. The penciling method lead to the least amount of cooling in the compartment. The continuous method using the narrow fog setting produced a temperature inversion in the compartment, where hot upper layer gases were forced into the lower layer, increasing the average temperature there. Such a temperature inversion in the compartment is undesirable, so the narrow fog nozzle setting should be used with care in this type of compartment fire.

In terms of impact at the firefighter, the continuous wide angle fog method lead to a much larger temperature increase when compared to the other methods. The burst tactic produced about half the increase at the firefighter level, but the duration of exposure to the increased temperature was much longer. The two straight stream methods and the narrow fog method produced very little increase in temperature near the firefighter during suppression. As the penciling tactic produced much less compartment cooling than the straight stream method with approximately the same impact at the firefighter, the utility of the penciling tactic is brought into question.

When comparing different numbers of bursts, a slightly greater temperature reduction in the compartment was observed as the number increased, but no amount of burst suppression produced the same level of cooling as the continuous method, even when more water was used than in the continuous method. Further more, as the number of bursts increased, the impact at the firefighter also increased. These results suggest that if a bursting tactic is to be used, 2 bursts may be optimal, since the compartment cooling is still comparable, while the lowest increase in temperature of the environment near the firefighter is produced.

Tests conducted at either a higher nozzle discharge pressure or greater angle of attack show very little difference in compartment cooling when either the narrow fog or wide fog settings are used. For the straight stream setting, however, increased compartment cooling was observed at the higher nozzle pressure, and decreased cooling was observed at the greater nozzle angle. Of all the methods, only continuous narrow fog suppression lead to increased measured temperatures just outside the door. This was observed in both the higher pressure and larger angle tests, again indicating care should be taken when using the narrow fog nozzle setting for initial attack in a compartment fire.

The measurement of carbon monoxide in the area of the firefighter supports the temperature measurements, as greater levels of CO were measured for the wide angle fog methods in comparison to the other methods. This suggests that more of the upper layer gases, even if they have been cooled, are being forced into the area around the firefighter during suppression with the wide angle fog setting, which may be undesirable in certain situations.

When considering the temperatures measured on the protected side of the firefighter, very little change was noticed for the different suppression methods studied. This was not the case on the side exposed to ambient, as differences in temperature of as much as 40 K were observed. This suggests that as long as firefighters are properly protected, the different suppression methods will not have large impacts on them. If there are any exposed surfaces, however, large temperature differences may be felt depending on the method of suppression. The protected heat flux sensors verify these results, except when the continuous wide angle fog suppression method is used, as increased heat flux was measured during the tests. This suggests that even though the thermocouples do not measure a noticeable temperature difference, the continuous wide angle method may have an impact on the firefighter, even under their gear.

When considering only peak levels of compartment cooling, continuous wide angle fog suppression delivered at a nozzle discharge pressure of 700 kPa was the best method tested. However, when the impact of suppression on the firefighter is also taken into account, the straight stream method delivered at 700 kPa and aimed towards the top of the back wall in the compartment (20° angle of attack) produces the largest amount of integrated compartment cooling, while leading to the smallest increases in temperature and carbon monoxide concentration in the area of the firefighter.

6.2 Recommendations for Future Work

First, in order to ensure the fuel load creates a hot layer similar to what would be observed in a fully developed compartment fire, a compartment fire using typical furnishings should be tested. If the developed hot layer temperatures and amount of cooling due to the different suppression methods in the present compartment are similar to those outlined in this research, then wood crib fuel loads could be used for future fire suppression tests in other compartments.

As the results from this experiment can only be used to determine the most appropriate initial attack suppression method for similar types of fires in the same sized compartment under the same conditions, a number of future tests should be conducted to expand the range of conditions. Data from future tests involving different sizes and geometries of compartments, as well as different ventilation conditions, could be used with the data presented here to determine the most effective and safest initial or prolonged attack suppression methods in terms of compartment cooling and firefighter safety for a number of different fire scenarios.

In terms of the experiment, there are several modifications that should be made before future tests are conducted. These modifications would increase the reliability and accuracy of the data measured. In order for the experiment to produce more accurate results of the heat flux measured just outside the compartment door, the backside surface temperature of the skin simulant heat flux gauges should be regulated. If cooling water was supplied to the backside surface of each of the gauges, both of the assumptions necessary for accurate results using the sensors could be satisfied.

One of the goals of the experimental set-up was to remove the uncertainty induced by the human operator on the suppression action. By implementing a fixed stand to deliver the suppression, the variability induced by the operator having to hold and aim the nozzle was removed, increasing the constancy of the suppression delivery point and aim. Unfortunately, it was not possible to remove the operator entirely, as the valve controlling the flow of suppression water was not automated. If possible, the valve controlling suppression water flow should be automated to further increase the repeatability of the suppression, and make it possible to ensure the same quantity of water is used for all of the suppression methods, removing one more variable in the experiments.

REFERENCES

[1] Fahy, R.F. U.S. fire service fatalities in structure fires, 1977-2009. Technical Report Index No. 1531, National Fire Protection Association, Quincy, MA, 2010.

[2] Ontario Office of the Fire Marshal. Ontario Fire Incident Summary. http://www.ofm.gov.on.ca/en/Media%20Relations%20and%20Resources/Statistics/All%20Fire%20Incidents.asp. Accessed May 2011.

[3] Flynn, J.D. Fire service performance measures. Technical Report No. USS85, National Fire Protection Association, Quincy, MA, 2009.

[4] Ontario Office of the Fire Marshal. Ontario Structure Fires: Response time statistics, 2009.

[5] U.S. Fire Administration/National Fire Data Center. *Structure Fire Response Times*. Topical Fire Research Series, Vol. 5, Issue 7, 2006.

[6] Drysdale, D. *An Introduction to Fire Dynamics*, John Wiley and Sons, Chichester, 2nd edition, 1985.

[7] Karlsson, B., and Quintiere, J.G. *Enclosure Fire Dynamics*, CRC Press, Boca Raton, FL, 1999.

[8] Walton, W.D., and Thomas, P.H. *The SFPE Handbook of Fire Protection Engineering*, Estimating temperatures in compartment fire, pages 3.134-3.147. National Fire Protection Association, Quincy, MA, 2nd edition, 1995.

[9] Waterman, T.E. Room flashover – criteria and synthesis. *Fire Technology*, 4:25-31, 1968.

[10] Hägglund, B., Jansson, R., and Innermark, B. Fire development in residential rooms after ignition from nuclear explosions. FOA Report C 20016-D6 (A3). Forsvarets Forskningsanstalt, Stockholm, 1974.

[11] Fang, J.B. Measurement of the behaviour of incidental fires in a compartment. Technical Report NBSIR 75-679, National Bureau of Standards, Gaithersburg, MD, 1975.

[12] Liant, F.M., Chow, W.K., and Lui, S.D. Preliminary studies on flashover mechanism in compartment fires. *Journal of Fire Sciences*, 20:87-112, 2002.

[13] Gross, D., and Robertson, A.F. Experimental fires in enclosures. In *10th Symposium (International) on Combustion*, pages 931-942, The Combustion Institute, Pittsburgh, PA, 1965.

[14] Babrauskas, V. Peacock, R.D., and Reneke, P.A. Defining flashover for fire hazard calculations: Part II. *Fire Safety Journal*, 38:613-622, 2003.

[15] ISO 9705. Fire Tests – Full Scale Room Test for Surface Products. International Organization for Standardization, Geneva, Switzerland, 1993.

[16] Lock, A., Bundy, M., Johnsson, E., Opert, K., Hamins, A., Hwang, C., and Lee, K.Y. Chemical species and temperature mapping in full scale underventilated compartment fires. Technical Report 20899-8661, National Institute of Standards and Technology, Gaithersburg, MD, 2010.

[17] Hakkarainen, T. Post-flashover fires in light and heavy timber construction compartments. Journal of Fire Sciences, 20:133-175, 2002.

[18] Janssens, M. and Parker, W.J. Oxygen consumption calorimetry. Chapter 3 in *Heat Release in Fires,* Babrauskas, V., and Grayson, S.J., editors. Elsevier, New York, NY, 1992.

[19] Lai, C.M., Ho, M.C., and Lin, T.H. Experimental investigations of fire spread and flashover time in office fires. *Journal of Fire Sciences*, 28:279-302, 2010.

[20] Nelson, F.W. *Qualitative Fire Behaviour*, International Society of Fire Service Instructors, Ashland, MA, 1991.

[21] Chow, W.K. Performance of sprinkler in atria. *Journal of Fire Sciences*, 14:466-488, 1996.

[22] Rasbash, D.J., Rogowski, Z.W., and Stark, G.W.V. Mechanisms of extinction of liquid fires with water sprays. *Combustion and Flame*, 4:223-234, 1960.

[23] Evans, D.D. Calculating sprinkler actuation time in compartments. *Fire Safety Journal*, 9:147-155, 1985.

[24] O'Neill, J.G., and Hayes, W.D. Jr. Full-scale fire tests with automatic sprinklers in a patient room. Technical Report NBSIR 79-1749, National Bureau of Standards, Washington, D.C., 1979.

[25] O'Neill, J.G., Hayes, W.D. Jr., and Zile, R.H. Full-scale fire tests with automatic sprinklers in a patient room. Phase II. Technical Report NBSIR 80-2097, National Bureau of Standards, Washington, D.C., 1980.

[26] Blevins, L.G., and Oliphant, J.C. Drop size measurements in a fire sprinkler using an agricultural testing method. In Annual Conference on Fire Research Book of Abstracts, Beall, K.A. editor. Technical Report NISTIR 6242, National Institute of Standards and Technology, Gaithersburg, MD, 1998.

[27] Ren, N., Baum, H.R., and Marshall, A.W. A comprehensive methodology for characterizing sprinkler sprays. *Proceedings of the Combustion Institute*, 33:2547-2554, 2011.

[28] Tao, C. and Kalelkar, A.S. Effect of drop size on sprinkler performance. *Fire Technology*, 6:254-268, 1970.

[29] Zhou, X. and Yu, H.Z. Experimental investigation of spray formation as affected by sprinkler geometry. *Fire Saefty Journal*, 46:140-150, 2011.

[30] Back, G.G., DiNenno, P.J., Leonard, J.T., and Darwing, R.L. Full scale tests of water mist fire suppression systems for navy shipboard machinery spaces: Part II – Obstructed spaces. Technical Report NRL/MR/6180--96-7831, Naval Research Laboratory, Washington, D.C., 1996.

[31] Liu, Z., and Kim, A.K. A review of water mist fire suppression technology: PartII – Application studies. *Journal of Fire Protection Engineering*, 11:16-42, 2001.

[32] Royer, K. Water for Fire Fighting. Bulletin No. 18, Engineering Extension Service, Iowa State University, Ames, IA, 1959.

[33] Chang, C.H., and Huang, H.C. A water requirements estimation model for fire suppression: a study based on integrated uncertainty analysis. *Fire Technology*, 41:5-24, 2005.

[34] Hadjisophocleous, G.V. Water flow demands for firefighting. *Fire Technology*, 41:173-191, 2005.

[35] Linder, K.W. Water supply requirements for fire protection. Chapter 6 in *Fire Protection Handbook*, 17th edition, Hall, J.R. Jr., and Cote, A.E., editors. National Fire Protection Association, Quincy, MA, 1981.

[36] Särdqvist, S., and Holmstedt, G. Water for manual fire suppression. *Journal of Fire Protection Engineering*. 11:209-231, 2001.

[37] Torvi, D., Hadjisophocleous, G., Guenther, M.B., and Thomas, G. Estimating water requirements for firefighting operations using FIERAsystem. *Fire Technology*, 37:235-262, 2001.

[38] MacInnis, S. Personal communication, Kitchener Fire Department, Kitchener, ON, 2010.

[39] Akron Brass Company. Turbojet nozzles. http://www.akronbrass.com/uploadedFiles/Products/2011/Nozzles/Turbojet_Nozzles.pdf. Accessed May 2010.

[40] Wieder, M.A. Pumping Apparatus Driver/Operator Handbook. Smith, C., and Brakhage, C., editors. Fire Protection Publications, Oklahoma State University, Stillwater, OK, 1999.

[41] Grimwood, P., and Kesmet, K. *Tactical Firefighting*. Firetactics and Crisis & Emergency Management Centre, Belgium, 2003.

[42] Svensson, S. The Operational Problem of Fire Control. Ph.D. thesis, Lund University, Lund, Sweden, 2002.

[43] Svensson, S., and Lundström, S. Live fire tests on suppression of post-flashover fires using manually applied high and low pressure water sprays. In *Interflam '99 Conference Proceedings*, pages 47-57, 8th International Fire Science & Engineering Conference, Edinburgh, Scotland, 29th June – 1st July, 1999.

[44] Särdqvist, S., and Svensson, S. Fire tests in a large hall, using manually applied high- and low-pressure water sprays. *Fire Science and Technology*, 21:1-17, 2001.

[45] Scheffey, J.L., and Williams, F.W. The extinguishment of fires using low flow water hose streams – Part I. *Fire Technology*, 27:128-144, 1991.

[46] Scheffey, J.L., and Williams, F.W. The extinguishment of fires using low flow water hose streams – Part II. *Fire Technology*, 27:291-320, 1991.

[47] Grimwood, P. Hartin, E., McDonough, J., and Raffel, S. *3D Tactical Firefighting. Training, Techniques, and Tactics*. Fire Protection Publications, Oklahoma State University, Stillwater, OK, 2005.

[48] Tavoularis, S. *Measurement in Fluid Mechanics*, Cambridge University Press, New York, NY, 2005.

[49] Moffet, R.J. Experimental Methods in Heat Transfer. *Proceedings of the First World Conference, Experimental Heat Transfer, Fluid Mechanics, and Thermodynamics*, pages 13-31, World Academy of Science, Engineering and Technology, Dubrovnik, Yugoslavia, 1988.

[50] Incropera, F.P., Dewitt, D.P., Bergman, T.L., and Lavine, A.S. *Fundamentals of Heat and Mass Transfer*. John Wiley & Sons, New York, NY, 6th edition, 2007.

[51] Lam, C.S. Thermal Characterization of a Pool Fire in Crosswind With and Without a Large Downwind Blocking Object. Ph.D. thesis, University of Waterloo, Waterloo, Ontario, Canada, 2009.

[52] Gardon, R. A transducer for the measurement of heat-flow rate. *Journal of Heat Transfer*, 82:396-398, 1960.

[53] Vatell Corporation. Thermogage Circular Foil heat Flux Gages. Vatell Corporation, Christiansburg, VA, 2001.

[54] McCaffrey, B.J., and Heskestad, G. A robust bidirectional low-velocity probe for flame and fire application. *Combustion and Flame*, 26:125-127, 1976.

[55] Weisinger, J. Characterization of the University of Waterloo Live Fire Research Facility Wind Generation System. M.A.Sc. thesis, University of Waterloo, Waterloo, Ontario, Canada, 2004.

[56] White, F.M. *Fluid Mechanics*. McGraw-Hill, New York, NY, 6th edition, 2008.

[57] International Sensor Technology. Hazardous Gas Monitors. http://www.intlsensor.com/pdf/infrared.pdf. Accessed Feb 2011.

[58] Delta F Corporation. Delta F Non-Depleting Coulometric – Paramagnetic. http://www.delta-f.com/O2Guide/O2GuidePara.html. Accessed Feb 2011.

[59] Crown, E.M., and Dale, J.D. Evaluation of flash fire protective clothing using an instrumented mannequin. Technical Report prepared for Alberta Occupational Health and Safety Heritage Grant Program, University of Alberta, Edmonton, AB, 1992.

[60] B.J. Wolf Enterprises. Pyromark High Temperature Paint. B.J. Wolf Enterprises, Agoura Hills, CA, 2009.

[61] Torvi, D.A. Heat Transfer in Thin Fibrous Materials Under High Heat Flux Conditions. Ph.D. thesis, University of Alberta, Edmonton, Alberta, Canada, 1997.

[62] Henrique, F.C. Jr. Studies of thermal injuries v. the predictability and the significance of thermally induced rate processes leading to irreversible epidermal injury. Archives of Pathology, 43:489-502, 1947.

[63] Stoll, A.M., and Chianta, M.A. Method and rating system for evaluation of thermal protection. *Aerospace Medicine*, 40:1232-1238, 1969.

[64] FTT. Users' Guide for the LSHRCalc Software Package, Fire Testing Technology Limited, West Sussex, 2001.

[65] Heskestad, G. Heat of combustion in spreading wood crib fires with application to ceiling jets. *Fire Safety Journal*, 41:343-348, 2006.

[66] Buchanan, A.H. Structural Design for Fire Safety, John Wiley and Sons, Chichester, 2002.

[67] Moran, M.J., and Shapiro, H.N. *Fundamentals of Engineering Thermodynamics*. John Wiley and Sons, Hoboken, NJ, 5th edition, 2004.

[68] OMEGA Engineering, Inc. *The Temperature Handbook*. Stamford, CT, 21st century, 2nd edition, 2000.

[69] National Instruments Corporation. FieldPoint operating instructions, FP-TC120 and cFP-TC-120 8-channel thermocouple input modules. http://www.ni.com/pdg/manuals/373344a.pdf. October 2002 edition, Accessed February 2011.

[70] Francis, J., and Yau, T.M. On radiant network models of thermocouple error in pre and post flashover compartment fires. *Fire Technology*, 40:277-294, 2004.

[71] Pitts, W.M., Braun, E., Peacock, R.D., Mitler, H.E., Johnsson, E.L., Reneke, P.A., and Blevins, L.G. Temperature uncertainties for bare-bead and aspirated thermocouple measurements in fire environments. In *Thermal Measurements: The Foundation of Fire Standards*, Gritzo, L.A. and Alvares, N.J., editors, pages 3-15, American Society for Testing and Materials, West Conshohocken, PA, 2002. ASTM Special Technical Publication 1427.

[72] Brohez, S., Delvosalle, C., and Marlair, G. A two-thermocouples probe for radiation corrections of measured temperatures in compartment fires. *Fire Safety Journal*, 39:399-411, 2004.

[73] Setra Sensing Solutions. Model 267 and 267MR Differential Pressure Transducers Installation Guide. Setra Sensing Solutions. Boxborough, MA, 2002.

[74] Servomex Group Limited. Servomex Emissions Analyzers, ServoPRO 4900. Servomex Group Limited, East Sussex, UK, 2010.